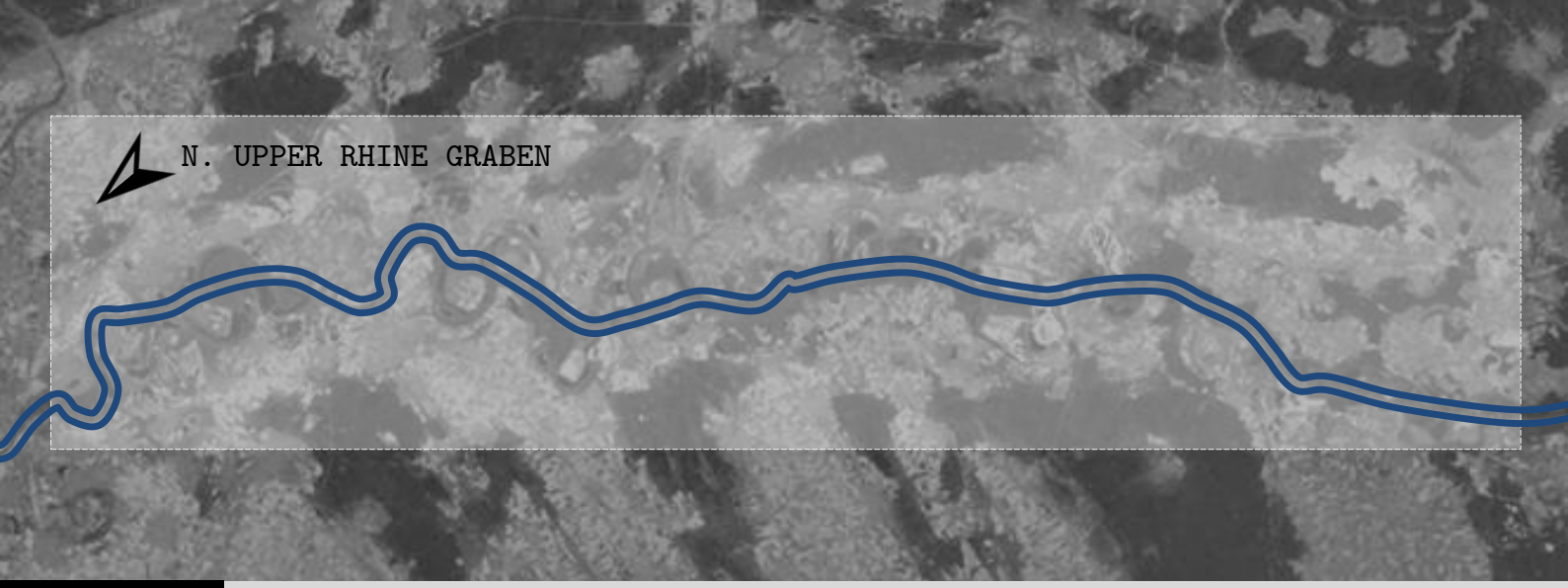

Master of Science Thesis

Analysis of measured data of sediment nourishments in the Rhine River

A. Emmanouil

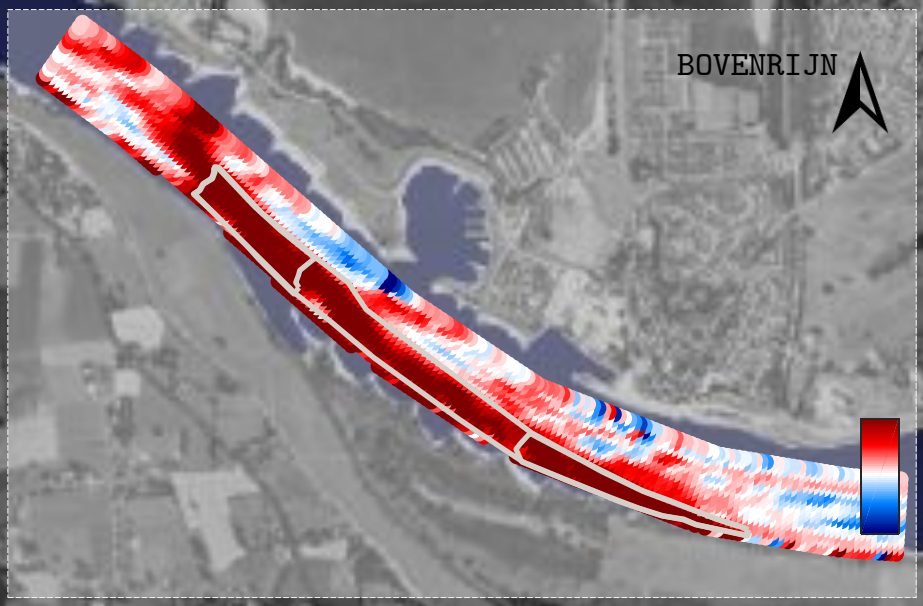

TU Delft

ANALYSIS OF MEASURED DATA OF SEDIMENT NOURISHMENTS IN THE RHINE RIVER

Cover: The maps of the two study areas at the Rhine with flow direction from right to left. Bovenrijn is depicted at bottom figure and the Northern Upper Rhine Graben at the top figure.

Analysis of measured data of sediment nourishments in the Rhine river

by

Antonios Emmanouil

in partial fulfilment of the requirements for the degree of

Master of Science
in Civil Engineering

at the Delft University of Technology,
defended publicly on Wednesday December 20, 2017 at 16:00 PM.

Student number:	4510828	
Chair:	Prof. dr. ir.W. S. J. Uijttewaal	Delft University of Technology
Supervisor:	Dr. ir. A. Blom	Delft University of Technology
Thesis committee:	Dr. ir. C. J. Sloff	Deltares, Delft University of Technology
	Dr. E. Viparelli	University of South Carolina
	Dipl.-Ing. Anke Becker	Deltares

TU Delft Delft University of Technology

PREFACE

The present document comes as the final product of my Master studies in Delft University of Technology during the past two years. Conducting research for the MSc Thesis has been a long, challenging, but most of all inspiring educational journey. I consider that i have benefited in two main ways from it. First, i was introduced to the world of river morphodynamics which i expect to keep me challenged in the days to come and second i was able to explore the limits of personal determination.

To start with i would like to thank the members of my committee for their valuable input in the present thesis. In addition, i would like to thank dr. ir. Astrid Blom for the time she has spent in supervising and especially for her patience and determination in improving my reporting ability, hoping that this is reflected in the present document. For all the support, comments, and amazing working hours together, i would like to especially thank Liselot, Meles, and Victor as well as all other beautiful people i met in the WaterLab. Finally, i am gratefull to Lina, Panos and other friends for the personal support during this research.

Antonios Emmanouil,
Delft, 13/12/2017

ABSTRACT

Sediment nourishments have become an attractive alternative to hard measures in counteracting long-term river bed degradation. Due to the large degree of uncertainty concerning mixed sediment morphodynamics, river authorities conduct field studies to collect data that will help in the calibration of morphological models, eventually used to design effective mitigation measures.

In the present study, we analyse measured data from two field experiments in the Rhine river, that monitored the fate of the mixed-size nourished sediment. In the first study case, we analyse data from a 5 year monitoring campaign at the reach below the most downstream weir in the Rhine river. The sieving analyses of the soil samples collected from the bed of the study reach, reveal the concentrations of various tracer granite fractions at several vertical layers, lateral positions and cross sections along the streamwise direction in the study reach. Second, we studied the early development of the nourishment pilot study initiated in 2016 at Lobith, a reach situated further downstream in the Rhine river. In spite of the early stage of the nourishment, due to intensive monitoring of the pilot, data are collected in dense time intervals by means of bed surveys, radioactivity measurements for the detection of tracer sediment as well as soil samples, revealing the initial morphodynamic trends in the study reach.

In both study cases we predominantly focus on the migration of nourished sediment in all directions and the main physical processes that regulate the feedback between flow and mixed sediment morphodynamics. We conclude that nourished sediment disperses along the streamwise direction, gets mixed into larger depths as it migrates downstream, but also follows certain paths along the mitigated meandering reaches. We find that especially vertical mixing of nourished sediment is a major control on its streamwise migration. Regarding certain of these aspects, the various grain size fractions of the nourished sediment were seen to behave differently. For example finer fractions migrated downstream faster, but were also mixed in larger depths below Iffezheim.

In the present study we assess the influence of flow temporal and spatial variability, but also the influence of small and large scale processes which are relevant in mixed sediment morphodynamics. The feedback between flow and mixed sediment morphodynamics is key in explaining the main physical processes controlling the fate of nourished sediment, yet more work needs to be done to assess which are the dominant small and large scale physical mechanisms when mixed-size sediment feeding in lowland rivers is considered.

NOTATIONS

f	[-]	sampled grain size fraction index
i	[-]	sampled cross-section index
v	[-]	sampled vertical layer index
n	[-]	sampled lateral position index
s	[-]	crossing index
Rkm	[km]	Rhine river chainage
T	[%]	total tracer concentration per cross section
T_N	[-]	normalised total tracer concentration per cross section
Rkm_{mean}	[km]	Rhine kilometre of the mean parameter
I_u	[%]	T integral as a function of distance from the upstream end
I_d	[%]	T integral as a function of distance from the downstream end
$Rkm_{\ 99\%\ \text{front}}$	[km]	Rhine kilometre of the 99% front parameter
F	[%]	fractional tracer concentration per cross section
F_N	[-]	normalised fractional tracer concentration per cross section
Q_w	$[m^3/s]$	water discharge
S_N	[-]	normalized fractional sediment discharge
TL	[%]	total tracer concentration as a function of lateral position per cross section
FL	[%]	fractional tracer concentration as a function of lateral position per cross section
TL_N	[-]	normalized total tracer concentration as a function of lateral position per cross section
$\overline{FL(n=inner)}$	[%]	campaign averaged fractional tracer concentration closer to inner bends
$\overline{FL(n=outer)}$	[%]	campaign averaged fractional tracer concentration closer to outer bends
$\overline{FL}$	[%]	campaign averaged fractional tracer concentration
$Rkm_{\mathrm{N,s}}$	[km]	chainage location of the nearest crossing s to the examined cross-section i
X_P	[-]	bend crossing conditions distance parameter
$L_{\mathrm{B,U}}$	[km]	streamwise extent of the upstream bend closest to the examined cross-section i
$L_{\mathrm{B,D}}$	[km]	streamwise extent of the downstream bend closest to the examined cross-section i
FV	[%]	fractional tracer concentration as a function of depth per cross section

CONTENTS

chapter

ONE

INTRODUCTION

1.1 Context

Long-term bed degradation is one of the dominant morphodynamic responses in engineered rivers like the Rhine and Danube, to anthropogenic and natural changes in climate, flow and sediment transport regime (Gölz, 1994; Habersack et al., 2013). For example, a cumulative erosion of 7 meters in a period of 100 years is reported at the Upper Rhine Graben (Buck, 1993). Moreover, in the Dutch Rhine branches the bed has degraded from 1 to 2 meters locally during the past century (Sieben, 2009).

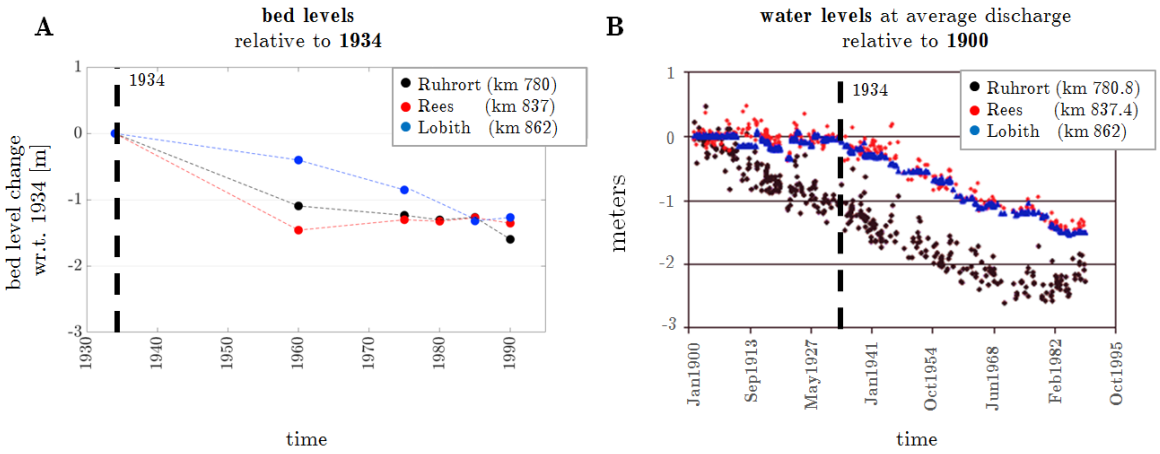

Figure 1.1: **Panel A.** Bed levels [m] relative to 1934 at Ruhrort, Rees and Lobith (data source: Paarlberg et al. (2016)). **Panel B.** Water levels [m] at mean discharge relative to 1900 for three locations (gauging stations) with colors relative to Panel A (from Van Vuren (2005)). In both panels a vertical line is plotted for 1934 to facilitate the comparison between bed and water level measurements. It can be seen that degrading beds are followed by lowering water levels. For all locations a cumulative incision of 1.3 m is demonstrated for the period 1934-1995.

Such bed incision is followed by lowering water levels (Fig.1.1) and may lead to adverse effects for various aspects of river management such as navigation, ecology, existing infrastructure, bifurcation stability and flood protection (Frings et al., 2014b). In Fig.1.2 some characteristic examples of problems related to bed degradation are illustrated. Panel A treats non-erodible layers that are exposed and hinder navigation while Panel B and C treat the lowering of water levels, leading to decrease of the available depth in river harbours and to lowering of groundwater tables with effects on floodplain vegetation.

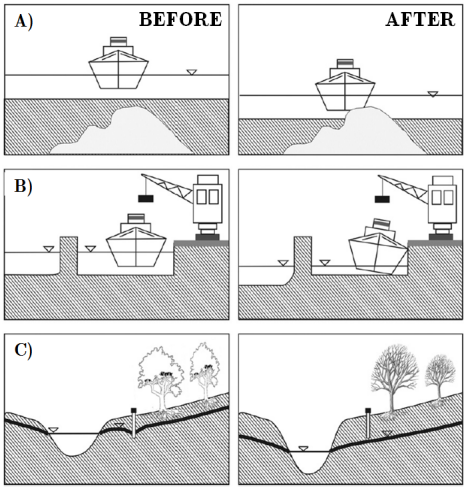

Figure 1.2: Problems emerging from river bed degradation to navigation (A), infrastructure (B) and ecology (C). The figures are modified by Frings et al. (2014b) and were originally created from Gölz (1994).

In order to design effective mitigation measures, knowledge concerning the ongoing degradational process is indispensable (Wohl et al., 2005). Depending on the anticipated current and expected characteristics of adjustment, the spatial scale over which degradation occurs, and the triggering factors, different strategic approaches may be followed. These strategies consist of measures such as: (a) halting of mining activities, (b) re-allocation dredging, (c) local training measures (e.g. lowering of groynes and/or implementation of training walls) and (d) sediment feeding. For example, following accelerated rates of degradation at the upstream Rhine reaches during the period 1980-1990 (Ten Brinke and Gölz, 2001), the Dutch river authorities decided to halt removal dredging and feed all the sediment dredged from shallows for navigation purposes to upstream deeper locations (Sieben, 2009) (Fig.1.3).

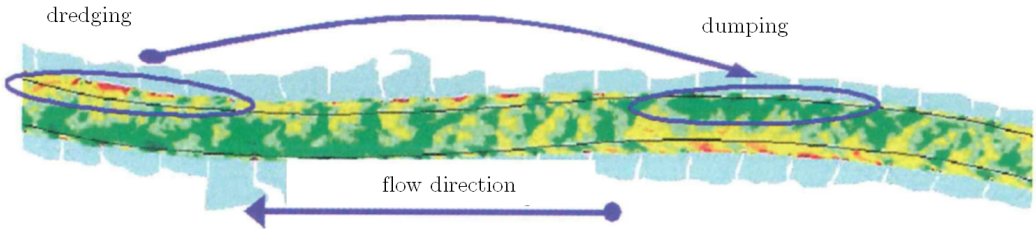

Figure 1.3: Dredging from shallows and feeding at upstream deep locations. source: Ten Brinke (2005).

It is not trivial to fully anticipate and predict the time and space varying degradational process. This is due to the fact that there are numerous potential triggers with various effects overlapping in time, but also spatially varying hydraulic conditions resulting in different degradational properties (e.g. incision rates) for different reaches of the same river, and the uncertainty regarding future morphodynamic changes. Such levels of complexity with respect to river bed degradation are met for instance in the German Rhine reaches. The possibly ongoing response to past centuries river training measures (e.g. Tulla works), the recent (2000s) narrowing by extension of groynes (Frings et al., 2014b), the blockage of bedload sediment behind weirs at the upstream end (Iffezheim), and at the tributaries of the freely-flowing German reach (e.g. Neckar, Main and Moselle), are most probably only some of the controls on the current degradation of the riverbed. This bed incision is expressed by neither constant nor uniform rates of degradation (Gölz, 2008).

To this end, a dynamic bed stabilization strategy is followed for the German Rhine reaches, which is a representative example of a combination of mitigation measures. It is dynamic in the sense that it is adjusted to the temporally varying imbalances of the sediment budget, while bed stabilization measures are selected predominantly based on the longitudinal extent of degradation. When relatively short river sections are degrading, dredging and dumping activities (i.e., re-allocation dredging) and

local training works (e.g. lowering of groynes, fixed layers) are implemented. On the contrary, when degradation evolves within larger river sections, sediment nourishments are performed (Fig.1.4).

Figure 1.4: Sediment nourishments with barges. Image courtesy: **A.** Kondolf (1997) (photograph taken below Iffezheim weir) **B.** Rijkswaterstaat (screenshot from animation).

Future morphodynamic change is uncertain, when designing mitigation measures for bed degradation, which is characterized by large time scales (De Vriend, 2015). For example, Guerrero et al. (2013) demonstrate how certain climate scenarios could yield excessive sedimentation for the Parana river. That being said, inflexible structural measures that would achieve short term mitigation of degrading rivers, could potentially aggravate adverse effects on the long term (e.g. for navigation). Following from their susceptibility to future adjustments, repeated sediment nourishments could address this uncertainty more effectively. Moreover, the operational flexibility of sediment augmentation allows for adjustments at a shorter time scale. Humphries et al. (2012) demonstrate how sediment pulse dynamics closely relate to the discharge hydrograph. This implies that for instance the supplied volume of sediment can be modified according to the changing flow conditions.

On these grounds and combined with their environmentally sound character, sediment nourishments are becoming an increasingly attractive alternative to hard measures. They have been applied for almost four decades by the German authorities, as a sustainable alternative to further impoundments of the Rhine (Gölz, 2008) but also implemented in the erosion stretch of Elbe (Schmidt and Faulhaber, 2001). Supply of artificial sediment was also initiated in 1995 for the degrading freely-flowing reach of Danube east of Vienna, by the Austrian river authorities (Habersack et al., 2015) where sediment of the natural range is continuously fed to the river. Additional examples come from projects in impounded mountainous rivers at the USA and Japan, where sediment augmentation measures are aimed jointly at ecological restoration and counteracting bed degradation (Kondolf and Minear, 2004; Bunte, 2004; Kantoush and Sumi, 2010). Finally, a pilot study was initiated in 2015 at Lobith from the Dutch river authorities, to assess the effectiveness of the measure in arresting bed degradation at the Dutch Rhine branches.

Effectively, there are several ways through which sediment nourishments can counteract bed degradation. First, the added sediment can be seen as a direct increase in bed level. Further, supposing that the augmented volume is large and distributed along an accountable distance, it may disturb the flow such that it induces spatial flow depth gradients favourable for upstream deposition of sediment. Third, provided that the nourished sediment is sufficiently mobile, it may reduce the deficit of sediment supply from upstream. Finally, provided that the nourished sediment is coarser than the bed sediment it has a stabilizing effect by armouring of the bed surface. In that way, the sediment transport capacity decreases and underlying sediment is protected from entrainment by the flow. By adjusting the specifications of augmented sediment (e.g. feeding frequency, volume, grain size characteristics, geometry, dumping location) a different counteracting effect may become dominant. The proper choice for that adjustment results mainly from the characteristics of the degradational process to the extent that it is understood. In fact, a clearer distinction between nourishment strategies is made on the basis of the grain size characteristics of the added sediment.

At one hand, river authorities feed sediment that is significantly coarser than the original bed

sediment to achieve rapid bed stabilization. This is done in order to level streamwise positive gradients in sediment transport capacity, by coarsening the downstream section of a degrading reach (Sloff and Sieben, 2008). Such sediment transport gradients leading to degradation could for example follow after incision of a downstream adjacent reach and consequent lowering of the base level. This strategy, often termed bed stabilization feeding, has been applied just upstream from the German-Dutch border for almost three decades (Fig.4.10). There, nearly immobile sediment with a mean grain size up to 50 times coarser than the mean grain size of the bed material is fed, reaching up to 25% of the sediment source for the whole Niederrhein reach (Frings et al., 2014a).

The disadvantage of this approach is that it is sustainable only when it is applied along the whole extent of a reach, as otherwise a deficit of sediment supply may develop for downstream sections, consequently leading to a downstream migrating erosional wave. In fact, concerning the nourishment of coarse gravel and cobbles at the lower Niederrhein, despite contributing effectively to bed stabilization in this reach, it is hypothesized by Blom (2016) to be contributing to the ongoing erosion at the downstream adjacent Dutch Rhine branches. Fig.1.5.A demonstrates the evolution of bed levels at the reaches close to the German-Dutch border area. It can be seen that after the initiation of coarse gravel and pebble nourishments in 1990 (Fig.1.5.B), the reaches of Lower Niederrhein get stabilized or even demonstrate aggradation (e.g. Rhine-km 840-850). The Bovenrijn has remained more or less stable after 2000 while erosion in the Waal persists at decreased rates compared to the past. Moreover, since 1976 13.6 Mt of mining waste were supplied in the Niederrhein to fill the subsidence funnels. At the same period, the extensive removal dredging of the past e.g. (Emmanouil, 2017) was replaced by re-allocation dredging while finally since 2000, fine gravel is also nourished more or less at the same locations as the coarser material, to increase the bedload supply at Niederrhein (Frings et al., 2014a).

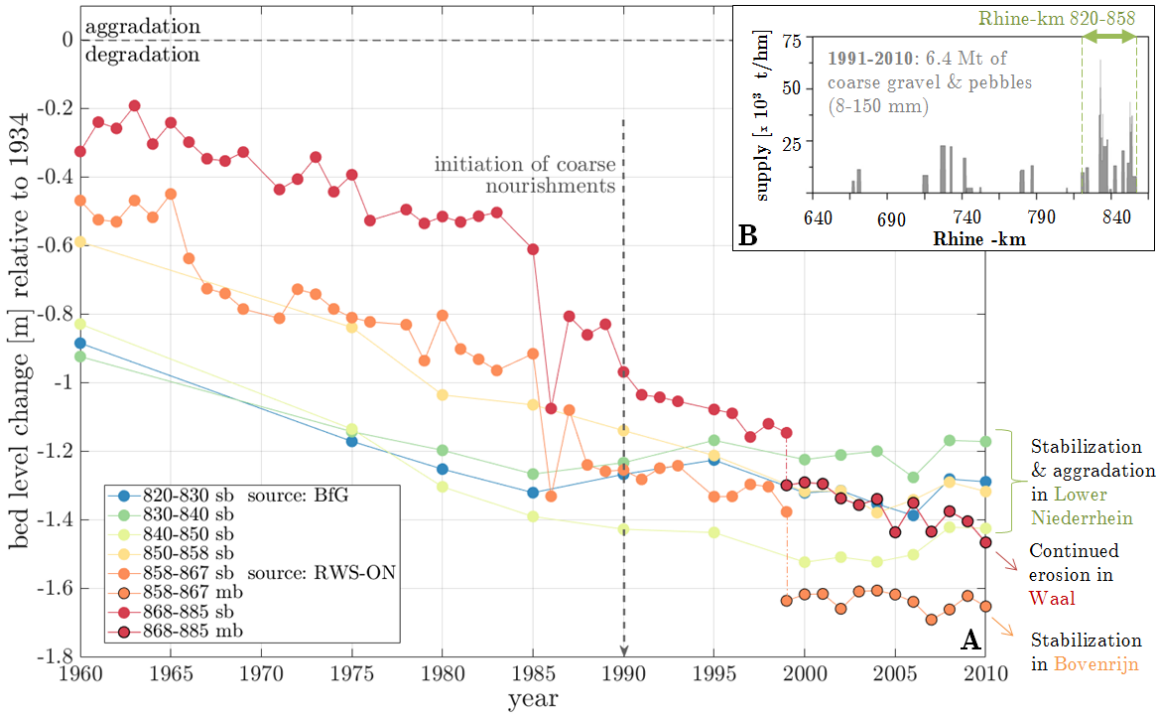

Figure 1.5: **Panel A:** Reach averaged bed level changes relative to 1934 for Lower Niederrhein, Bovenrijn and Waal. Note that the discontinuity seen in 1999 for the Bovenrijn and the Waal reaches, follows from the change in the method of bed level surveys. Single-beam were changed to multi-beam echo soundings (source of data: BfG and Rijkswaterstaat). **Panel B:** The amounts of nourished coarse gravel and pebbles during 1991-2010 are given for the Niederrhein reach. Most of the nourishments were performed at the most downstream reach, just upstream the German-Dutch border. (source: Frings et al. (2014a)).

The hypothesis by Blom (2016) is also supported by experiments in laboratory conditions by Berkhout (2015). In these experiments an erosional wave was found to precede the nourished bed wave in the case that the latter was coarser than the material in the bed.

Apparently bed stabilization nourishments have the potential to become a sustainable mitigation practice only for short reaches that do not extent upstream from free flowing river sections. This is the case for instance east of Vienna, where a 48 km free flowing reach of Danube river is situated upstream from Gabcikovo dam. Degradation there, has lowered the bed by 1 meter in 50 years (see Fig.1.6.A). The latter continues at a rate of approximately 2 cm/annum despite the addition of 194.000 m^3 gravel on a yearly basis since 1995 (Pessenlehner et al., 2016). In search of alternative approaches to arrest the ongoing degradation, the Austrian river authorities have initiated the Bad Deutsch-Altenburg pilot study. The aim is to effectively counteract the ongoing erosion by reducing the bedload transport at the degrading reaches by nearly 90%. To this end, 113.000 m^3 of artificial sediment was fed to the river. It consisted of gravel within the natural grain size spectrum, yet with a mean grain size double (ca. 52 mm) the mean grain size of the bed material (ca. 26 mm). The tested approach is termed as granulometric bed improvement, which is demonstrated in Fig.1.6.B. The addition of an approximately 25 cm layer of coarse material on top of the bed is expected to coarsen the bed surface, diminish the bedload transport, and eventually arrest bed degradation at the reach. The main difference from the coarse nourishments performed at the Lower Niederrhein is that the downstream adjacent reach of the Danube's mitigated stretch is not free flowing as the Dutch Rhine branches; it is impounded from the downstream situated Gabcikovo dam (Habersack et al., 2015).

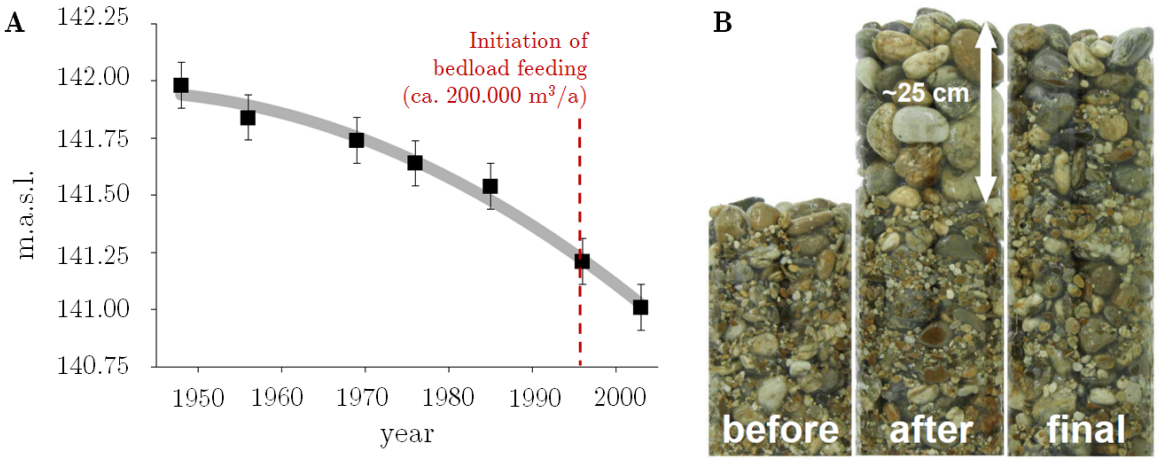

Figure 1.6: **Panel A:** Bed degradation of river Danube, east of Vienna.(source: viadonau) **Panel B:** A schematic of granulometric bed improvement is demonstrated as tested in the pilot study Bad Deutsch-Altenburg east of Vienna. Three time instances are shown. Before the addition of the artificial sediment, after the nourishment (forming a layer of ca. 25 cm), and after the turbation of nourished sediment with the natural sediment (source: Tögel (2011)).

So far, we mainly addressed the so-called bed stabilization nourishments. The other feeding strategy, already mentioned, concerns sediment that corresponds more to the natural grain size spectrum. This strategy is followed when the objective is to counteract degradation characterized by a deficit of upstream sediment supply (e.g. following from sediment retention behind dams, or training works that increase the overall sediment transport capacity of a reach). Then sufficiently mobile sediment needs to be fed at a certain frequency or even continuously (Gölz, 2008). Such feeding is the most common in the Rhine. Frings et al. (2014b) demonstrated by means of a sediment budget analysis, that sediment nourished to reduce the deficit from upstream, provided almost half of the sediment source during 1985-2006 for the northern Upper Rhine Graben and Rhenish Massif (Fig.1.7). Moreover, it was implemented in the degrading reaches of the Elbe river e.g. (Gabriel et al., 2009), and in Danube river since 1995 as was discussed previously.

Obviously, the mobility of augmented sediment which is key in such nourishments is related to its grain size characteristics. After sediment is fed, it behaves as a slowly downstream migrating wave consisting of multiple waves (respective to its often multiple fractions) migrating at different speeds. In previous tracer studies, a celerity in the order of a few kilometres per year was found to characterize the migration of such waves for the upstream free flowing Rhine (Gölz et al., 2006). From an operational and economic point of view, the behavioural aspects of such a wave, are of

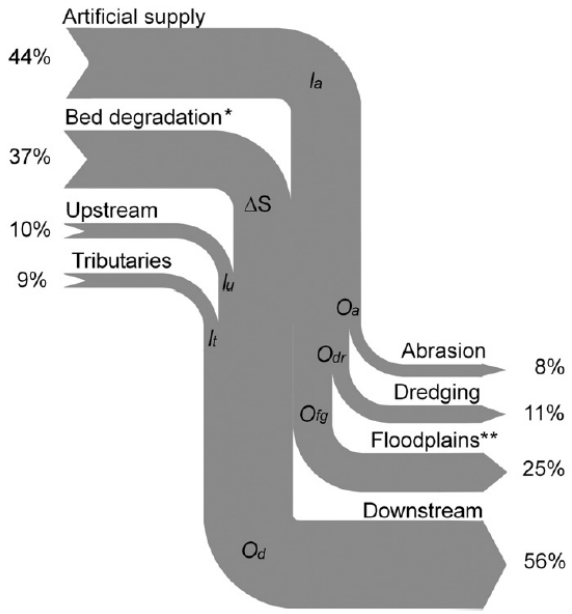

Figure 1.7: Sediment budget analysis for the period 1985-2006 by Frings et al. (2014b) for the northern Upper Rhine Graben and the Rhenish Massif. Almost half of the sediment input to the studied reach (44%) was estimated to originate from bedload feeding. Most of this sediment is fed below Iffezheim weir at the upstream end of the freely-flowing Rhine. Despite the large amounts of sediment feeding the river bed still shows degradation. Note that only 20% of the sediment source comes from upstream and the tributaries.

critical importance since these characterize the efficiency of the measure. An optimal result is accomplished when the counter effects of the nourishment are prolonged, while the required volume of sediment, and frequency and duration of feeding are restrained (Sloff and Sieben, 2008). River engineers have keen interest in understanding and predicting how the nourished wave aspects like the order of the downstream migration rate, its dispersion rate, and the overall effects on the bed levels and texture of the mitigated reaches, depend on the characteristics of the feeding material. While the volume and geometry of the nourished sediment are, to the largest extent, constrained from the established allowances for navigable depth, its grain size characteristics prove to be key in optimizing the mitigation practice.

Despite the principle of nourishments closer to the bed grain size range, being to reduce the deficit of upstream sediment supply, the nourished sediment in most cases (e.g. downstream from Iffezheim and in Bovenrijn pilot study) is designed somewhat coarser than the sediment of the bed surface. The latter also means, that the nourished sediment is even coarser with respect to the sediment transported as bedload, which usually has a characteristic grain size smaller than the material of the bed surface.

There are several reasons why river managers design the so-called bedload nourishments with somewhat coarser material than the bed and bedload material. First, supposing that the sediment fed would correspond to the grain size of the bedload, it is to be expected that it would be quickly flushed downstream and its effects would be felt only for a short period at the degrading reach, rendering continuous feeding and hence relatively large volumes inevitable. Moreover, it is hypothesized that gradual coarsening of the bed would increase the shear stress needed by the flow for sediment transport (analogous to bed stabilization nourishments) arresting bed degradation faster, with decreased volumes of nourished sediment (Sloff and Sieben, 2008). Additionally, it is possible that the (long-term) bed coarsening may lead to a reduction of the transverse bed slopes, and thus of the dredging requirements for navigation purposes (Mosselman et al., 2004).

A compromise between sufficient mobility of nourished sediment and coarsening of the degrading riverbed is the main objective of nourishments applied currently in practice. It is common that the nourished sediment is characterized by a wide grain size distribution. The sorting range of the supplied mixture is designed such that it corresponds to the natural grain size range of river bed (Gölz et al., 2006), while the nourished sediment becomes overall relatively coarser by means of

under-representation of the finer river bed fractions (Sieben, 2017). The finer fractions are expected to migrate faster downstream reducing the sediment deficit of long degrading reaches (e.g northern Upper Rhine Graben) whereas the coarser to adjust the bed texture and prolong the effects of sediment nourishments.

1.2 Scope of the present study

During the past decades, as the supply of artificial sediment becomes an increasingly attractive mitigation practice for river bed degradation, there has been an increasing effort in optimizing the behaviour of the non-uniform nourished sediment. Numerous field studies have been performed at various rivers (e.g. the Rhine, the Danube, the Elbe) but also in some cases at multiple reaches along the same river (e.g. field experiments at Iffezheim, Mittelrhein and Niederrhein by BfG and at Bovenrijn by RWS). In most of these studies multi-fractional tracer sediment is employed, and monitored at various time instances after its feeding into the reaches. The field experiments aim mostly at providing site-specific information concerning the fate of nourished sediment at reaches with certain hydraulic conditions and valuable data for the calibration of mathematical models, with the use of which following nourishing campaigns are designed. Nevertheless, not only field but also laboratory experiments have been employed in some cases to provide more understanding about the evolution of nourished sediment pulses. The latter concern, to their larger extent, nourishments at mountainous rivers aimed jointly at counteracting bed degradation and ecological restoration and focus more on the qualitative aspects of the pulse evolution compared to field studies.

However, we still lack understanding about the morphodynamic processes governing the behaviour of nourished sediment, the effects on the bed level and texture of the mitigated reaches, the interactions of its various fractions and finally the feedback with hydrodynamics. In the present study we aim at providing more insight on the intrinsic aspects of sediment nourishments focusing on the dominant morphodynamic processes.

The **objectives** of the present research, are to provide insight on the characteristics of the temporal changes linked with the behaviour of mixed-size sediment fed in lowland rivers as well as to assess the main physical mechanisms dominating this.

The research **questions** formulated are as follows.

a. What characterizes the downstream migration of mixed-size nourished sediment fed in lowland rivers?

b. What is the trajectory of mixed-size nourished sediment fed in meandering reaches?

c. What characterizes the vertical mixing of mixed-size nourished sediment at lowland rivers?

d. Which are the main physical mechanisms that control the observed behaviour?

e. Which are the effects of sediment nourishments on textural changes in the studied reaches?

In order to answer the research questions a combination of literature survey and data analysis are performed. The **methodology** is as follows. First, we analyse data from two field experiments in the Rhine (Iffezheim and Bovenrijn). Then we focus on the main physical mechanisms that can provide explanations concerning the main findings of our data analysis. To this end we employ simple hand-calculations, conduct further literature survey and provide physical argumentation.

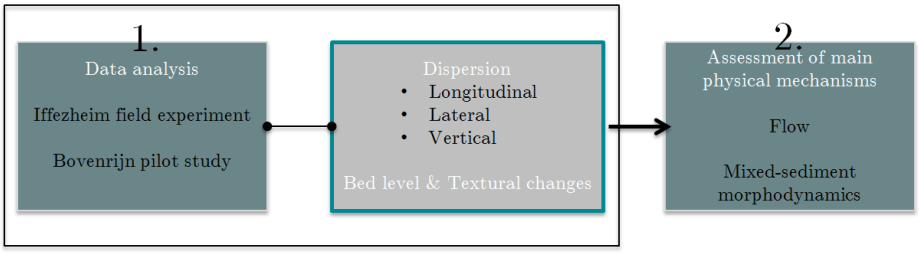

Figure 1.8: Followed methodology in steps.

chapter

TWO

IFFEZHEIM FIELD EXPERIMENT

2.1 Introduction

A long monitored field experiment was conducted in the German Rhine below Iffezheim weir to study the evolution of the sediment that was fed downstream from the barrage since 1978. In October 1996, tracer sediment was fed across the whole width of an approximately 1 km river stretch forming a layer with thickness of approximately 20 cm. It was monitored for a period of 5 years until 2001.

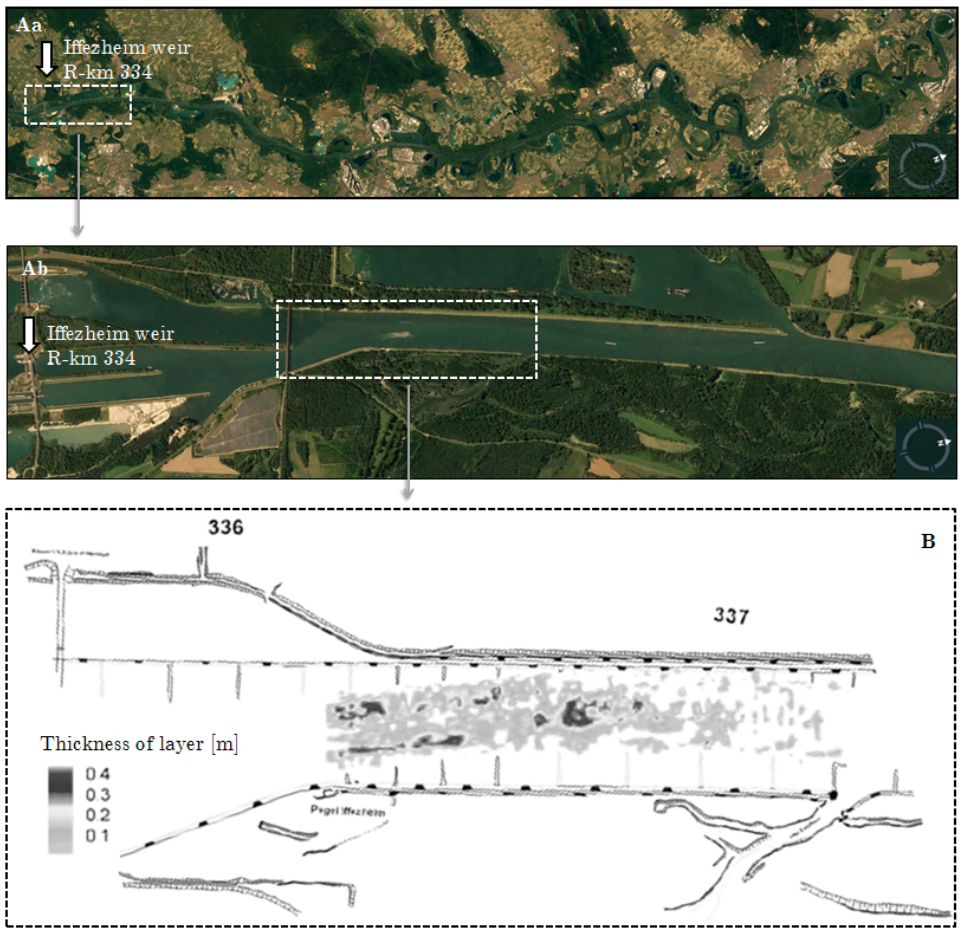

Figure 2.1: In all panels flow is from left to right. **Panel Aa** A screen-shot of the study reach as taken from Google Earth. At the very right-hand side of the map Mannheim is located at Rhine-km 425. **Panel Ab** A screen-shot of the study reach as taken from Google Earth, zoomed at the straight feeding stretch below Iffezheim weir (Rhine-km 334). **Panel B** Bed level surveys by WSA revealing the thickness of the nourished sediment (source: Gölz et al. (2006))

2.1.1 Characteristics of the study reach

In the following, we define our study reach from the longitudinal extent of tracer material during the monitoring period. The Rhine stretch under consideration starts at Iffezheim (Rkm-334) and extends to Speyer (Rkm-404). The study area is characterized by the presence of the weir located at the upstream end which acts as a barrage of sediment load to downstream reaches. In response to lack of sediment supply from upstream due to the presence of dams (Frings et al., 2014b), and the Tula regularization works in the 20^{th} century (Droge et al., 1992), the bed at the study reach has been degrading at high rates in the past.

Nevertheless, during the tracer experiment the bed level changes were characterized by modest alternating erosion and sedimentation (Fig.2.3.A). The decreased degradational rates compared to the past, followed to a certain extent from the large amounts of artificial sediment that has been continuously fed below the barrage since 1978. During the monitoring period of the field experiment (1996-2001), approximately 1 million m^3 was fed at the same stretch as in the tracer experiment. This continuous feeding exceeds by 3 orders of magnitude the amount of tracer sediment (e.g. Fig.2.2) and was distributed as much as possible uniformly with time (Kuhl, 1993).

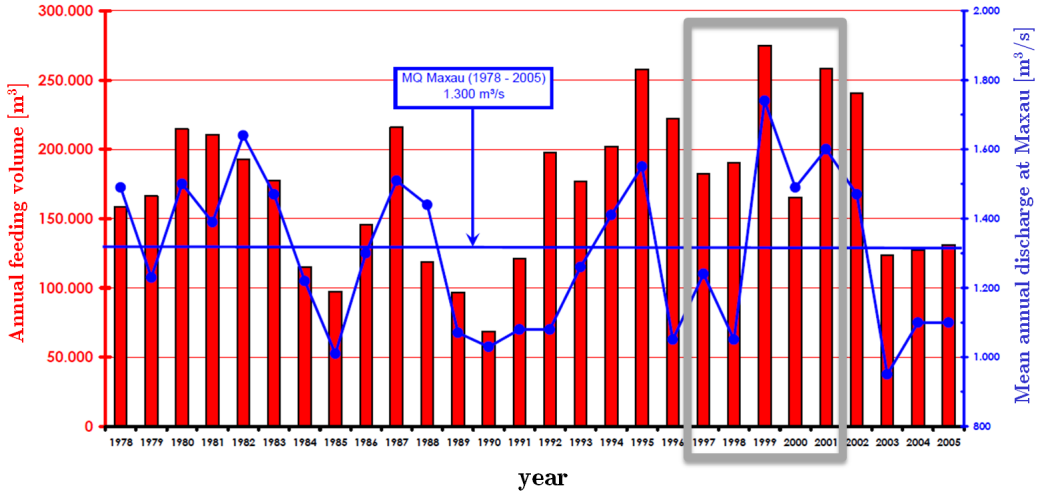

Figure 2.2: Feeding volumes below Iffezheim from the start of nourishments at Iffezheim (1978) up to 2005 plotted with the mean yearly discharge at Maxau gauging station. Approximately 1 million m^3 of sediment had been fed during the monitoring period 1997-2001 denoted by the grey box(source of figure: Gölz et al. (2006)).

Furthermore, the shear stress exerted by the flow on the bed remains more or less constant for the larger part of the reach before reducing further downstream (Fig.2.3.B). A downstream fining pattern is present for the grain size of the bed surface and subsurface sediment yet it is milder for the first half of the study reach and intensifies further downstream. This pattern depicted in Fig.2.5 holds also for the caliber of the bed-load material (Frings et al., 2014b).

The longitudinal patterns in the grain size of the bed material and bedload but also the transport rates of the latter are explained by the increase of river width with downstream distance (ca. 50% increase from Rhine-km 350 to 425) (see Fig.2.5,D). The slope at the study reach is approximately 3.810^{-4} and decreases slightly downstream (Fig.2.5,C). The gradual decrease of longitudinal slope and increase of width follow from the base level control at Mainz Basin, exerted by the uplifting of the Upper Rhine Graben tectonic unit (Frings et al., 2014b).

The planform geometry of the reach is characterized by the presence of transverse groynes alternating at its banks, while the sinuosity generally increases with downstream distance where large bends are present. Further, the gravel addition together with the construction of groynes have reduced the transverse slopes and increased the bed levels at the deep parts of the cross sections as indicated by the comparison of bed surveys between 1976 and 1992 (Kuhl, 1993). This is the case especially at cross sections located closer to the Iffezheim weir.

The mean discharge at Maxau gauging station which is located at the study area (Rkm-362), is 1310 m^3/s while the mean high discharge is 3390 m^3/s for the period 1965 to 1999. Within the monitoring period, in 1999, a flood wave that lasted during spring and summer, was associated with

a 1/100 years discharge of around 4300 m^3/s as can be seen in Fig.2.7. Finally, gravel dunes were reported by WSA from echo sounding surveys at discharge rates of 3000 to 3500 m^3/s (Fig.2.4). These dunes have a height of a few decimetres and length of around 20 to 50 meters.

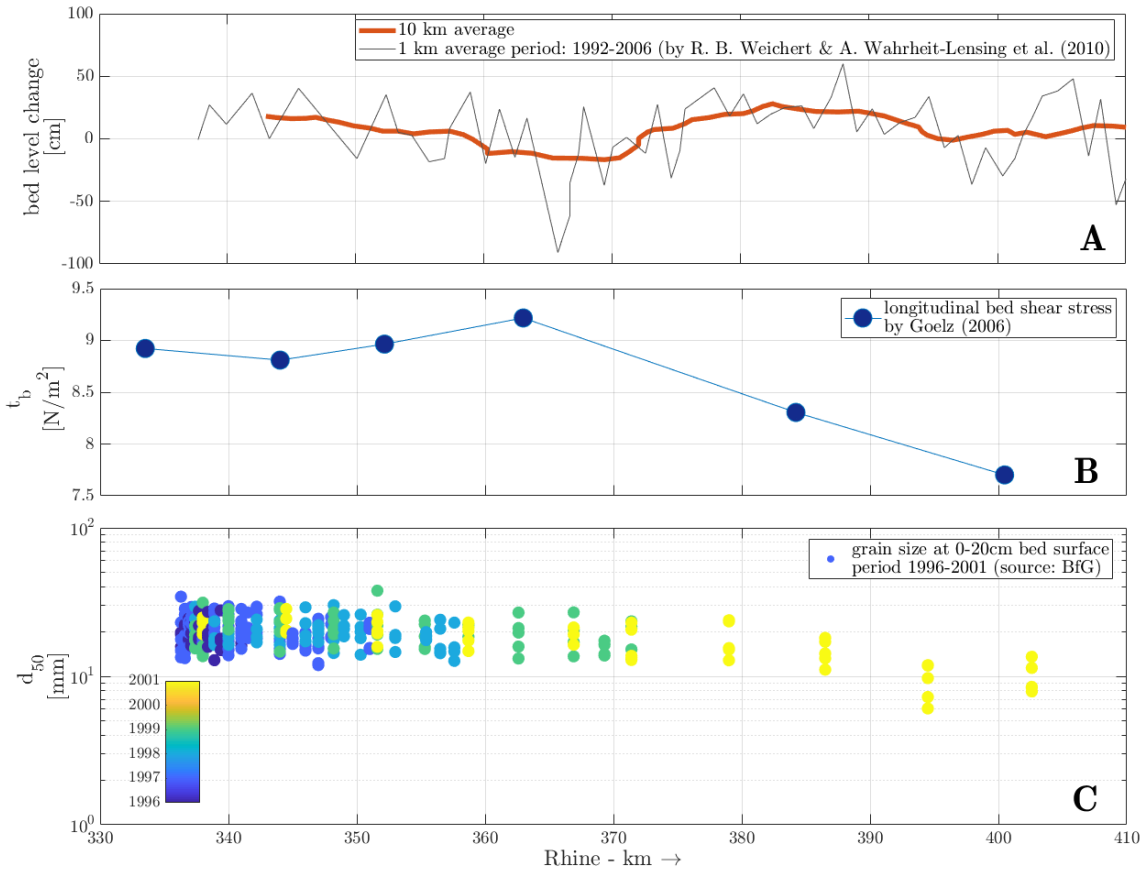

Figure 2.3: **Fig.A** - Bed level changes at the study reach for the period 1992-2006. **Fig.B** - Bed shear stress at the study reach. **Fig.C** - d_{50} characteristic grain size of the bed surface at the study reach, for the period 1996-2001.

Figure 2.4: Gravel dune at the study reach photographed inside the diving bell of Carl Straat vessel (image courtesy: WSA, BfG).

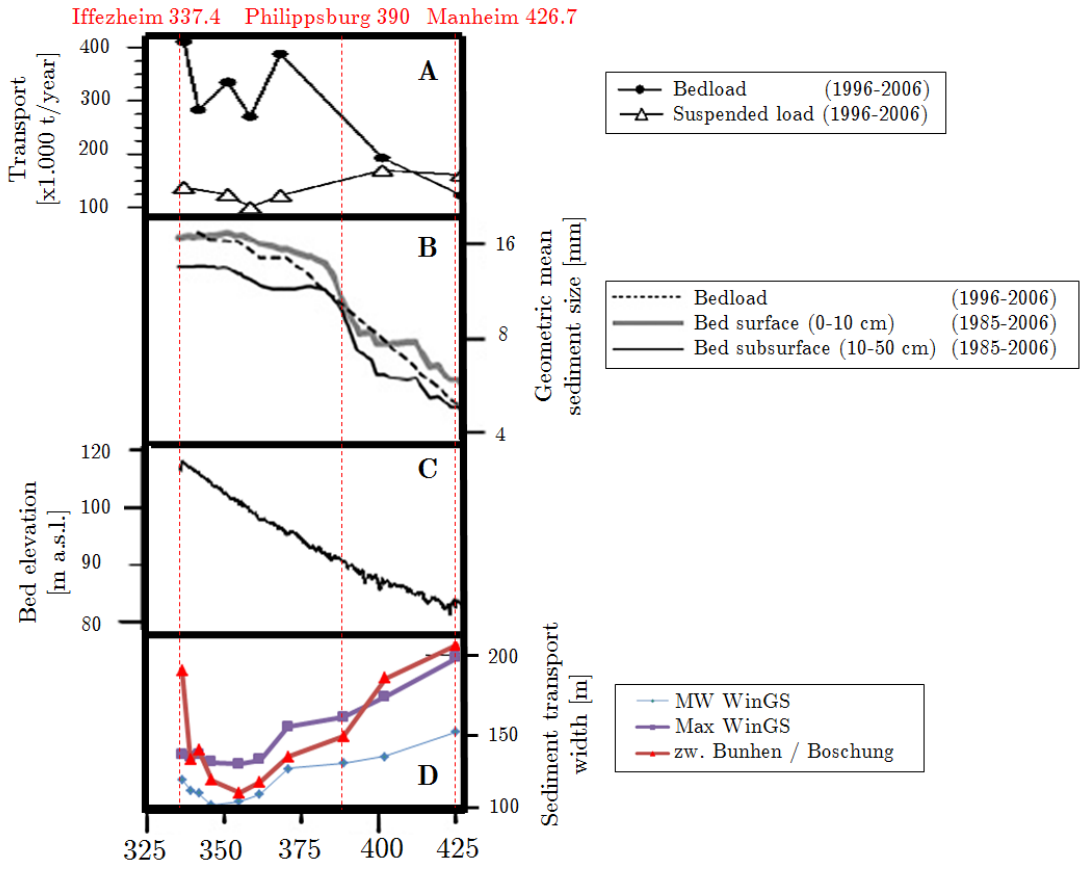

Figure 2.5: Key morphodynamic aspects at the study reach (330-425 Rhine-km). **Panel A**: Bedload and suspended load measurements at the study reach. **Panel B**: Geometric mean size of bed-load (1996-2006), and bed (sub)surface material (1985-2006). **Panel C**: Longitudinal profile of the river bed. **Panel D**: Sediment transport width. source: Frings et al. (2014b)

2.1.2 Supplied sediment characteristics

There were several different mixtures supplied below Iffezheim from 1978 to 1991 as can be seen in Fig.2.6. Sand, as well as the finer gravel fractions were not included in most cases. The specifications of feeding material were also determined by the availability of sediment at the gravel market. Since 1991, relatively finer sediment is nourished which additionally includes a sand fraction, and corresponds to a large extent to the composition of the bed material thereon (Gölz et al., 2006).

The field study was aimed to assess how sediment fed below Iffezheim behaved. Thus, the mixture supplied was characterized by multiple grain size fractions with specifications similar to those continuously fed since 1991. The sediment that was fed at the grain size range of 4-63 mm was granite and served as tracer. It was broken at a quarry and characterized by angular grains which together with its unique color, allowed for its visual detection at the soil samples. The very fine gravel fraction of 2-4 mm was excluded from the mixture since it would not be possible to differentiate it from the original bed sediment of the same range. Nevertheless, the sand fraction supplied since 1991, was included in the mixture even though it would not act as tracer, to act as lubricant by reducing the possibly increased effect of grain interlocking stemming from the enhanced angularity of granite compared to the sediment previously fed.

A total mass of 28.000 tons of tracer sediment was fed. During the feeding of tracer sediment no other nourishments were performed below Iffezheim. Most of the tracer sediment ($\backsim$ 35%) consisted of a coarse gravel fraction (16-31.5 mm) whereas the median grain size of the bed surface at the time of feeding was around 20 mm (Fig.2.3). Table 2.1 summarizes the volumes of each fraction that were supplied.

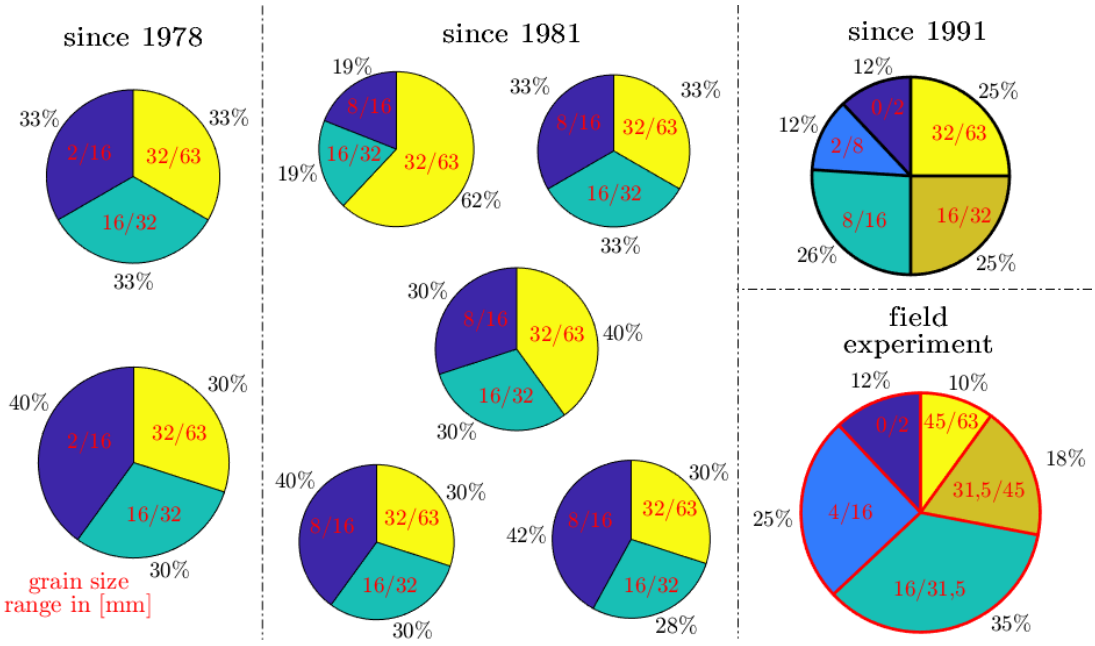

Figure 2.6: The mixtures supplied below Iffezheim since 1978 and the sediment mixture supplied in the field experiment. (source of data: Gölz et al. (2006))

Table 2.1: Specifications of sediment added downstream from Iffezheim after Gölz et al. (2006).

Fraction [mm]	Mass [ton]	Tracer	percentage %
0-2	-	No	12
4-16	7947	Yes	25
16-31.5	11128	Yes	35
31.5-45	5731	Yes	18
45-63	3192	Yes	10

2.1.3 Temporal and spatial resolution of monitoring

Six monitoring campaigns were conducted in total, with decreasing frequency in time. The temporal density of the monitoring campaigns is demonstrated in Fig.2.7 with the discharge measured at Maxau gauging station.

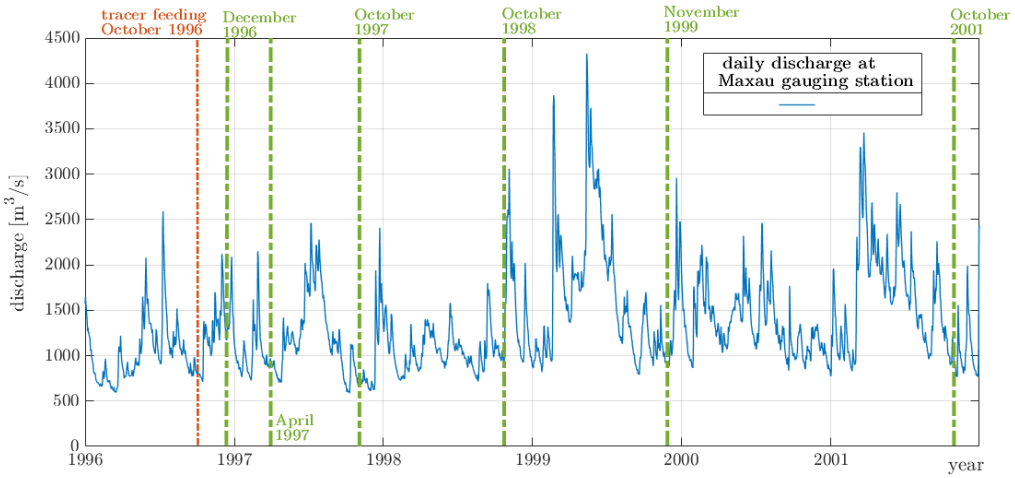

Figure 2.7: Discharge series at Maxau gauging station, next to Iffezheim dam plotted against the dates of tracer feeding and monitoring.

During these campaigns the Carl Straat vessel (see Gölz et al. (2006)) equipped with a diving bell was used and sediment samples were taken directly from the river bed after it was visually inspected. Soil samples were taken from 9 to 13 streamwise cross-sections per monitoring campaign. Since the tracer sediment migrated downstream with time, the longitudinal extent of the reach monitored increased with time and the streamwise spatial resolution decreased accordingly.

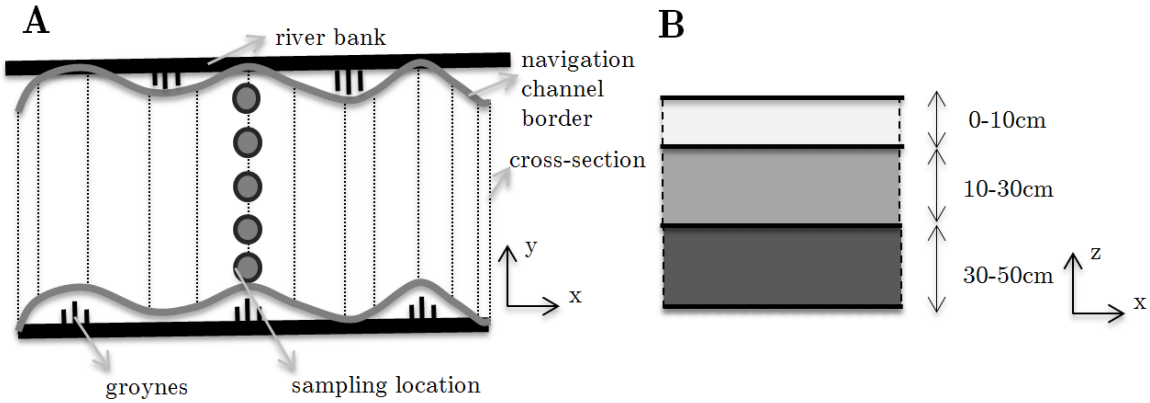

Figure 2.8: Schematic for the sampling resolution during Iffezheim field experiment. x denotes streamwise, y lateral and z vertical direction respectively.

For the vast majority of the cross sections, 5 transverse locations were sampled, more or less spread at equal space intervals within the navigation channel i.e., between the tips of opposite groynes.

Sieving analysis was conducted for three vertical layers per sampling location. These are the top 10 cm (0-0.1 m), and two layers of 20 cm below (0.1-0.3 m and 0.3-0.5 m). Nevertheless, only for the two top layers (0-30 cm) information is available for all monitoring campaigns and transverse locations. Soil samples from the deepest layer (30-50 cm) were taken only from one location per cross-section, starting from the third monitoring campaign. Finally, during the last two monitoring campaigns soils samples were taken from the groyne fields but also liquid nitrogen was used to extract freeze cores from a layer of approximately 1.5 meters.

2.1.4 Tracer recovery

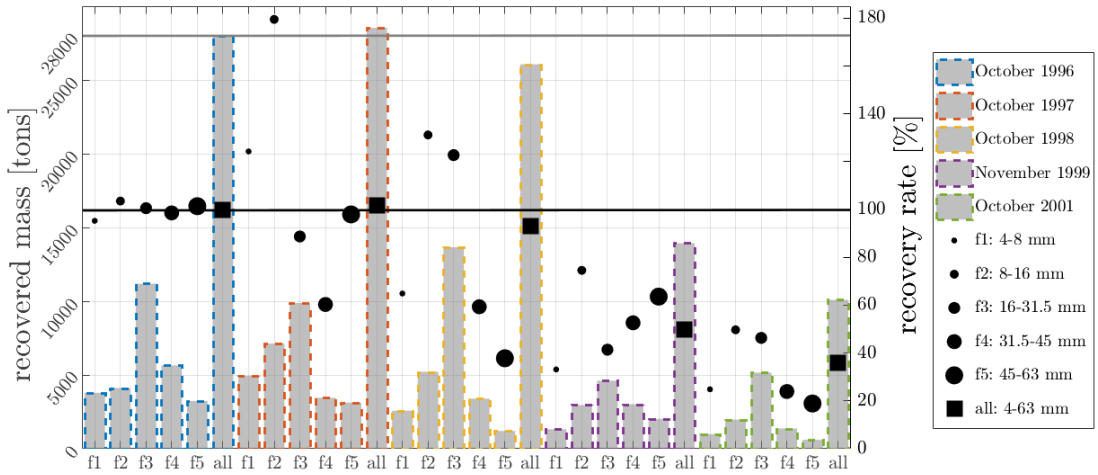

Figure 2.9: Tracer recovered mass (left y axis) and recovered rate (right y axis) for total (all) and respective size fractions (f1,f2,f3,f4,f5) (x-axis) plotted per monitoring campaign (with different color). Unrealistic recovery rates larger than 100% can be seen for certain fractions. These are explained by the limitations of the mass balance approach. Plotted data are retrieved from Gölz et al. (2006).

According to a mass balance for the top 50 cm performed by Gölz et al. (2006), it was revealed that the total tracer recovery was close to 100% for the first four monitoring campaigns, while it was below 50% for the two last campaigns. In Fig.2.9 it can also be seen that there were no specific tracer fractions that demonstrated systematically larger or lower recovery rates.

Analyses of the freeze cores during the last two campaigns reveal that part of the tracer sediment moved to deeper strata (found at depths up to 1.5 m) after the 1/100 years flood in 1999. Furthermore, samples collected from the groyne fields reveal that a part of tracer sediment had deposited there. Finally, due to the angular shape of the granite fed, it is hypothesized that a part of tracer was lost in abrasion processes (Gölz et al., 2006).

2.2 Data Analysis

2.2.1 Temporal changes of tracer concentration in streamwise direction

For the analysis of the longitudinal changes of the tracer sediment first the concentration of the total tracer sediment was assessed and then the concentration per size fraction. The objective of the present analysis is to assess and quantify the downstream migration of tracer sediment both concerning its bulk volume (`Total Tracer Concentration`) and the respective tracer fractions (`Fractional Tracer Concentration`).

2.2.1.1 Total tracer concentration

For the present analysis the concentration of tracer sediment was computed at each streamwise location reported, as the laterally and depth averaged concentration of tracer sediment in the soil samples. The simple mathematical equation that describes the `Total Tracer Concentration` ($T[\%]$) is:

$$T(i)[\%] = \frac{\text{Mass of tracer sediment at cross section i}}{\text{Mass of soil samples at cross section i}} * 100 \tag{2.1}$$

In Fig.2.10 the `Total Tracer Concentration` is given for the six monitoring campaigns with frozen x-axis. It can be seen that the temporal evolution of the tracer sediment is characterized by spreading and consequent reduction of local tracer concentrations (by two orders of magnitude from the beginning to the end of the monitoring campaign). The spreading is expressed by a downstream migrating front whereas the trail of the signal remains very close to the point of origin demonstrating very limited downstream migration. Nevertheless, the initial symmetry over the vertical axis is not heavily affected with time. Moreover, for the last monitoring campaign, it can be seen that two signals have formed one leading the other. Nevertheless, the total tracer concentration at the cross sections where the leading wave is located, is by an order of magnitude smaller.

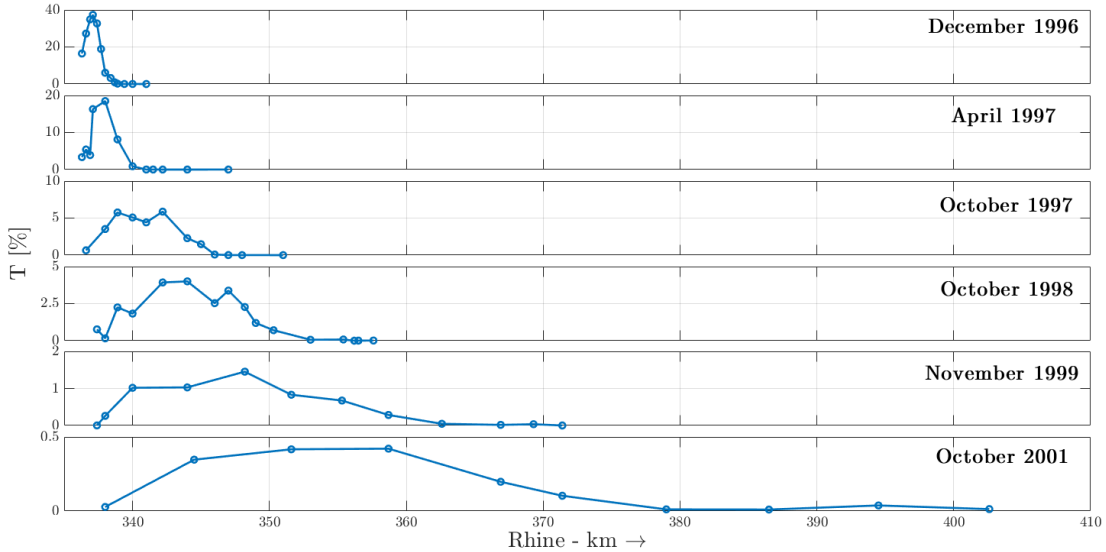

Figure 2.10: Temporal change of total tracer concentration $T[\%]$ in longitudinal direction.

Four parameters are employed here in order to quantify the temporal evolution of the tracer sediment. In Fig.2.11 the temporal evolution of the streamwise location of the **front**, the **99% front**, the **mean**, and the **max** T is given. The location of the front was extracted for each campaign by locating the most downstream cross-section were non-zero T was found. Similarly, the location of the max corresponds to the streamwise location where T attains its maximum value. While the first two parameters are inherently defined on the spatial (streamwise) sampling grid, for the determination of the mean and the 99% front parameters, the signals were linearly interpolated on a constructed grid using a space interval of 10 meters. Following consistency considerations the interpolation at the upstream and downstream ends of the signals, continues up to the last cross-section (marching upstream and downstream respectively) where a non-zero concentration is measured.

The mean locations, are determined by finding the minimum difference of T integrals, starting from the most upstream (I_u) and most downstream (I_d) sampled cross-section respectively. Thus the mean parameter essentially expresses the median of the concentration signals.

$$Rkm_{mean} = Rkm(|I_{\mathrm{u}}(x) - I_{\mathrm{d}}(x)| = min) \tag{2.2}$$

where,

Rkm_{mean} is the Rhine kilometre of the mean parameter

I_u is the T integral as a function of downstream distance starting from the most upstream sampling cross section

I_d is the T integral as a function of upstream distance starting from the most downstream sampling cross section

Furthermore, the locations of the 99% front parameter are determined by locating on the 10-meter constructed grid, the streamwise location of the I_u that satisfies the condition described below;

$$Rkm_{\ 99\%\ \mathrm{front}} = Rkm(I_{\mathrm{u}}(x) = 0.99 * I_{\mathrm{u}}(x_{\mathrm{max}})) \tag{2.3}$$

where,

x_{max} is the most downstream cross section where a non-zero concentration is measured.

The latter parameter is defined in addition to the front parameter, in order to indicate the position of the leading edge of the wave with respect to the bulk volume of the tracer sediment. It can be expected from the interpolation method that the streamwise location of the 99% front parameter is going to be located somewhat upstream from the location of the front parameter. Their difference indicates the degree that the latter serves as a good indication considering the migration of tracer sediment as a wave, while we retain full information on the longitudinal extent of the tracer sediment.

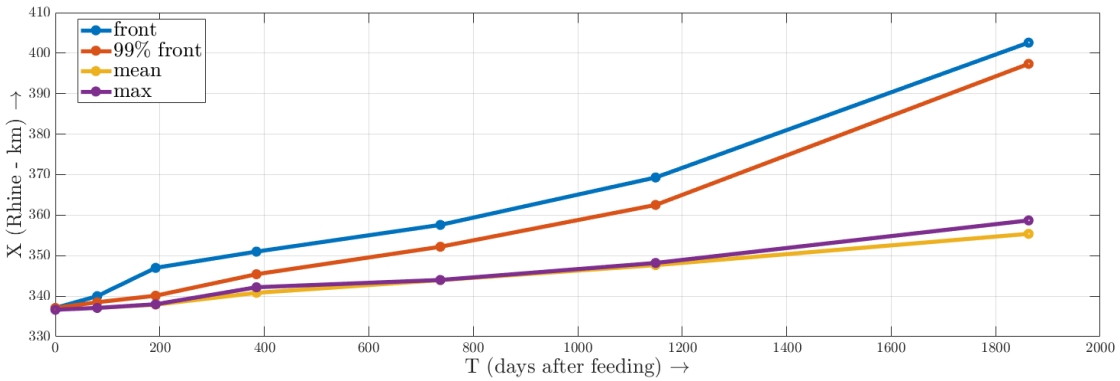

Figure 2.11: X-T diagram for the front, 99% front, max, and mean T parameters. Average celerities are as follows; $C_{front} = 13km/y$,$C_{99\%,front} = 9.3km/y$, $C_{mean} = 3.4km/y$, $C_{max} = 4km/y$

The mapping of the temporal evolution of the considered parameters is given in Fig.2.11. The locations of max and mean T lie very close for all monitoring campaigns, while the front and 99% front migrate downstream approximately 3.5 and 2.5 times faster respectively. Furthermore, the

migration celerity of the mean and the max T (slope of the line) remains nearly constant, while larger variations are identified when the front and 99% front are considered.

2.2.1.2 Fractional tracer concentration

In order to study how the tracer concentration changes in longitudinal direction depend on the grain size characteristics of supplied sediment, the five fractions are treated independently using the same analysis as in the previous section. Similarly, the `Fractional Tracer Concentration` ($F[\%]$) is now defined at each sampling cross section, as the laterally and vertically averaged value of:

$$F(i)[\%] = \frac{\text{Mass of tracer sediment of fraction f at cross section i}}{\text{Mass of soil samples at cross section i}} * 100 \tag{2.4}$$

In Fig.2.12 instead of F the `Normalized Fractional Tracer Concentration` (F_N) is plotted for the six monitoring campaigns. The F_N is extracted by dividing the F at each and every cross-section by the max F of all cross sections per monitoring campaign.

$$F_N(i)[-] = \frac{F(i)}{max(F)} \tag{2.5}$$

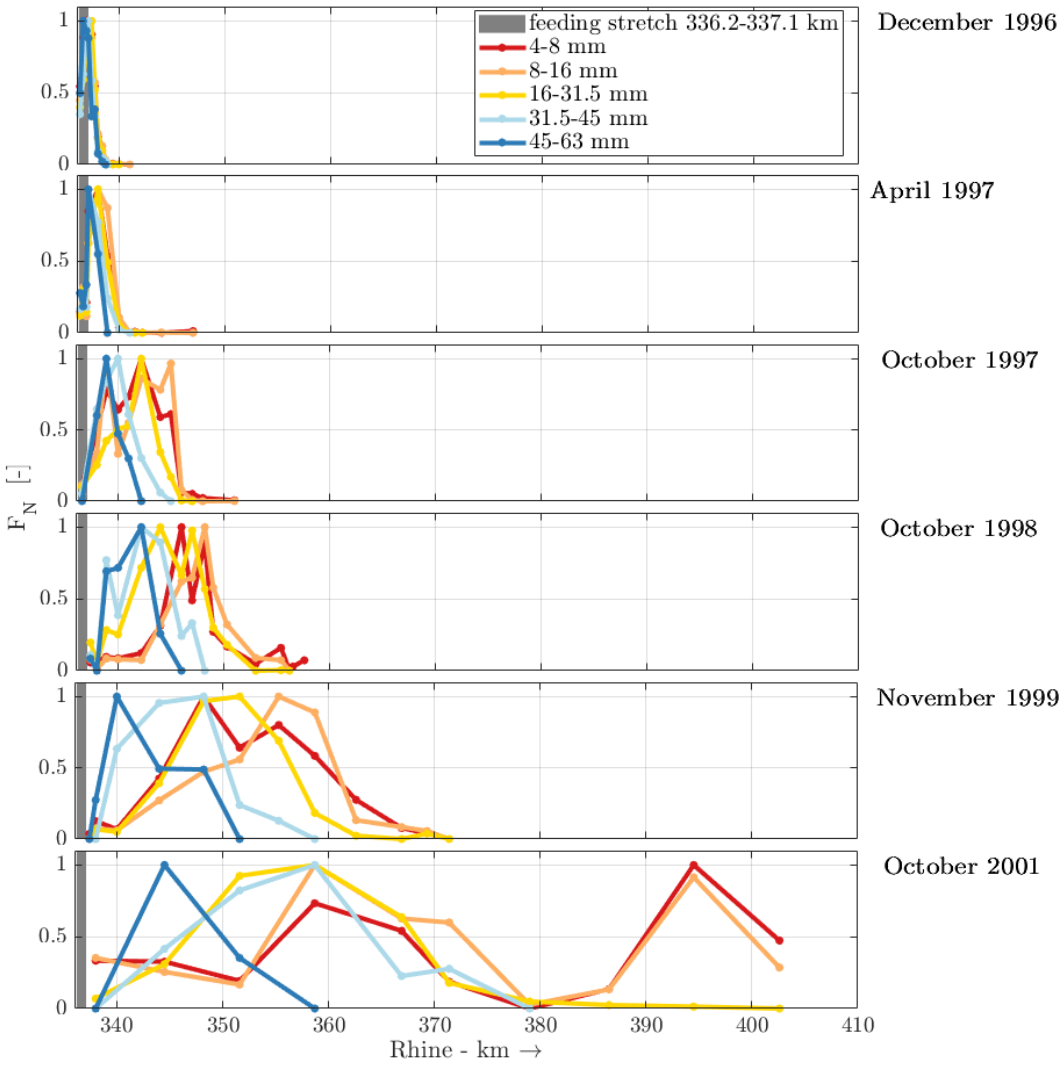

Figure 2.12: Normalized fractional tracer concentration F_N per monitoring campaign. The grey area denotes the feeding stretch.

The values of $max(F)$ are given per monitoring campaign and per size fraction in Table 2.2. Plots of the non-normalized F can be found in the Appendix.

Table 2.2: Maximum F[%] values per monitoring campaign, against which Fig.2.12 was normalized.

campaign	$4-8mm$	$8-16mm$	$16-31.5mm$	$31.5-45mm$	$45-63mm$
December 1996	0.8	4	21.9	8	5.5
April 1997	0.4	1.7	11	4.2	3.8
October 1997	0.1	0.6	4.7	1.6	1.7
October 1998	0.2	0.6	2.7	0.9	1
November 1999	0.03	0.2	0.6	0.4	0.7
October 2001	0.01	0.02	0.2	0.2	0.2

Fig.2.12 demonstrates how all fractions spread longitudinally with time. Nevertheless, this spreading varies strongly between different fractions; the finer fractions generally lead the coarsest and spread more starting from the first monitoring campaign. All fractions though, both spread and migrate downstream with their trails having exited the feeding stretch by the 4th campaign. The two finest fractions demonstrate very similar signals at all campaigns, while this also holds for the two coarsest fractions until October 1998.

Furthermore, only at the last monitoring campaign the two finest fractions are split in two parts, forming separate signals of nearly equal $max(F)$. One wave is located at the (upstream) stretch with the three relatively coarsest tracer fractions and one is leading at the front. Finally, looking at data presented in Table 2.2, the $max(F)$ is generally smaller for the finest fractions that have spread more, while it is the largest for the middle fraction that had the largest share in the initially fed mixture.

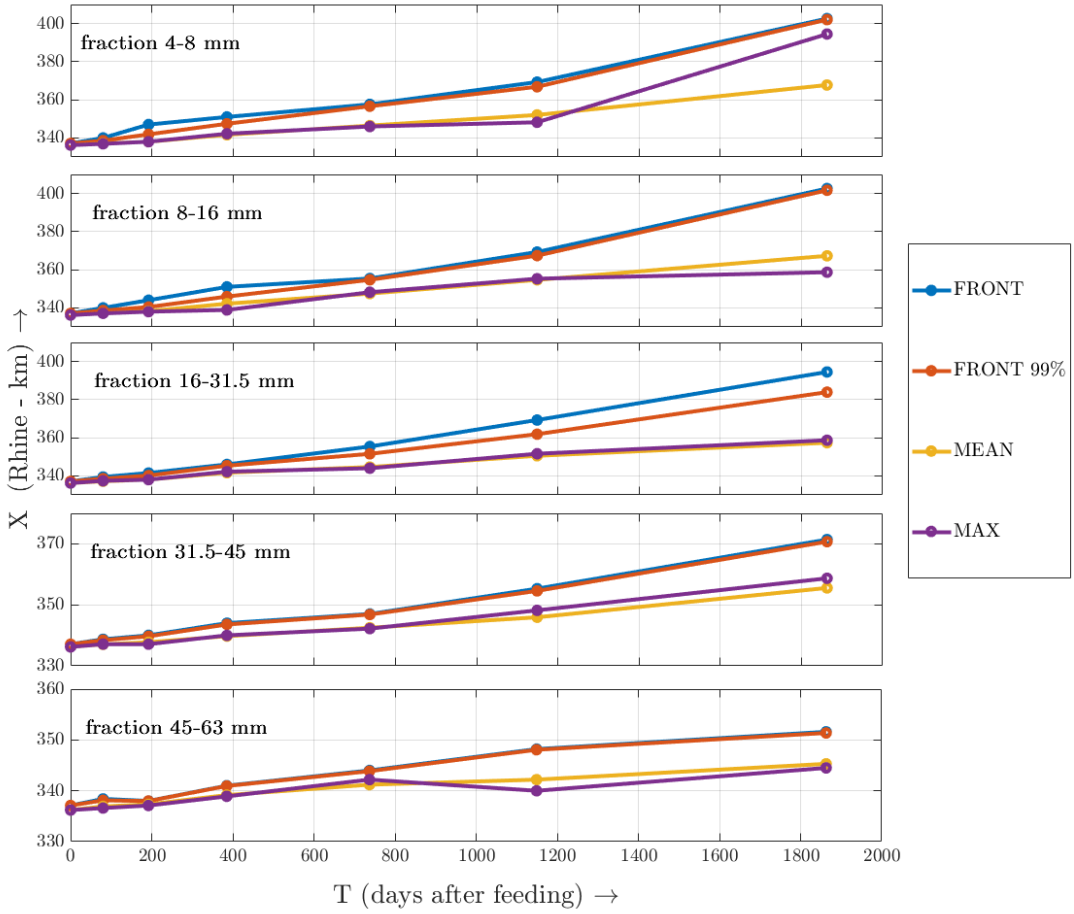

Figure 2.13: X-T diagram of the front, 99% front, mean, and max F parameters.

As in the previous section the locations of the max, mean, front and 99% front F parameters are presented for the six monitoring campaigns. The results in Fig.2.13 demonstrate more or less the same qualitative aspects as the ones already discussed for the T case; the front and 99% front parameters, show increasing spatial deviation from the mean and max. The two latter in most cases follow each other, with significant exception found for the finest tracer fraction (4-8 mm), following from the positioning of its $max(F)$ at the leading (split) signal at the last monitoring campaign.

By comparing visually the deviation of the front and the mean parameters between the various tracer fractions, it can not be clearly stated how the spreading compares between the tracer fractions. To this end, Table 2.3 gives the average celerities per size fraction and a quantitative comparison between the front and 99% front average celerities with the average celerity of the mean.

Table 2.3: Average celerities and quantitative comparison of the the characteristic celerities per size fraction.

parameter	4/63mm	4/8mm	8/16mm	16/31.5mm	31.5/45mm	45/63mm
C_{front} **[m/s]**	13	13	12.2	10.1	6.3	3.1
$C_{99\%,front}$**[m/s]**	9.3	10.8	10.2	8.1	6	3
C_{mean}**[m/s]**	3.4	5.3	5.6	4.3	3.4	2.1
C_{max}**[m/s]**	4	7.4	4.4	4.6	3.8	1.8
$C_{front} \div C_{mean}$**[-]**	3.82	2.45	2.18	2.35	1.85	1.48
$C_{99\%,front} \div C_{mean}$**[-]**	2.74	2.04	1.82	1.88	1.76	1.43

Both quotients reveal that the spreading intensity increases with decreasing grain size of the tracer fraction. In other words, finer tracer fractions spread more. All the examined fractional quotients are smaller than the quotient produced in the previous analysis that was not accounting for separate size fractions. The signal of the bulk tracer volume spreads more than the fractional signals.

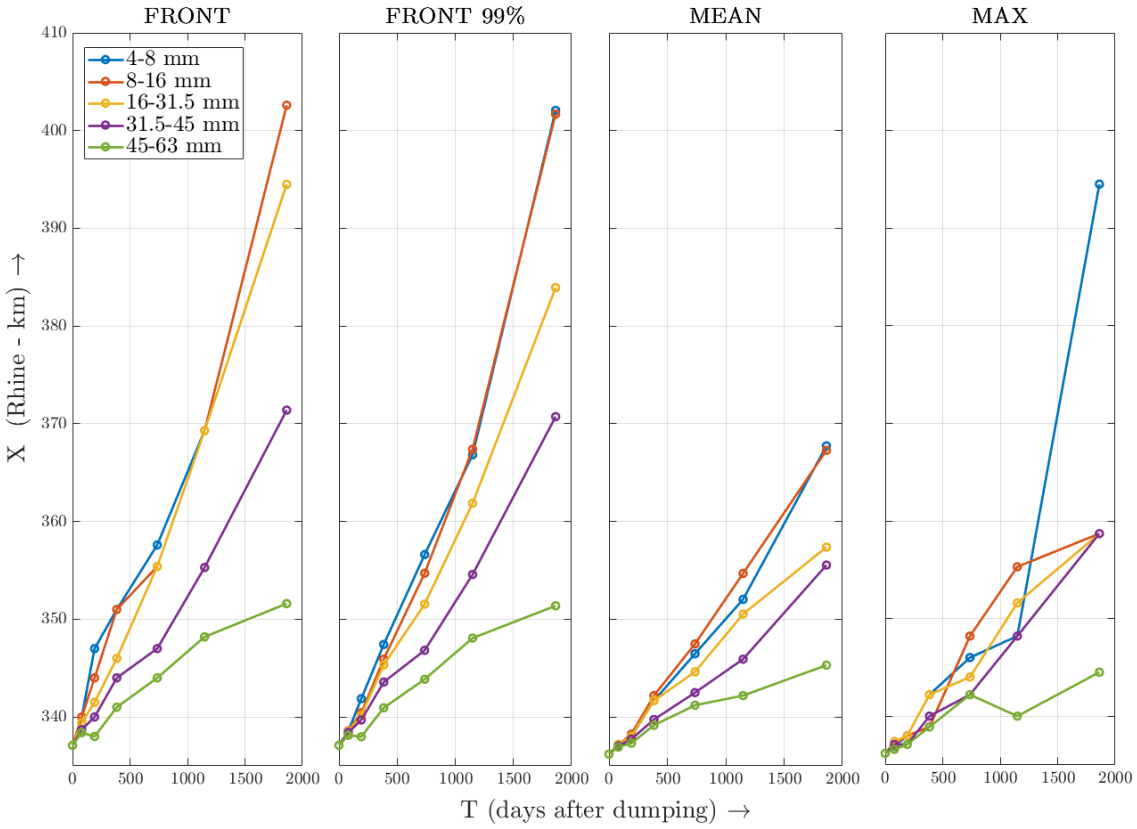

Figure 2.14: X-T diagram of the streamwise location of the front, 99% front, max, and mean F parameters.

In Fig.2.14 the same is plotted as in Fig.2.13 yet in the latter, results are presented for each studied parameter with frozen y and x axes. It can be seen that for all parameters in most cases the finest fractions lead. Nevertheless, it is revealed how the fronts of the two finest fractions follow each other very well. Further the location of the mean for the finest fraction, for all monitoring campaigns except for the last lags behind the respective location of the slightly coarsest fraction. It is also revealed for the last campaign that the location of the max for the finest fraction almost coincides with the location of its front i.e., the max concentration is found at the leading signal that was detected previously for both finest fractions.

2.2.2 Temporal changes of tracer concentration in lateral direction

2.2.2.1 Approach and methodology

The objective of the following analysis is to determine the trajectory of tracer sediment along the meanders of the study reach. We are also interested in possible differences between the trajectory followed by the various tracer fractions, as these might be linked with the longitudinal or even the vertical spreading of the latter. Therefore, as in the previous analysis, here we focus both on the lateral evolution of the `total` and the `fractional tracer concentration`. TL and FL express the same quantities that were defined previously and the only difference lies on the averaging process that is followed. Hereby, the respective total and fractional concentrations are not averaged both vertically and laterally and hence are not cross-sectional. Instead, these are determined at each transverse (sampling) location n per cross section i, by averaging only over the sampled vertical layers v.

The first stage of the present analysis concerned data preprocessing and geo-referencing and is presented in large detail in the Appendix. This allowed to later assess the temporal changes of tracer sediment in lateral direction, using three approaches. For the first two approaches we worked on a cross-sectional level. The first was to locate the position of the maximum tracer concentration per cross section. The second approach was to compare the average tracer concentrations closer to the inner and outer bends of the navigation channel per cross section. Both of the approaches in conjunction with the location of the measured cross-section along a meander provide a complete picture of the temporal changes of tracer concentration in the study reach. Finally, in order to assess if there are any differences between the trajectory followed by the various tracer fractions, we compared the average concentrations per monitoring campaign closer to the outer and inner bends for three merged fractions. Especially, for this last approach the sampling intensity of cross-sections per monitoring campaign far from bend crossings was additionally studied.

2.2.2.2 Total tracer concentration

Fig.2.15 demonstrates the TL for all monitoring campaigns. At first, tracer concentration varies longitudinally with lower concentrations found at downstream located measured cross-sections. As tracer sediment spreads downstream with time, the local tracer concentrations reduce by two orders of magnitude, when comparing the colorbar limits at the first and last campaign. These patterns were already observed in the analysis of the temporal changes of tracer concentration in longitudinal direction. From the present analysis we can observe that the tracer concentrations vary additionally in a cross-stream direction. Although samples corresponding to an individual cross-section demonstrate similar orders of magnitude of tracer concentrations, lateral variations can still be observed.

In order to additionally observe the lateral patterns at the cross sections where tracer concentrations are by orders of magnitude smaller a normalization against the $max(TL)$ of each cross section i is performed. The mathematical expression for this normalization method is

$$TL_N(n,i)[-] = \frac{TL(n,i)}{max(TL(n,i)) \text{ at respective cross section i}} \tag{2.6}$$

In that way, the position of the max tracer concentration can be straightforwardly detected at each cross-section, while information is still kept for the lateral structure of tracer sediment. Fig.2.16 demonstrates the results after this normalization procedure. The results presented in this figure are more interesting as we move earlier in time when a single meander is more densely sampled at a streamwise direction (e.g. monitoring campaign of December 1996).

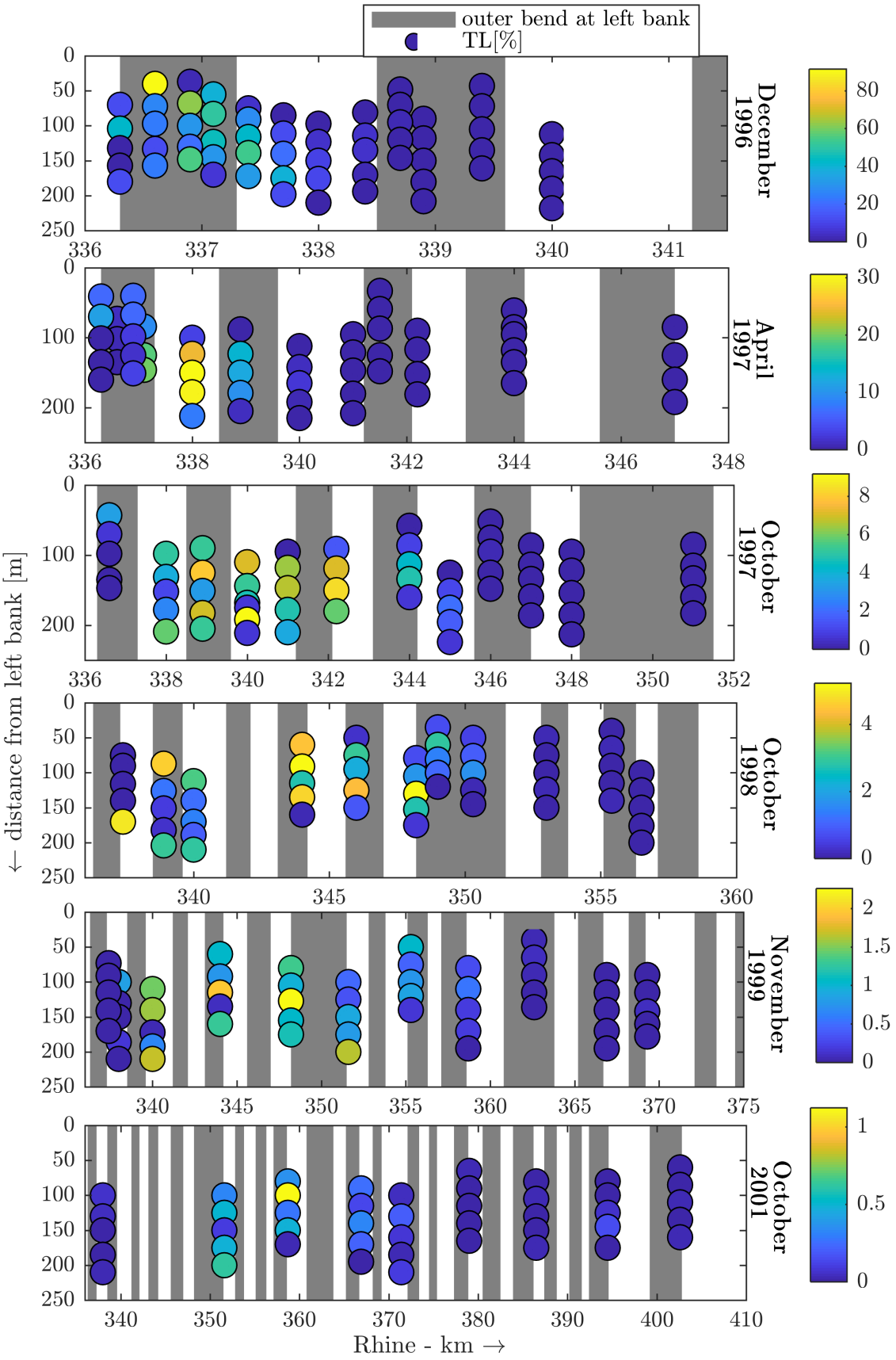

Figure 2.15: TL at transverse locations along each cross section. The cross sections removed in the data preprocessing are kept in this figure.

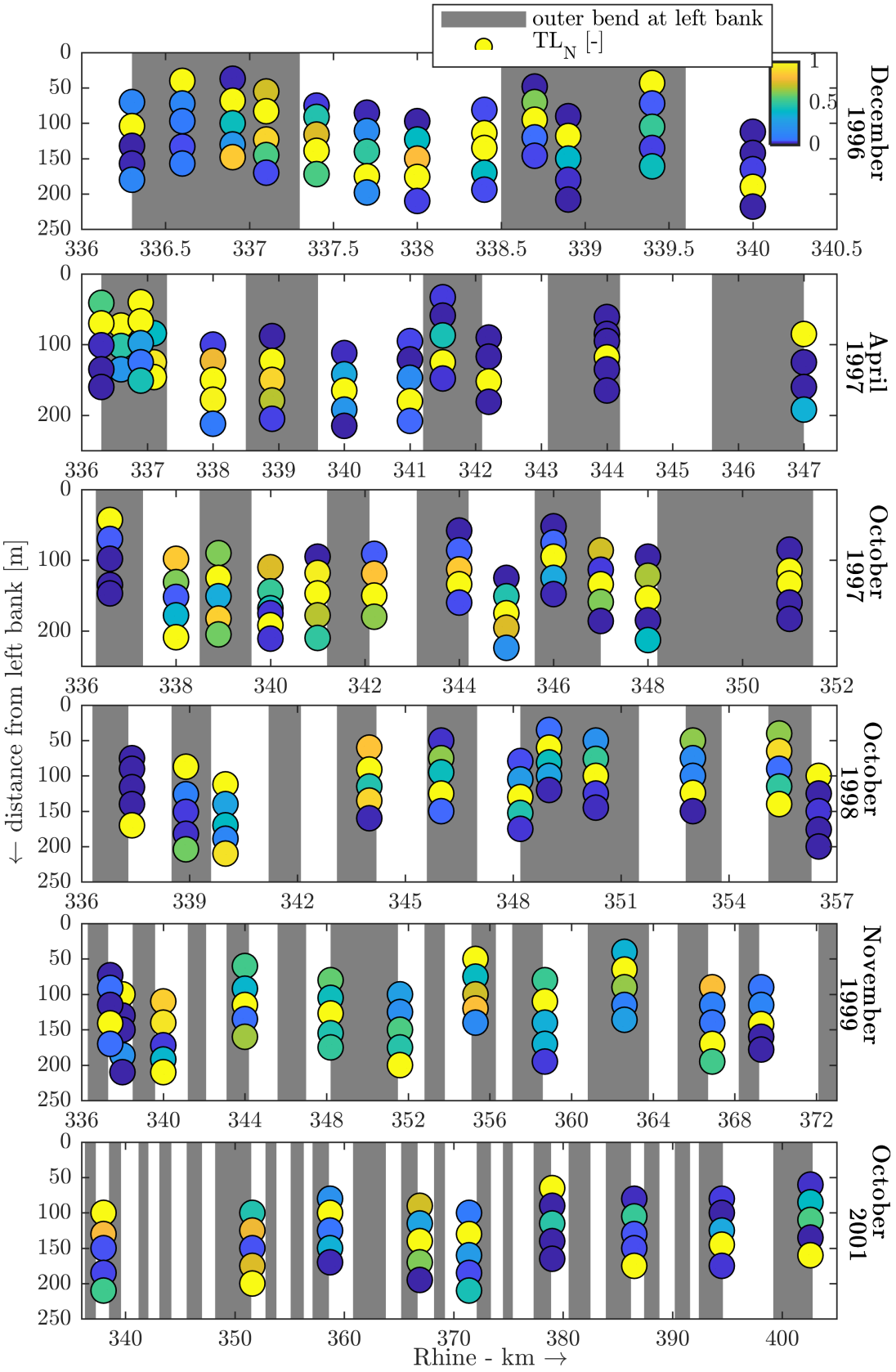

Figure 2.16: TL_N at transverse locations along each cross section. Yellow dots correspond straightforwardly to the transverse location of the max tracer concentration per cross section. The cross sections removed in the data preprocessing are not demonstrated here.

For this first monitoring campaign the location of the maximum concentration per cross-section clearly changes from one outer bend to the next. Closer to bend crossings the maximum concentration is often found closer to the axis of the navigation channel. At later campaigns the $\max(TL_N)$ lies more frequently closer to the axis of the navigation channel (the middle sampled location). However, at later campaigns the cross-sectional sampling intensity decreases far from the extracted bend crossings as we will see later.

To further explore the lateral distribution of tracer sediment along the river meanders we now compare the mean concentrations between the samples closer to the outer and inner bends rather than looking at the location of the maximum concentration at each cross-section. The qualitative aspects we are investigating with respect to the tracer sediment migration remain the same as in the previous approach. To perform this comparison, the tracer concentrations were first averaged depending on the number of samples per cross section according to the simple procedure demonstrated in Table 2.4.

Table 2.4: Averaging process for the extraction of left and right half average tracer concentrations. The numerical subscripts denote the lateral location of the individual samples with respect to the inner and outer bend of the meander. $n = 1$ denotes the location closest to inner bend.

sampled n locations per cross section i	average concentration closer to the inner bend [%]	average concentration closer to the outer bend [%]
4	$(TL_N(1,i) + TL_N(2,i))/2$	$(TL_N(3,i) + TL_N(4,i))/2$
5	$(TL_N(1,i) + TL_N(2,i))/2$	$(TL_N(4,i) + TL_N(5,i))/2$
6	$(TL_N(1,i) + TL_N(2,i) + TL_N(3,i))/3$	$(TL_N(4,i) + TL_N(5,i) + TL_N(6,i))/3$

It is worth to notice that the averaging process treats the normalized tracer concentrations. This is done for representation purposes, and since both the normalization and the comparison are performed on a cross-sectional level the procedure is not introducing any artefacts in our analysis. In Fig.2.17 the results of this comparison can be seen. The flag dots are used for representation purposes and denote whether the tracer concentration is larger closer to the outer bend (green) or not (red). Through the present approach more samples at each cross-section are involved compared to the previous approach.

The results indicate that not only the maximum tracer concentration is located closer to the outer bends as was seen before, but also the mean tracer concentration at the half of the navigation channel closer to the outer bends exceeds the respective concentration of the other half closer to the inner bends of the studied cross sections. As the flag dots indicate this is not always the case, especially at cross-sections sampled that are situated closer to bend crossings. Again the most interesting survey is the one from December 1996 when the evolution of tracer sediment along three meanders was densely sampled.

Finally, for the last campaign of October 2001 we can see the largest share of red dots amongst the cross-sections monitored compared to the other campaigns. This implies that the average concentrations closer to the inner bends exceed in most cross-sections the averaged concentrations closer to the outer bends. This can be explained first by the fact that the sampling intensity closer to bend crossings was increased for this monitoring campaign as it will be shown later, but also from the fact that the local tracer concentrations are less by at least two order of magnitudes compared to earlier monitoring campaigns. The latter means that for such small local concentrations the present approach may be not as valid. This holds to a certain extent for the campaign of November 1999.

It is already mentioned that the most interesting survey with respect to the present approach is the one of December 1996, two months after feeding, when the longitudinal spreading of the tracer sediment amounted to a few kilometres and the cross-sections monitored were concentrated on 3 meanders at the upstream end of our study reach. Fig.2.18 gathers the results of the two approaches followed and additionally plots the maximum TL_N on the map. Regarding this additional subplot where the extents of transverse groynes can clearly be seen, the maximum concentrations per cross-section are always found closer to the outer banks close to half extent of the meanders and closer to the axis of the navigation channel close to bend crossings.

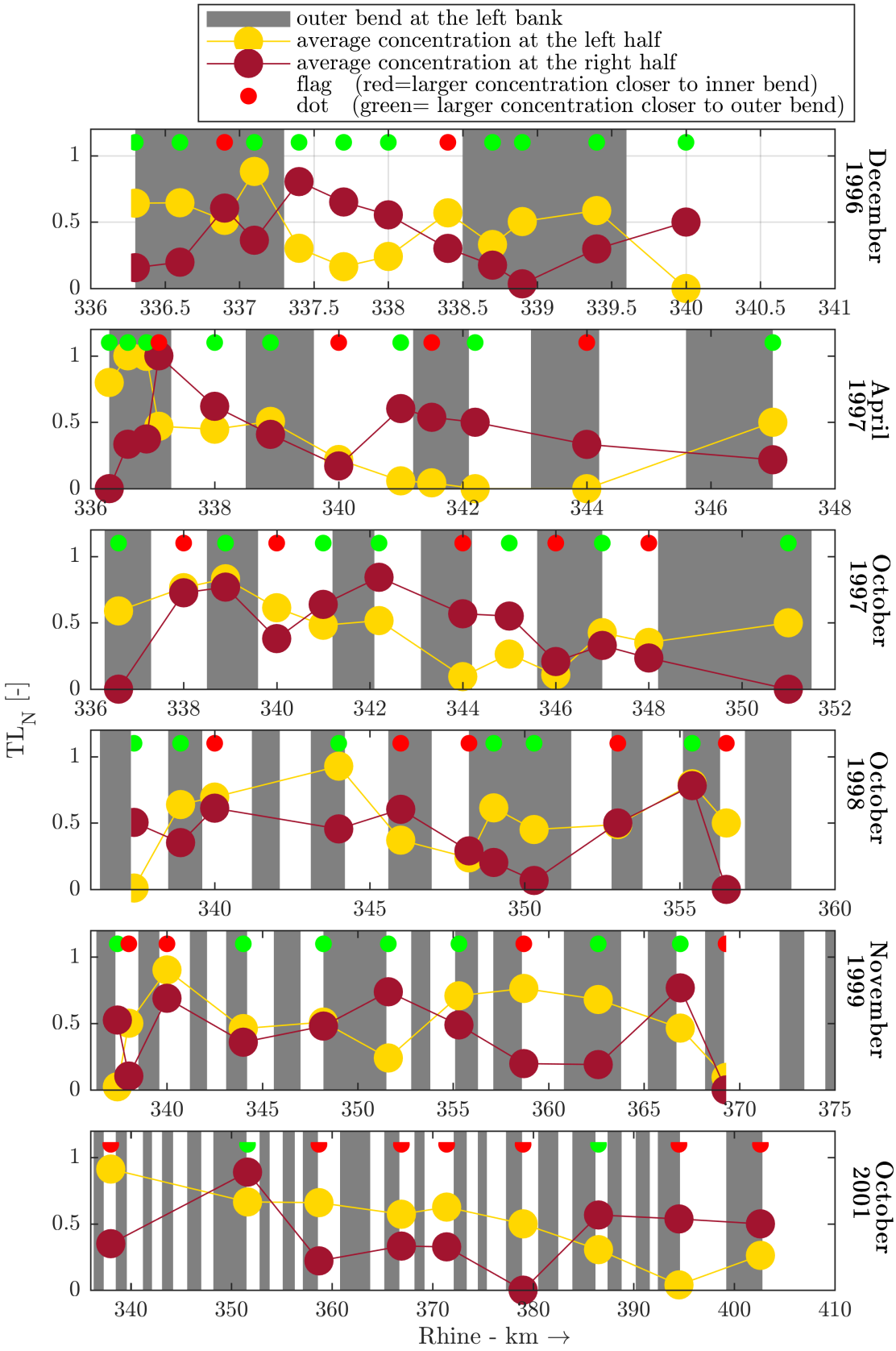

Figure 2.17: Averaged TL_N at each respective half of the navigation channel. When the concentration is larger at the outer bend (e.g. average concentration at left half larger than average concentration at right half and outer bend at the left half) a green dot is used as a flag. Conversely a red dot is used as a flag at the top of each subplot.

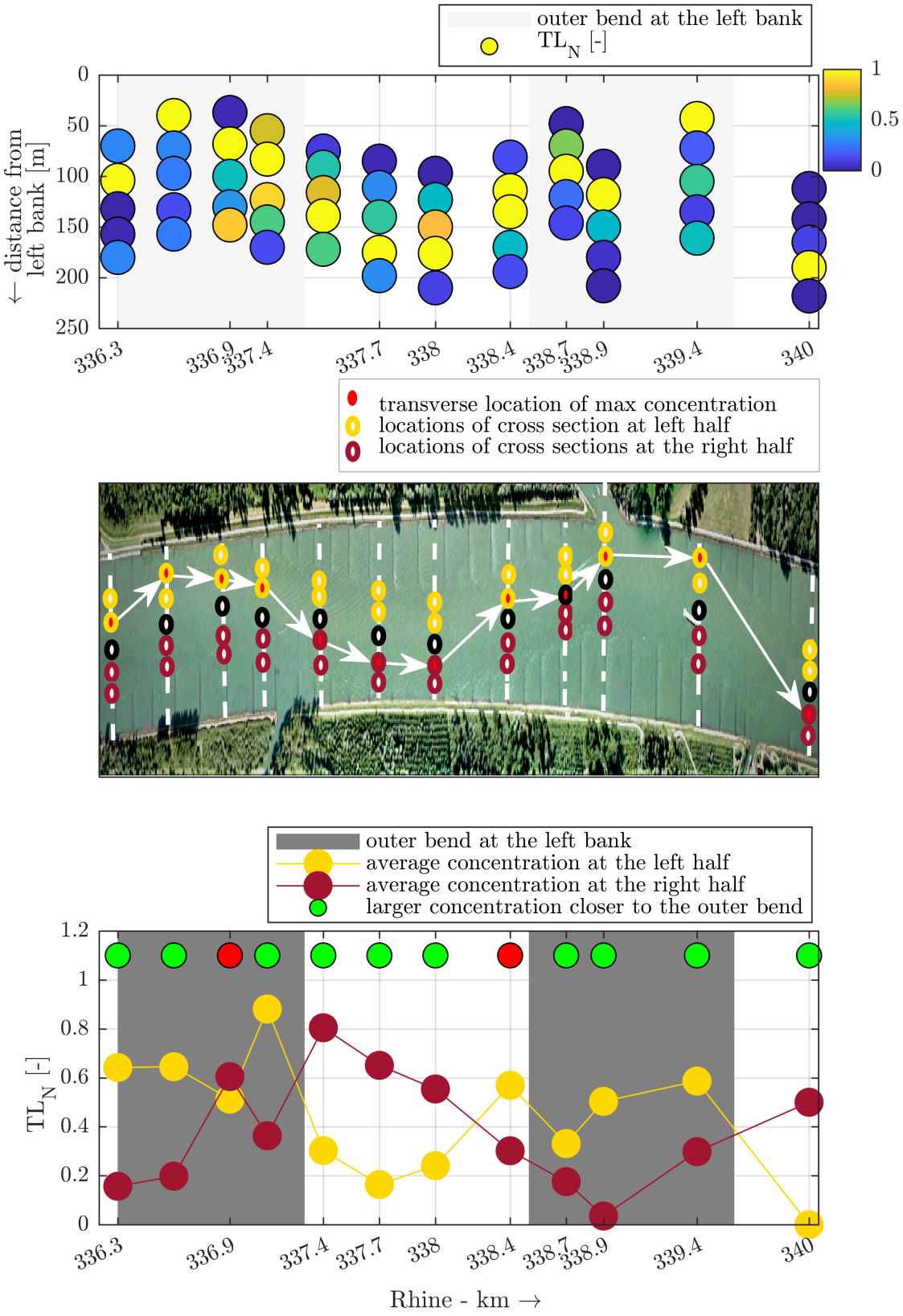

Figure 2.18: Trajectory of the max TL_N and comparison between the average normalized concentrations of the left and right half for December 1996.

2.2.2.3 Fractional tracer concentration

It is interesting to assess whether the pattern demonstrated in the `total tracer concentration` analysis holds for the various fractions of tracer sediment. To this end, the same analysis is repeated now for the FL. Before performing the analysis on a fractional level, the two coarsest and the two finest fractions were merged (essentially each treated as one fraction) such that sufficient and well weighted longitudinal and transverse coverage would be provided for all different fractions studied. The results per size fraction can be found in the Appendix. A meticulous study of these figures per size fraction, reveals that the patterns discussed for the bulk tracer sediment hold more or less for each tracer fraction.

Nevertheless, to demonstrate this finding at this stage of the document in a more elegant way, two mean values of FL are determined per monitoring campaign, which are later compared for each fraction. These averages are taken as;

- $\overline{FL(n = inner)}$ per campaign from all transverse locations n closer to inner bends
- $\overline{FL(n = outer)}$ per campaign from all transverse locations n closer to outer bends

In Fig.2.19 per monitoring campaign (x axis-subplots) and per (merged) size fraction (y axis-subplots) the two mean values of FL are compared. The last two monitoring campaigns are also shown but their background color differs. This is due to the fact that during these campaigns cross-sections measured closer to bend crossing locations. This issue is explored in more detail later. Finally a relative difference parameter is used to assist the interpretation of the compared values. The relative difference parameter is defined as

$$R.D.[-] = \frac{|\ \overline{FL(n = inner)} - \overline{FL(n = outer)}\ |}{\overline{FL}} \tag{2.7}$$

Where,
$\overline{FL}$ is the mean FL per monitoring campaign.

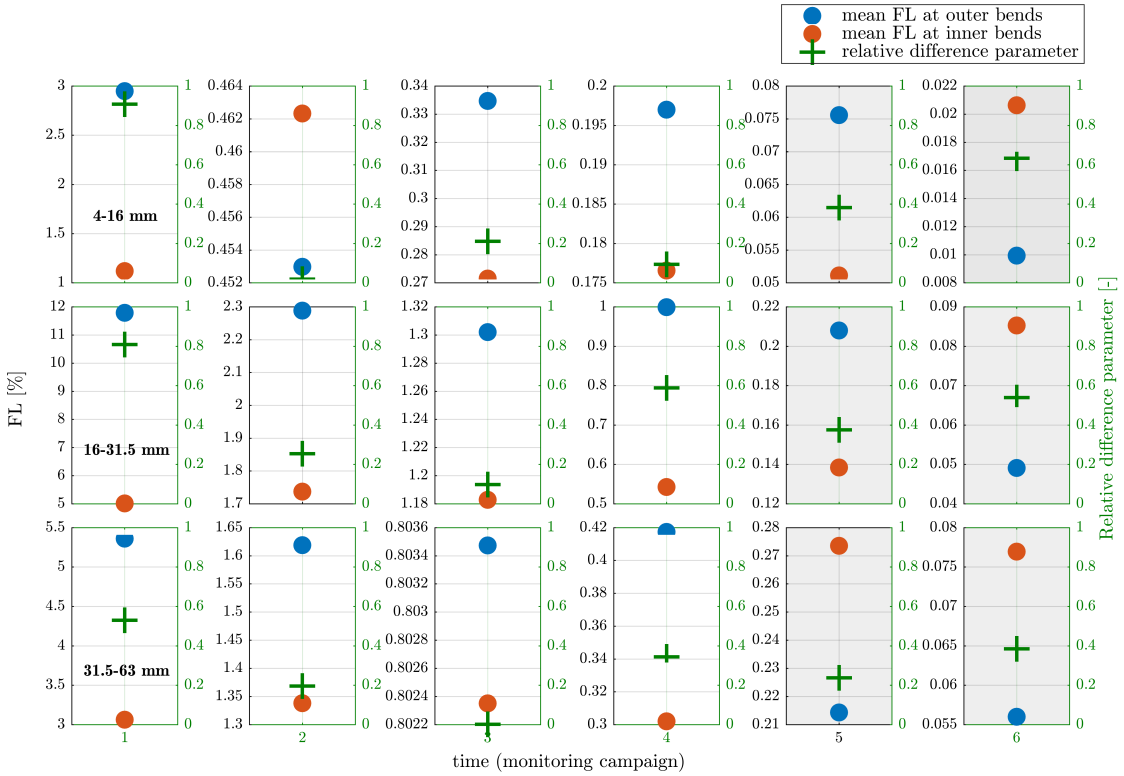

Figure 2.19: Comparison of $\overline{FL(n = inner)}$ (red) and $\overline{FL(n = outer)}$ (blue) for each merged fraction (y axis subplots) and per monitoring campaign (x axis subplots). When blue dots lie above red dots the fractional tracer concentrations are larger closer to the outer bends.

Fig.2.19 indicates that the average FL at the outer bends (blue dots) is larger than the average concentration at the inner bends (red dots) irrespective from which fraction is under consideration. This agrees with the results of the TL analysis. Only for the finest fraction (4-16 mm), this is not the case for the second monitoring campaign. Nevertheless, the two concentrations examined lie very close to each other as also indicated by the $R.D.$ parameter.

2.2.2.4 Determination of the sampling intensity far from bend crossings

Since the measured cross-sections differ between various campaigns, it is expected that there may be also significant differences with respect to the sampling intensity far from bend crossings. In other words, some campaigns may have been significantly more or less focused on locations where lateral sorting patterns are expected to be stronger. Such systematic differences limit the ability to compare explicitly results between various campaigns, or even the relevance of some campaigns for part of the analyses demonstrated above. The latter is especially the case for the last approach followed (see Fig.2.19).

It can be expected that closer to bend crossings, the cross sectional shape may deviate significantly from the bar and pool topography that yields larger depths towards the outer bends and lower depths towards the inner bends as well as that these are locations where lateral sorting patterns (which are considered here) are less strong. Gölz et al. (2006) note that the sampling during the last two monitoring campaigns was focused more at the locations of bend crossings. This is no surprise if we consider the temporal decrease in longitudinal sampling resolution (given that almost the same number of cross sections was sampled per monitoring campaign) following from the downstream spreading of the tracer sediment and hence the demand of increasing longitudinal coverage.

To address this issue an assessment of the sampling intensity of each monitoring campaign far from bend crossing is performed. To this end, each cross-section per monitoring campaign is studied for its respective location along the meanders based on whether the following condition is satisfied;

$$|Rkm(i) - Rkm_{\mathrm{N,s}}(i)| \geqslant X_p * \frac{L_{\mathrm{B,U}}(i) + L_{\mathrm{B,D}}(i)}{2} \tag{2.8}$$

Where,

Rkm [km] is the chainage location of the examined cross section i

$Rkm_{\mathrm{N,s}}$ [km] is the chainage location of the nearest crossing s to the examined cross-section i

X_p [-] is a distance parameter that expresses the percentage of the streamwise bend extent within the bend crossing influence

$L_{\mathrm{B,U}}, L_{\mathrm{B,D}}$ [km] are the lengths of the nearest upstream and downstream bends to the examined cross section i

When the above condition is satisfied for an examined cross section it means that it is situated far from the crossing at a minimum distance expressed by the right hand side. Note that for the study reach the mean meander length varies in the range 1 to 1.5 km for the six monitoring campaigns. Fig.2.20 demonstrates sampling intensity far from bend crossings by plotting the percentage of cross sections per monitoring campaign that satisfied relation 2.8. Note that various values for the distance parameter X_p are checked.

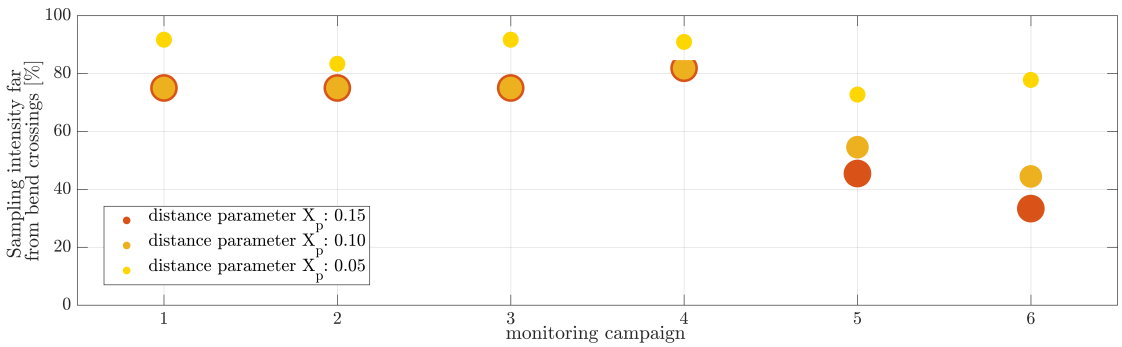

Figure 2.20: Sampling intensity far from bend crossings per monitoring campaign.

It is clear that for the first four monitoring campaigns (x-axis) the sampling intensity far from crossings remains at percentages larger than 70% showing little sensitivity for changing X_p parameter. On the contrary, for the last two campaigns the sampling intensity lies at percentages even well below 50% as the X_p increases. This is the reason why for the latter, a comparison between the campaign-averaged values of FL closer to inner and outer bends was not considered relevant and the respective results in Fig.2.19 are given with greyed backgrounds.

2.2.3 Temporal changes of tracer concentration in vertical direction

2.2.3.1 Approach and methodology

The objective of the present analysis is to assess how various tracer sediments are mixed over the river bed as they migrate downstream. This is interesting because the degree of vertical mixing controls the exposure of grains to the flow and thus potentially affects the downstream migration of the studied tracer waves. Here we perform only an analysis on a fractional level to study possible differences in the vertical mixing of various tracer fractions.

Therefore, the FV is now determined by considering the two uppermost vertical layers (0-10cm and 10-30cm), for which the various lateral samples taken per cross-section are averaged out. The selection of vertical layers treated in this analysis is based on the sampling resolution of the monitoring campaigns. As explained previously, information on the deepest vertical layer (30-50 cm), is only available for specific monitoring campaigns, and for non-consistent sampled transverse locations. Therefore for the following, while we underline that tracer sediment was generally mixed over a larger depth, for consistency we are only going to treat the two layers in the uppermost 30 cm of the bed. Finally it is worth noticing that only for the first monitoring campaign, data for the lowermost studied layer (10-30 cm) are available at a certain extent of the reach (for all transverse locations). Therefore in determining FV and comparing between the two vertical layers, we consider only this stretch that nevertheless resolves the largest part of the bulk tracer volume (km 337-339).

At this point, it was critical that the procedure in determining the FV at each layer v, would be performed by weighting the tracer mass in the samples at a certain layer against the total mass of soil samples at the same layer. The FV per cross-section and for all five tracer fractions was determined as a function of depth using the following mathematical expression;

$$FV(\text{v,i})\ [\%] = \frac{\text{Mass of tracer sediment of fraction f at layer v}}{\text{Mass of soil sample at layer v}} * 100 \tag{2.9}$$

2.2.3.2 Results

Figures 2.21,2.22,2.23,2.24,2.25, illustrate the longitudinal distribution of concentrations at the top and bottom layers for each and every studied tracer fraction. It can be seen that finer fractions tend to have larger FV in the deeper layer than in the surface, whereas coarser fractions have larger FV in the surface than in the deeper layer.

To illustrate this pattern in a different way, a similar analysis is made as in the previous section that treated the campaign averaged FL concentrations. In Fig.2.26 these are compared between the top and bottom layer per monitoring campaign (x-axis subplots) and per grain size fraction (y-axis subplots). The tendency of larger vertical mixing for finer fractions is indicated by the fact that mean FV at the bottom layer (red dots) lie more often above the mean FV at the top layer (blue dots) as we study the figure bottom-up (moving from coarser to finer tracer fractions). This result is even more striking considering that the coarsest tracer fractions follow the finest and are closest to the upstream nourishment area where sediment was continuously fed after the placement of the tracer material. Additionally, from Fig.2.3.A it can be seen that along the stretch that all sediments reside at least during the first four monitoring campaigns (330-370 Rhine-km) aggradational conditions are more enhanced closer to Iffezheim barrage than further downstream.

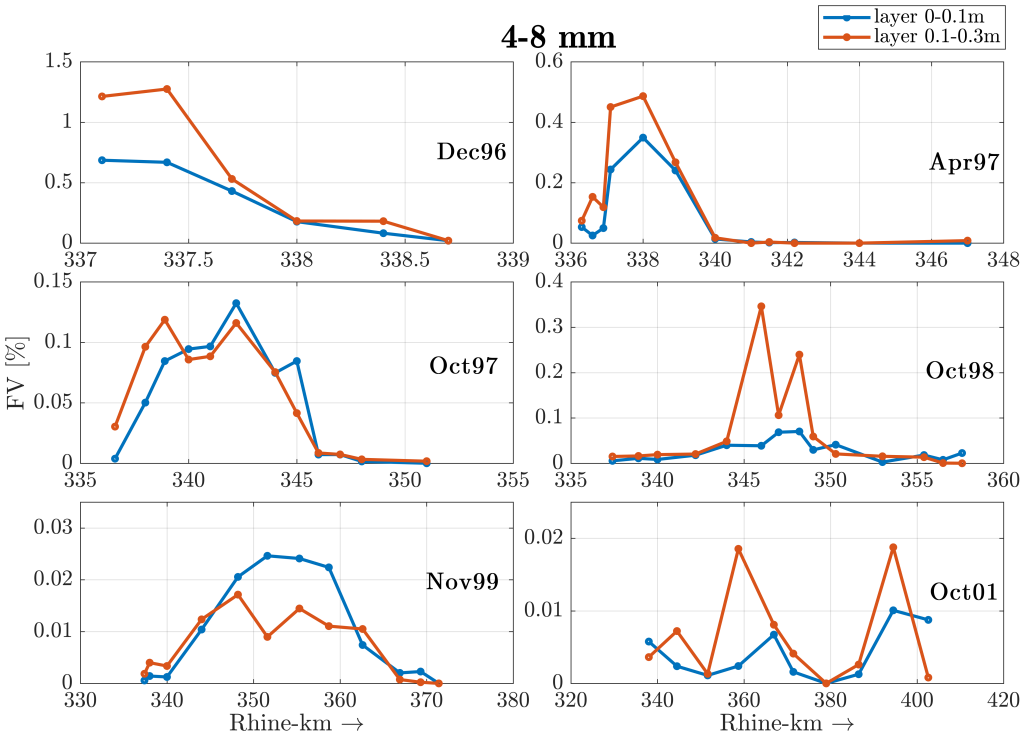

Figure 2.21: Comparison of FV at the layers 0-10cm (blue color) and 10-30cm (red color) for fraction 4-8 mm and per monitoring campaign.

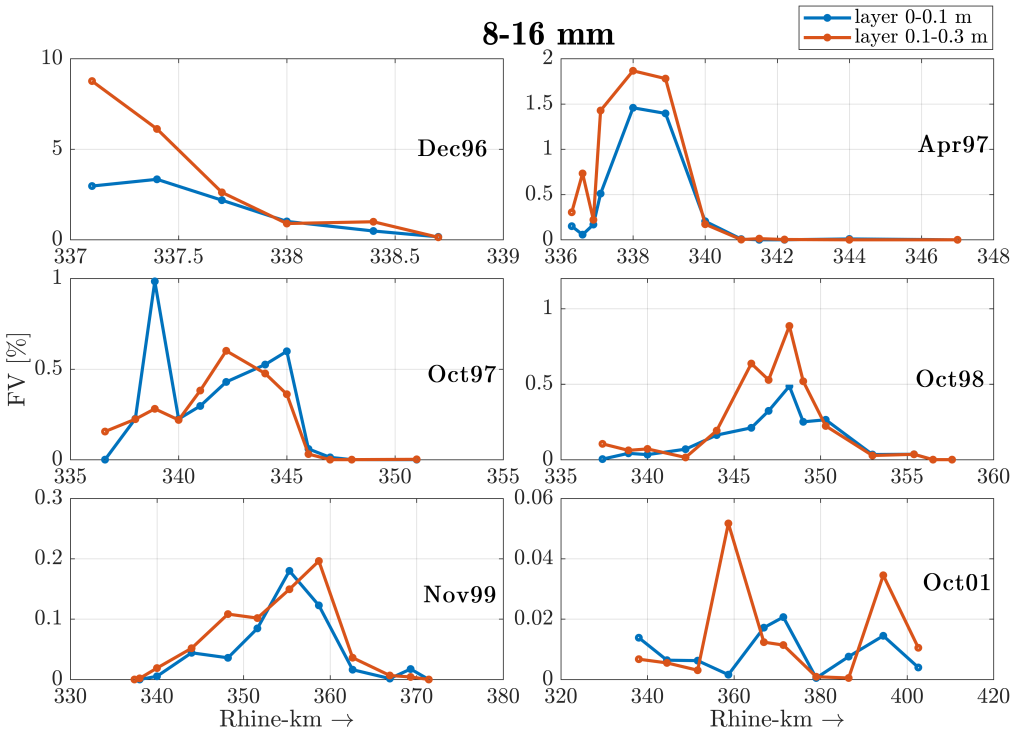

Figure 2.22: Comparison of FV at the layers 0-10cm (blue color) and 10-30cm (red color) for fraction 8-16 mm and per monitoring campaign.

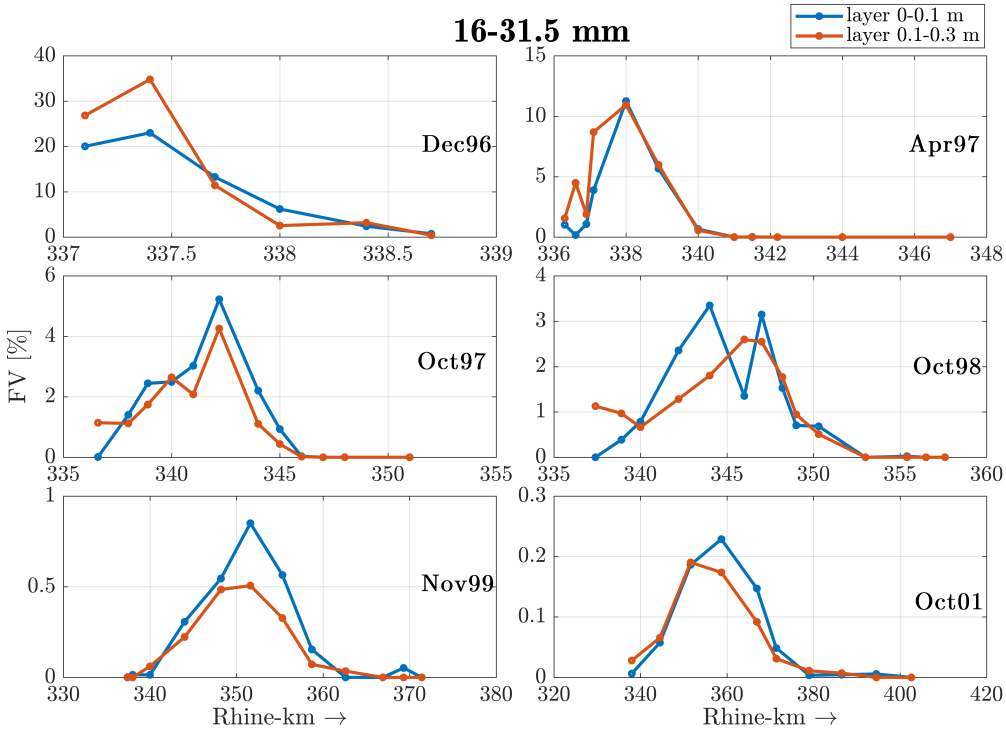

Figure 2.23: Comparison of FV at the layers 0-10cm (blue color) and 10-30cm (red color) for fraction 13-31.5 mm and per monitoring campaign.

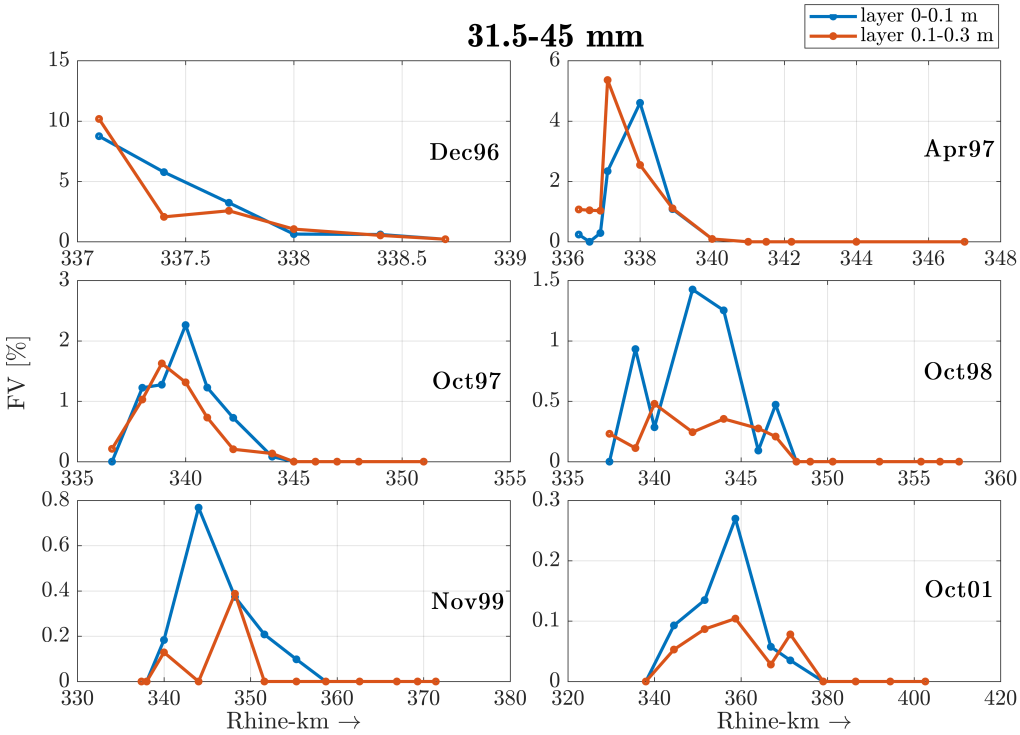

Figure 2.24: Comparison of FV at the layers 0-10cm (blue color) and 10-30cm (red color) for fraction 31.5-45 mm and per monitoring campaign.

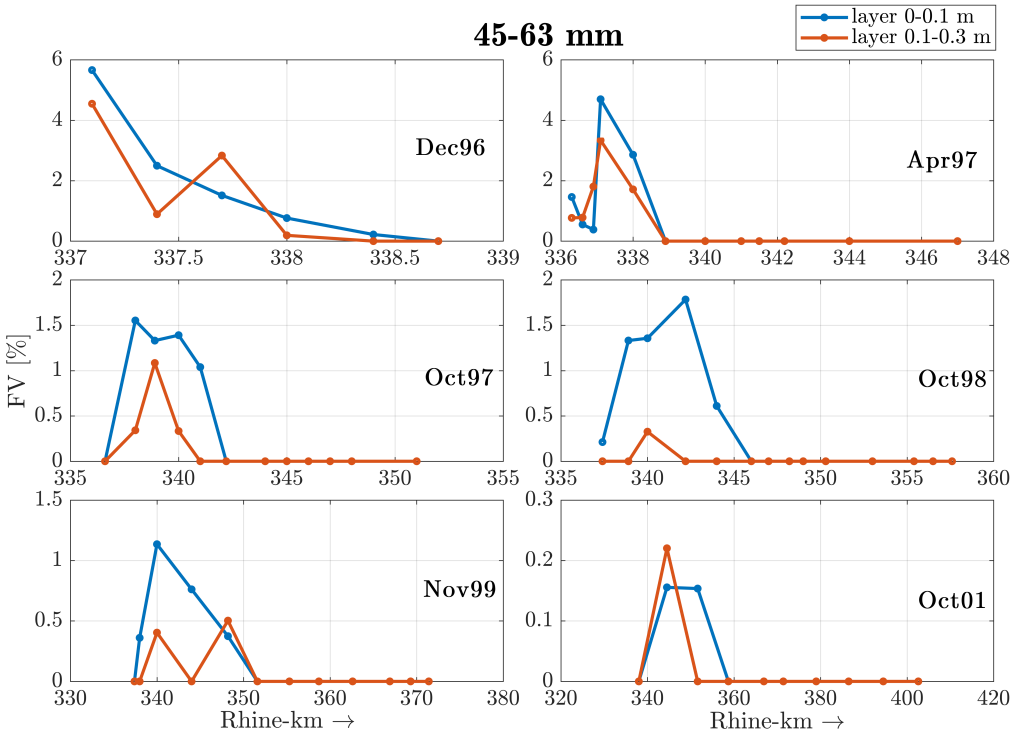

Figure 2.25: Comparison of FV at the layers 0-10cm (blue color) and 10-30cm (red color) for fraction 45-63 mm and per monitoring campaign.

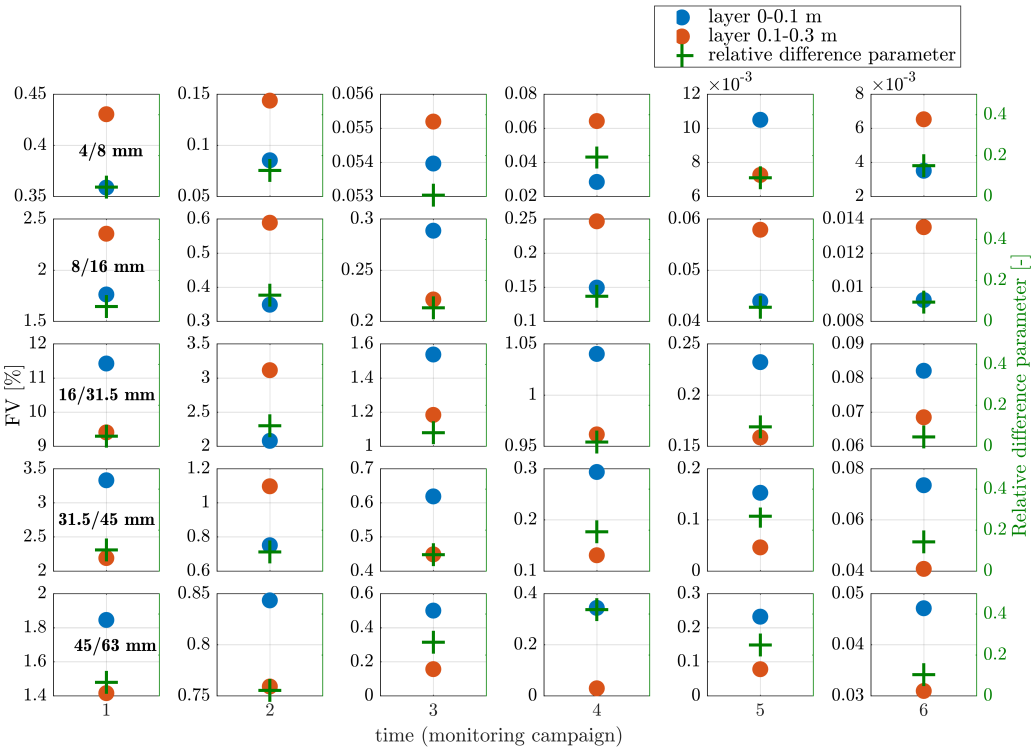

Figure 2.26: Comparison of mean FV at the layers 0-10cm (blue color) and 10-30cm (red color) per size fraction (y-axis subplots) and per monitoring campaign (x-axis subplots).

2.3 Conclusions

Concerning the temporal changes of tracer concentration in streamwise direction conclusions about the `total` and `fractional` concentrations can be summarized in the following;

a. The tracer signals reveal that the nourished sediment evolved through a combination of downstream migration and spreading.

b. All the parts of bulk tracer sediment were found to migrate downstream. The front of the tracer signals migrated downstream faster from the centroid (approximately 3 times concerning the bulk volume of tracer sediment) which in turn migrated downstream faster than the trailing edge. The tracer sediment in the last monitoring campaign had spread over a distance of approximately 60 km.

c. The degree of downstream migration and spreading was found to be different between the various tracer fractions. The finer tracer fractions migrated downstream faster and spread more compared to the coarser tracer fractions.

d. The downstream migration of tracer sediment was generally more enhanced in the monitoring campaigns shortly after the feeding of tracer sediment.

e. The variations of migration celerity were larger for the front of the tracer signals while the centroid of the signals migrated with almost a constant celerity during the monitoring period.

f. The occurrence of the 1/100 years flood before the fourth monitoring campaign was not found to have a significant influence on the downstream migration celerities.

g. The two finest tracer fractions studied, demonstrated close resemblance in their temporal changes. In fact, the finer of the two fractions migrated downstream slower than the coarser. Their signals formed peaks separated from the bulk volume of tracer sediment only 5 years following the feeding.

For the analysis of the temporal changes along the lateral direction conclusions about the `total` and `fractional` concentrations can be summarized in the following;

a. The maximum tracer concentration per cross-section studied was found to form a trajectory from one outer bend to the next. Close to bend crossings the maximum tracer concentrations were closer to the axis of the navigation channel.

b. The tracer concentrations closer to the outer bends of the meanders compared to the tracer concentrations closer to inner bends were found to be greater for most of the cross-sections examined.

c. These findings were seen to hold also at a fractional level.

Finally, concerning the temporal changes of tracer concentration in vertical direction, conclusions about the `fractional` concentrations can be summarized in the following;

a. The tracer concentration for the finer fractions was found to be systematically larger in the bottom layer compared to the top layer.

b. Conversely, for the coarser tracer fractions the concentration was larger at the uppermost vertical layer.

   As a result, the finer tracer fractions were found to mix more into deeper strata compared to coarser tracer fractions for all monitoring campaigns.

chapter

THREE

BOVENRIJN PILOT STUDY

3.1 Introduction

During April June and July 2016 sediment was nourished at the deep outer bend of Bovenrijn next to Lobith as part of a pilot study aiming to counteract bed degradation at the Dutch Rhine branches. The stretch of the nourished sediment starts from 862 and extends to 864.3 Rhine kilometre, while its thickness is restricted to approximately 30 cm such that the OLR-4m navigability condition is satisfied. The nourishment will be repeated in 2019 at the same Rhine reach.

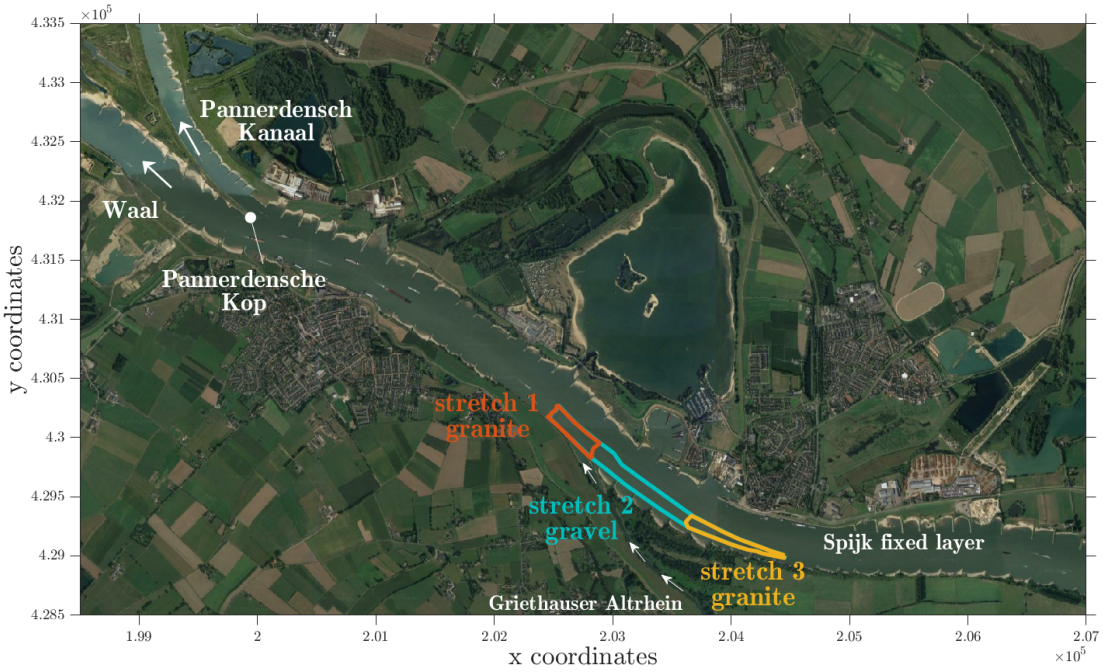

Figure 3.1: The study reach depicted with the polygons of granite and gravel stretches.

3.1.1 Characteristics of the study reach

The study reach is characterized by a two-dimensional morphology. The feeding area itself, is situated at the deep outer bend of Bovenrijn. The bar and pool topography yields strong lateral sorting patterns, characterized by finer sediment closer to the inner bed and coarser closer to the outer bend, despite the low sinuosity at the study reach. It can be seen from Fig.3.2 that these

sorting patterns are stronger closer to the bifurcation and do not necessarily extend upstream to the nourishment area. The nourishment front (denoted in Fig.3.2) initially resided at the location of crossing between the two adjacent meanders where nearly uniform cross-sectional texture can be observed from the coarser sampling grid upstream.

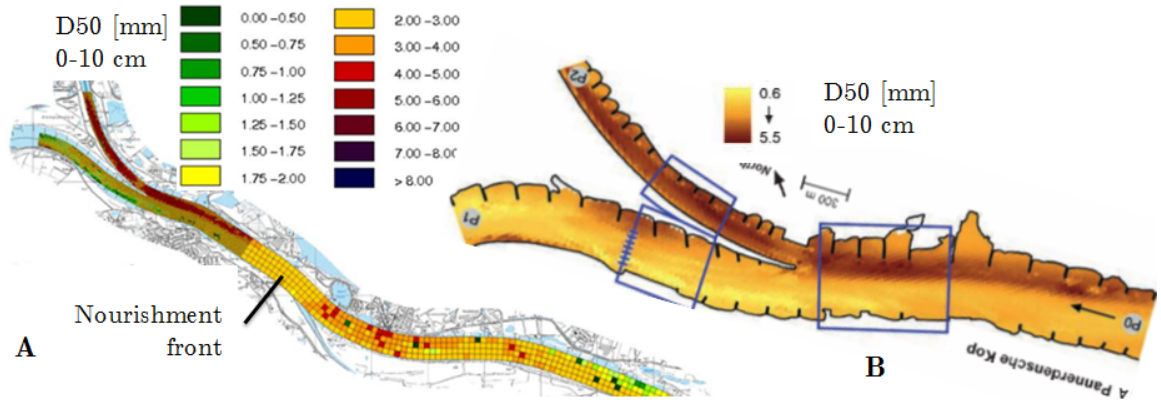

Figure 3.2: Flow is from right to left. Lateral sorting patterns of the surface texture at the study reach, as revealed by vibracore measurements taken in 2000/2001. The sampling resolution is larger at the bifurcation compared to further upstream, whereas the measurements were not taken at the same time period yielding an abrupt transition in panel A. Panel B zooms in the uniform grid at the bifurcation area. Source: TNO, Rijkswaterstaaat (Panel A), (Frings, 2008) (Panel B).

Pannerdensche Kop splits the Rhine to the Waal and Pannerdensch Kanaal. Furthermore, the study area is located at the downstream part of the Rhine's gravel sand transition (Frings, 2008). Therefore, a strong downstream fining pattern is present as can be seen in Fig.3.3. The bed at the Bovenrijn is gravel dominated and has become coarser during the recent years. Further downstream the Waal gradually becomes a sand-dominated reach.

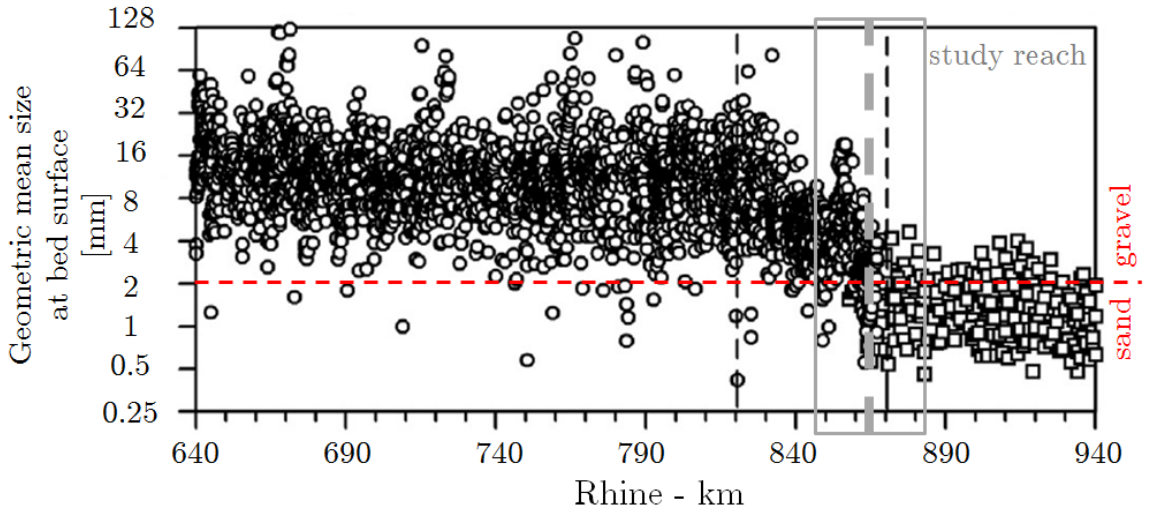

Figure 3.3: The grain size of the top layer of the river bed for Niederrhein, Bovenrijn and the Waal. The gravel-sand transition is denoted by the dashed back vertical lines. The study reach is denoted by the gray box while the nourishment location from the dashed vertical gray line. The figure is modified from Frings et al. (2014a).

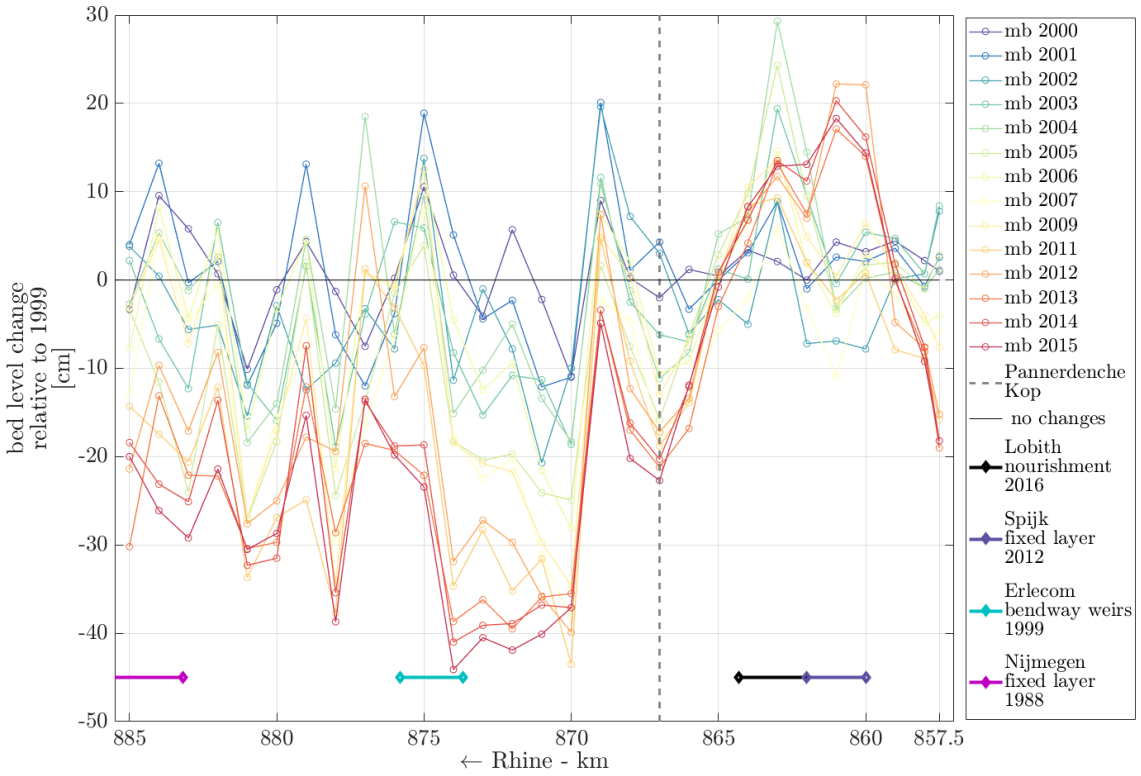

Figure 3.4: The recent development of bed levels relative to 1999 for the Bovenrijn and the upstream Waal. The multibeam measurements are averaged per 1 kilometre. Various relevant interventions at the study reach are depicted together with the nourishment stretch. Data source: Rijkswaterstaat-ON

Degradation has characterized the Dutch Rhine branches, as well as the German reach. Degradation at the Bovenrijn and the downstream adjacent reaches accelerated during the decade 1980-1990 having a form of a downstream migrating erosional wave (e.g. (Emmanouil, 2017)). However, since the late 1990s the riverbed of Bovenrijn shows overall stability (Fig.1.5) with the most recent development characterized by aggradation to the largest extent reaching up to 20 cm relative to 1999 (Fig.3.4). That being said the upstream adjacent reach of Lower Niederrhein in Germany have been stabilizing and aggrading earlier, since the early 90s to a large extent as a response to the nourishments initiated at the same period (Frings et al., 2014a). The same is not true for the downstream adjacent reach of Waal where erosion persists (Fig.3.4).

Dredging activities are often executed for the maintenance of the port that is located west of Lobith but also downstream from the mouth of Altrhein that joins Bovenrijn at the front of Stretch 1. Furthermore, in 2012 a fixed layer was placed in the shallow inner bend just upstream from the nourishment stretch (Rhine-km 860-862). The fixed layer is hypothesized to induce bed level changes at adjacent areas expressed by erosional waves (Sieben, 2017). Finally, the mean discharge at Lobith for the period 1901-2013 is 2200 m^3/s which corresponds to recent yearly averaged water level of 9.7 $m+NAP$. The formation of dunes is common for the Bovenrijn reach but for discharges exceeding 6000 m^3/s (Kleinhans et al., 2007). Dunes detected from bed level surveys at various flood events, demonstrate larger dimensions closer to the inner bends (e.g. (Ten Brinke, 2005)).

3.1.2 Supplied sediment characteristics

The nourished sediment consists of gravel part of which is granite. This serves as tracer sediment due to its natural radioactivity and is broken at a quarry. The non radioactive gravel (from the rest denoted as gravel) supplied originates from dredging and hence its properties correspond better to the original bed sediment at Bovenrijn. The granite is characterized by larger density, increased angularity and larger grain size compared to the rest of the added sediment. Therefore it is expected to be less mobile than the gravel. The gravel and granite were not mixed, but on the contrary were fed at three separate boxes (Fig.3.1). During the execution of the sediment feeding the aim was to

place the granite exclusively at the front and the trail (half of its total volume placed at each box) while the gravel exclusively at the middle of the stretch. The total volumes of granite and granite at the nourishment are the same. Both, are somewhat coarser the the original bed sediment (see Table 3.1). Moreover, the width of nourished sediment increases with downstream distance. The sediment specifications are given in Table 3.1.

Table 3.1: Grain size characteristics of the sediment nourished in Bovenrijn (source: RWS).

sediment	$\rho[kg/m^3]$	$D_m[mm]$	$D_{90}[mm]$	$D_{50}[mm]$	$D_{10}[mm]$	$volume[m^3]$
original bed	2650	8.8	19.5	7.4	0.4	-
added gravel	2620	9.7	18.8	9	4.3	35100
added granite	2740	12.7	22.8	11.6	4.3	35450

3.1.3 Temporal and spatial resolution of monitoring campaigns

The monitoring campaign of the field study consists of Multibeam echo soundings, Medusa measurements of radioactivity, Van Veen grab soil samples of the bed surface top layer, and finally water level and discharge measurements. There are no analyses available of the granite concentrations in soil samples to date as was the case with the monitoring of Iffezheim field experiment.

The spatial resolution of the Multibeam bed level measurements is 1x1 meter and covers the whole stretch of the nourishment over the whole width of the river, with some extra allowance (few kilometres) both upstream and downstream. The Medusa measurements also cover the same longitudinal extent yet resolving only the left half of the river where the nourishment is performed. Finally, the soil samples are taken from a stretch that extends from well upstream the nourishment stretch to a few kilometres downstream from the Pannerdensche Kop at each downstream channel (Waal and Pannerdensch Kanaal). The longitudinal space interval for the latter is 500 meters while two samples across the lateral were taken from every second sampled cross section. The latter lie 70 meters to the left and the right of the river axis.

Fig.3.5 shows the temporal resolution of the various monitoring campaigns and the execution periods for each stretch. It can be seen that the execution of Stretch 3 was intercepted by discharge exceeding 4000 m^3/s in June 2016.

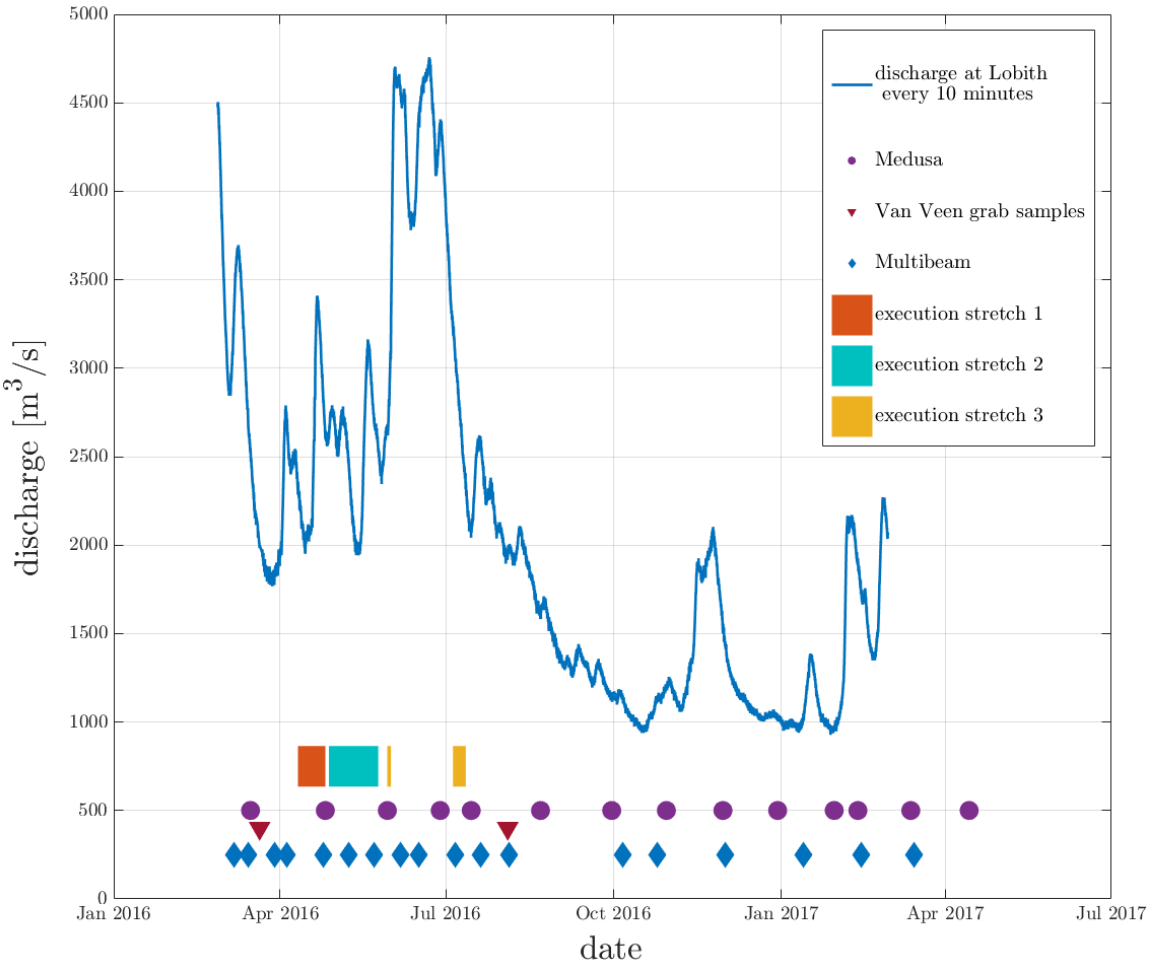

Figure 3.5: Temporal resolution of various monitoring campaigns plotted against the discharge measured at Lobith gauging station.

3.2 Data Analysis

3.2.1 Textural changes at the study reach

3.2.1.1 Comparison of bed composition surveys within the monitoring period

For the time being, there are two available measurements of the bed grain size distribution with respect to the field study. The first monitoring campaign was in March 2016, before the nourishment of granite and gravel, and was meant to serve a reference measurement. Unfortunately, the analysis of the soil samples provides information only for the grain size distribution for grain sizes below 2mm i.e. sand and clay sediments, but nevertheless provides information concerning the percentage of grains that exceeded these fractions i.e, gravel and pebbles. In August 2016 after the completion of the nourishment, a second measuring campaign was conducted. The analysis of these soil samples additionally provides information for the grain size distribution of all the fractions taken from the bed. Finally, no information is available for the tracer concentration in the samples.

Considering the available data, the analysis here is based on the percentage of soil material larger than sand which is a measure of coarseness of the bed surface. It has to be noted that depending the measuring procedure, the presence of extremely coarse elements on the bed (e.g. very large pebbles) can have a large impact on the results of this analysis. Their possible presence is also the reason why the term coarseness parameter is used instead of gravel content.

The coarseness parameter is plotted against x and y coordinates for the two sampling campaigns in Fig.3.6. It can be seen that generally the bed of Bovenrijn was coarser in March comparing

to August, possibly due to the occurrence of higher discharges before March. Generally speaking, following the occurrence of larger discharges, the surface texture might coarsen since it is likely that the finer material of the bed surface are preferentially transported downstream. Coarsening of the bed is visible at the bifurcation downstream which nevertheless is unlikely to be linked with the nourishment considering the large distance and the small interval period. Some coarsening can be identified at the front of the nourishment stretch as well as somewhat downstream. However, the spatial resolution is too small to allow for generalized conclusions with respect to the effects of the nourishment on the surface texture of the study reach.

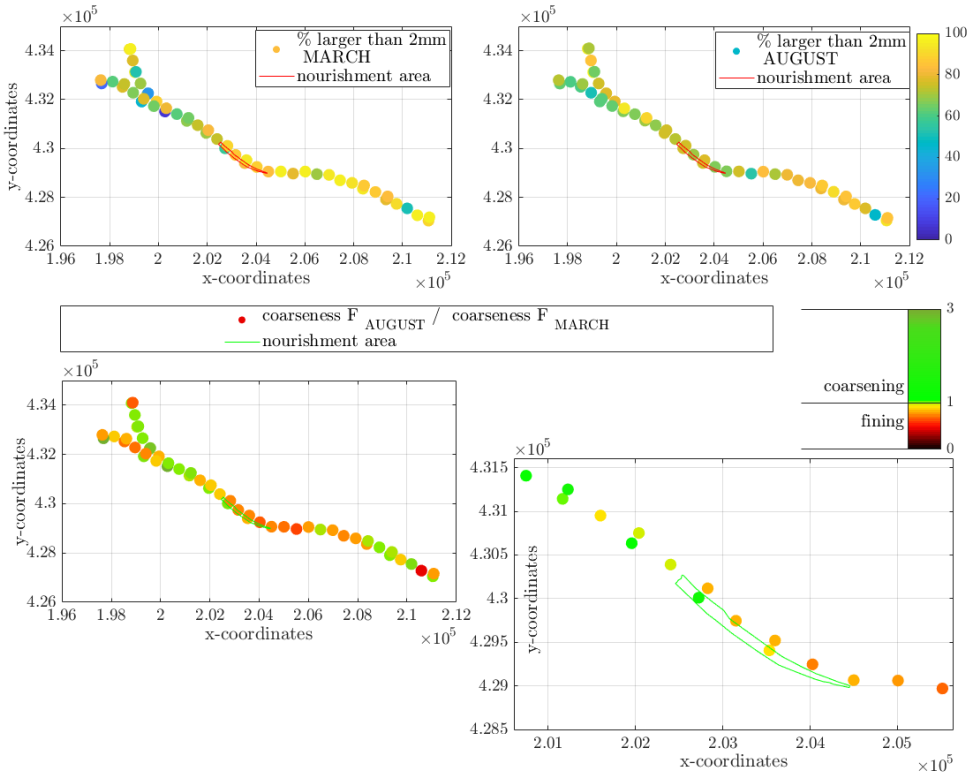

Figure 3.6: Comparison of coarseness parameter ($\% > 2mm$) between March and August 2016. At the subplots below, the colorbar indicates the difference between the coarseness parameter of the two campaigns. Red color indicates coarsening while blue color indicates fining. Data source: Deltares, Rijkswaterstaat-ON

3.2.1.2 Comparison of Van Veen grab samples between August 2016, 2008 and 1995

In Fig.3.7, a comparison is made between the d_{10}, d_{50} and d_{90} characteristic grain sizes of the August 2016, 2008 and 1995/96 sampling campaigns. All campaigns were made with the use of Van Veen buckets. Additionally, the characteristic grain sizes of the nourishment material are plotted. This comparison is interesting not only in order to assess the relative coarseness of the nourishment at Lobith with the present bed composition, but also in order to assess the past development of the bed texture. The data used are not laterally averaged but instead reveal information for three sampling locations per campaign one always situated at the river axis.

It can be seen from Fig.3.7 that the bed surface sediment has become significantly coarser over the period studied prior to the nourishment pilot study. The 2008 and 2016 soil samples do not indicate large differences in the surface texture i.e., the coarsening evolved predominantly in the period 1995-2008. It is worth to mention though that the spatial resolution of measurements in a streamwise direction is lower for the 1995 campaign compared to 2008 and 2016. Finally, at the upstream end of the study reach (km 855-858) where samples were not taken in 1995, a coarsening is revealed during the period 2008-2016.

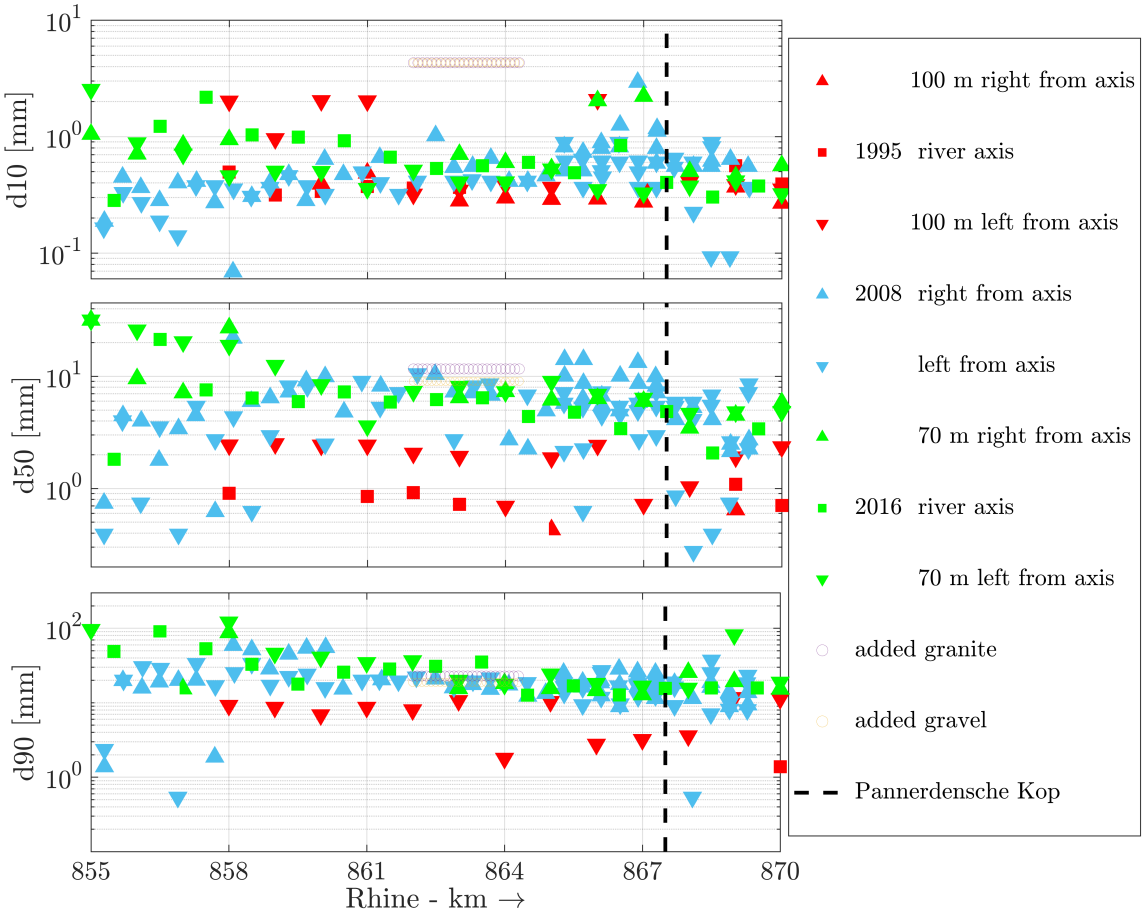

Figure 3.7: The grain size characteristics (d_{10},d_{50} and d_{90}) of the nourished sediment plotted in log-scale along with the Van Veen grab samples taken in 1995, 2008 and August 2016 from the bed surface of the study reach. Data source: Rijkswaterstaat-ON

To illustrate the temporal changes in the characteristic grain sizes of the study reach, the moving averages were calculated for each monitoring campaign and the changes between successive campaigns were calculated. The spatial window (2.5 km) that was used for the calculation, was determined such that the most upstream part (where 1995 measurements are not available) and the most downstream part (the Waal downstream from the Pannerdensche Kop) would be assessed separately. The resulted plots showed little sensitivity in changes of the moving average window.

Fig.3.8 demonstrates the results of the approach followed. Two are the interesting conclusions that can be drawn from studying the figure. First, the coarsening revealed in Fig.3.7 is more pronounced for the d_{50} and d_{90} between the first considered period. The second interesting finding is that this increase is more enhanced at the upstream end of the study reach. This spatial trend is more pronounced for the d_{90} of the first period, and for all characteristic grain sizes during the second. In fact, concerning the second period (2008 to 2016) it can be seen that this increase is very significant at the upstream end of the study reach changing by a factor 10 (at least) the diameter of the bed surface. Note that the August samples were somewhat finer than the March samples of 2016.

Finally, concerning earlier periods than the ones studied here (i.e., before 1995), it was seen from previous analysis (Emmanouil, 2017) of grab samples from the study reach that there were no statistically significant temporal trends linked with changes in the surface texture of the Bovenrijn. Regarding the nourished material, it is somewhat coarser compared to the present bed material. Especially the finest fractions of the bed material are not included in the grain size distribution of the added sediment.

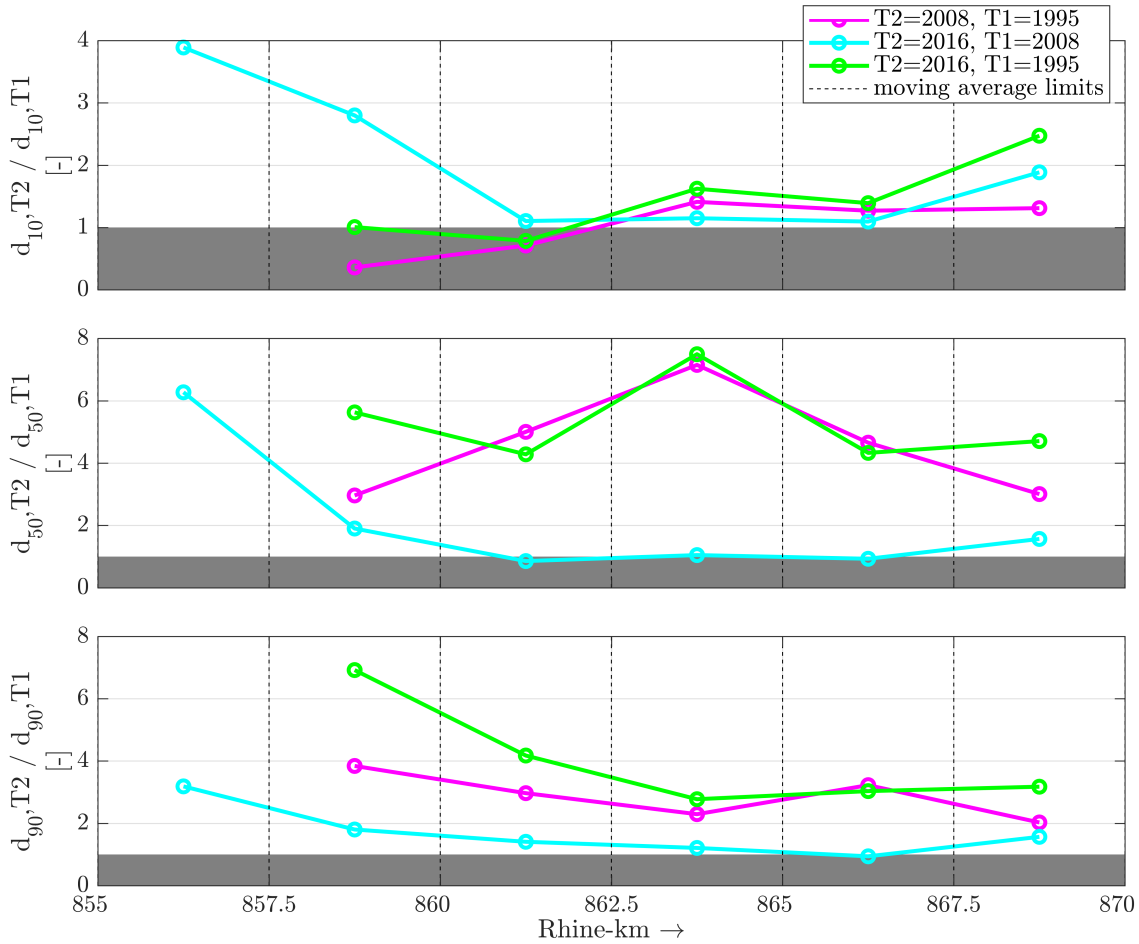

Figure 3.8: Temporal changes in characteristic grain sizes d_{10}, d_{50}, d_{90} in the study reach using the moving averages per campaign with a window of 2.5 kilometres.

3.2.2 Downstream and lateral migration of changes in topography

There are 10 Multibeam surveys available for this study. One is conducted before the initiation of the nourishment, and the rest follow after the completion of the first part of stretch 3. The data available have a resolution of 1x1 m. For the purposes of the present analysis, the bed level data were averaged on a 20x20 m reference grid for which, both the x,y coordinates and the streamwise and lateral (with respect to river axis) positions are known. This allowed to exclude the unwanted noise and the irrelevant small scale perturbations present at the signals. The reference grid was constructed based on the first available MB reference campaign grid (prior to the nourishment) which compared to the rest was spanning to a closest lateral and streamwise extent. Nevertheless, this was needed in order to calculate the bed level changes, and hence extract the nourishment as a bed wave feature. The averaging process was conducted by setting an algorithm which assigned each x,y coordinates of the 1x1 grids on the nearest x,y coordinates of the reference 20x20 m grid.

By subtracting the bed levels of April 2016 from the bed levels of the following campaigns the resulting bed level changes indicate the thickness of the nourished sediment and partly the changes related with its presence in the study reach. We will term this extracted feature as bed wave from now on. However, it is worth to notice that this does not necessarily either consist exclusively of nourished material or that it contains all the nourished material. Therefore we analyse a signal that has the potential to vary from the signals that were assessed in the previous Chapter. We will explore these differences later in this document. Having said that, in Fig.3.9 the bed wave is depicted for 3 selected monitoring campaigns the last of which corresponds to approximately 7 months after feeding.

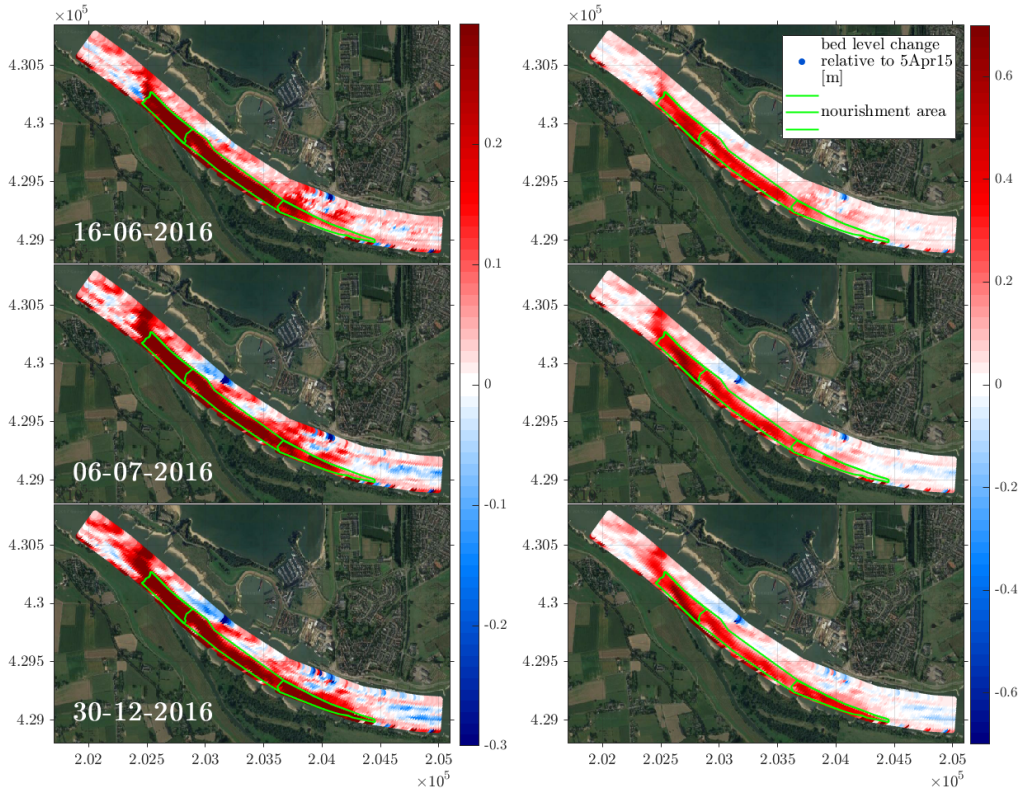

Figure 3.9: The bed wave depicted for 3 selected monitoring campaigns. Two colorbars are used with different limits ([-0.3 0.3] and [-0.7 0.7] meters). Red color denotes deposition and blue color erosion. The y axis gives the y-coordinates whereas the x-axis the x-coordinates in meters.

It can be seen that the front of the wave migrates very slowly downstream. Its front lies only a few hundredths meters downstream from its location right after the nourishment (indicated by the green polygon). This relatively slow migration is related with the low discharges that were measured at Lobith gauging station during the 8 month period considered here. In fact, only the one month occurrence of 4000 m^3/s water discharge seems to have led to significant migration of the front. The location of the latter in 30-12-2016 lies close to the one measured in 06-07-2016 corresponding to a time instance shortly after the passage of the high water event.

It is clear that the migration of the bed wave appears to evolve predominantly in a diagonal direction towards the outer bend at the downstream right bank. This can better be observed in Fig.3.10 where the bed level change are plotted as a function of river km and distance from the river axis for all the available measurements. Some other aspects concerning the bed level changes at the study reach can also be observed. For instance, there is mild erosion at the tip of the front which is restricted to approximately 10 centimetres, yet persists leading the front of the bed wave throughout the monitoring period. Erosion at the right half of the river axis and next to the nourishment area is attributed to maintenance dredging activities for the functioning of the neighbouring port (Sieben, 2017).

Even though the migration of the front was rather mild even during the high water event, this is not the case for the evolution of its thickness. During the high water event the thickness at stretch 1 (front granite box) was more than doubled reaching up to 70 cm locally. At least part of this sediment appears to originate from the gravel at stretch 2 which is the only box demonstrating locally thickness less than (the initial) 30 cm. There, erosion areas evolve predominantly close to the river axis. A distinct erosion pit is situated close to the front of stretch 2 next to the left bank. Fig.3.9 at the right Panel, demonstrates how sediment is deposited in a diagonal manner at stretch 1. At the upstream of this diagonal dark red line the erosion pit can be visually detected. It is worth to mention that this diagonal depositional ridge forms a continuous line with the Altrhein Griethauser tributary joining Bovenrijn at the front box. That could mean that the latter may play a role in the depositional pattern at stretch 1. The bed level changes between successive monitoring

campaigns are presented in the Appendix.

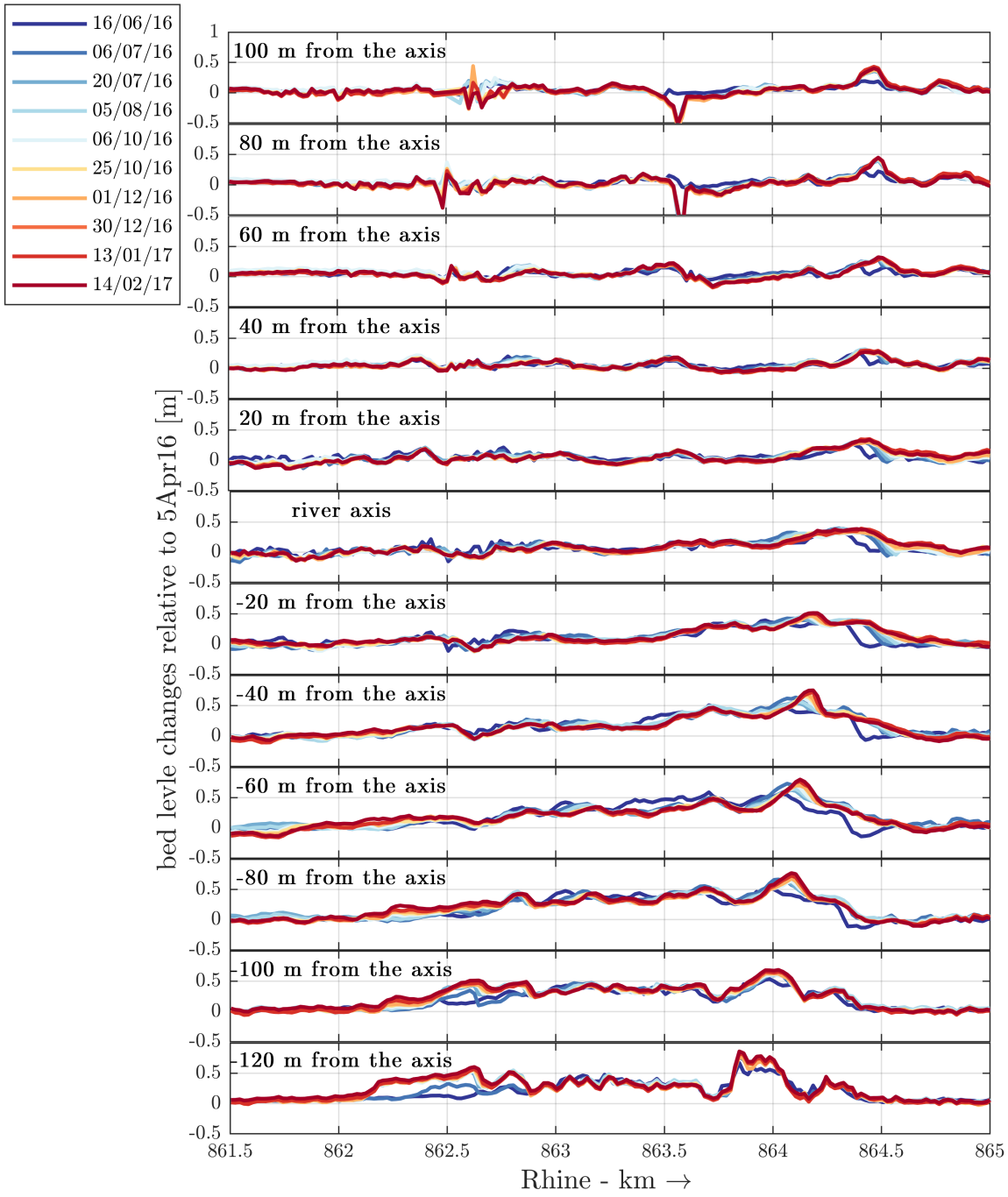

Figure 3.10: Bed level changes relative to 5 April 2016 for various distances from the river axis. Positive values indicate deposition and negative values erosion.

In order to study the migration of the front, and how it relates to the distance from the river axis, the bed wave signals (as taken from the bed level changes relative to 5 April 2016) were cross-correlated for each sequence of monitoring campaigns. The cross-correlation of two discrete functions f, g of a real variable x is a measure of similarity of two series as a function of the displacement of one relative to the other. It is defined as;

$$f \star g \equiv \overline{f}(-x) * g(x) \tag{3.1}$$

where, $*$ denotes convolution and $\overline{f}(x)$ is the complex conjugate of $f(x)$.

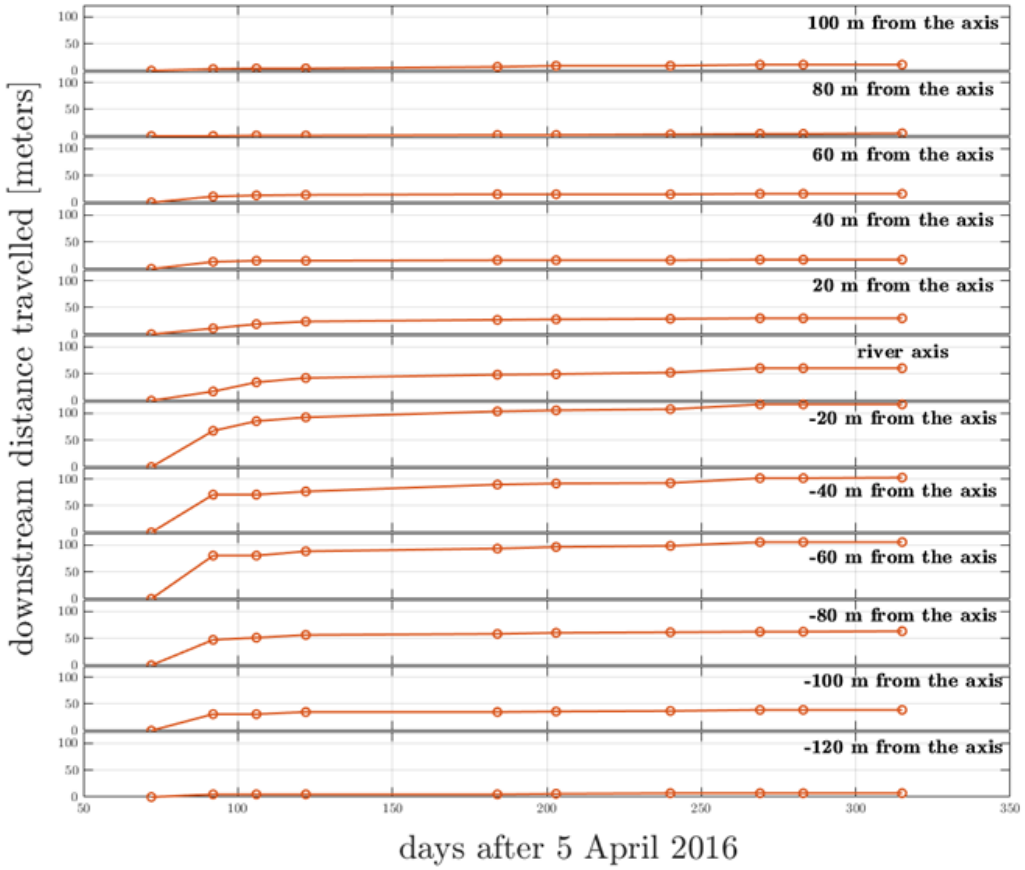

Figure 3.11: Migration of the bed wave signals (bed level change relative to 5 April 2016) at various transverse locations.

With the use of an algorithm, the smoothed (20x20 m) signals were interpolated in a streamwise direction, with a space interval of 1 meter. This allowed for the signals (per certain lateral distance from the river axis) to be cross correlated with a minimum lag of one meter. From the cross-correlation procedure, the maximum positive linear correlations resulted by negative lags of newer against earlier signals in time. The signal inputs used employed, covered the whole extent of the reference grid (861.5 to 865 km).

The lags corresponding to the maximum linear correlations, can be interpreted as downstream migration distances by the bed wave. The cumulative downstream migration per lateral distance from the river axis, is presented in Fig.3.11. The downstream migration celerity increases from the left bank towards the river axis, attaining its maximum 20 meters left from the axis. The migration of the signal close to the left bank is minimal and does not exceed 10 meters in 8 months. These results not only highlight the diagonal migration of the bed wave but also quantify the respective temporal changes. The maximum cumulative downstream distance travelled amounts 120 meters while the cross-sectionally averaged amounts approximately 40 meters during the period studied.

Note that part of the downstream migration is not observed in this analysis since the first available signal corresponds to a date approximately one and half month after the execution of stretch 1 when the wave had already migrated downstream to some degree.

As discussed earlier the downstream migration of the nourished sediment relates closely with the water discharge. To illustrate that, we determine the linear correlation between the cross-sectionally averaged downstream migration (as resulted from the cross-correlation analysis), and the water discharge measured at Lobith. To represent the latter, since the duration between monitoring campaigns is not constant, except for the mean discharge Q_M we use also its product with the discharge integral Q_I. In that way the effect of water discharge becomes weighted in a better way both against the relevant magnitude and the duration.

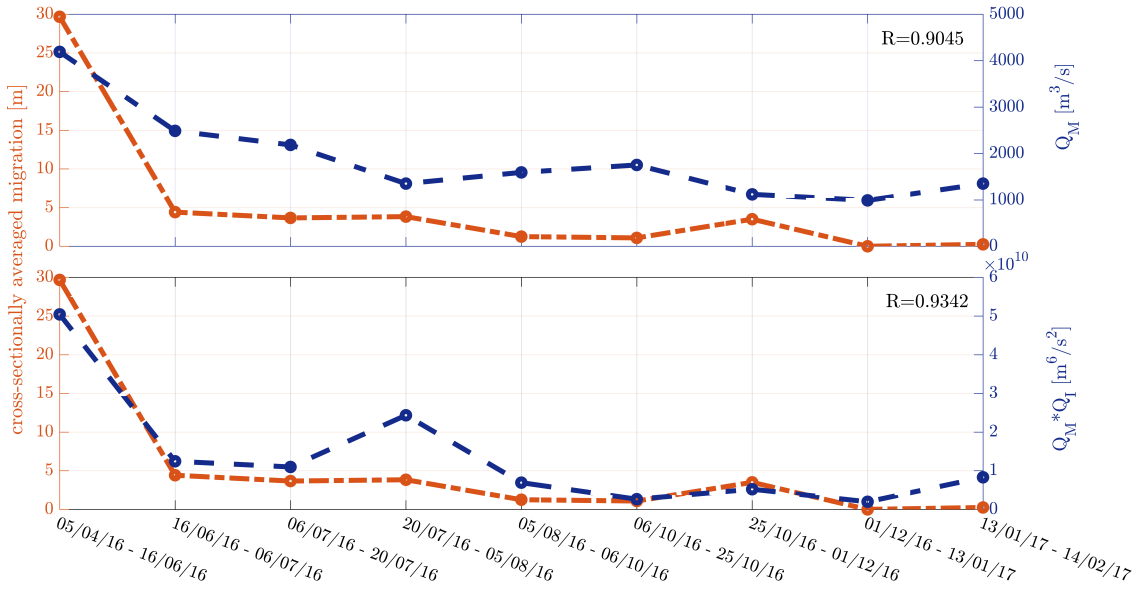

Figure 3.12: **Top panel**; Linear correlation between average studied migration and mean water discharge Q_M measured at Lobith during time intervals. **Bottom panel**; Linear correlation between average studied migration and the product of mean water discharge and discharge integral $Q_M * Q_I$ measured at Lobith during time intervals.

Fig.3.12 a confirmation of the previous analysis is provided. The linear correlation coefficient lies very close to 1.

3.2.3 Downstream and lateral migration of tracer sediment

The MEDUSA RhoC, provide a measure for the natural radioactivity of the river bed sediments (Eelkema, 2008). The sediment radiometric activity is taken by dragging a probe on the river bed with the use of a vessel. The measurents provide the intensities of the chemical elements in natural stones as Potassium (K), Thorium (Th), and Uranium (U) at the top layer (ca. 30 cm) of the bed surface. The relation that gives a measure for the radiometric activity is:

$$\text{Radioactivity } [Bq] = K/100 + Th + U \tag{3.2}$$

For the field experiment at Lobith, a background level of 25 Becquerel was determined by measuring the river bed prior to the feeding of the gravel and granite. The latter only, serves as tracer owing to its high radioactivity levels. Right after the feeding of granite, Medusa measurements revealed a radiation of ca. 120 Bq at the stretches 1 and 3. The temporal evolution of granite at the top bed layer can thus be assessed by changes in the signals of later measurements.

In Fig.3.13 measurements of radioactivity are plotted against the respective bed level measurements that reveal the evolution of the bed wave. Focusing on the left panel of the figure, it can be seen that the granite at the front stretch migrates downstream without crossing towards the downstream right bank as is the case for the bed wave. The granite stays at the left bank and is resolved further downstream from the the front of the bed wave. Therefore granite is seen to migrate downstream slightly faster.

The signal taken at the front stretch quickly diminishes to background levels denoting little presence of the granite at the top surface layer there. This can be explained either by a complete advancement of the granite at the front stretch further downstream, or by its burial into larger depths by deposited sediment from upstream. In fact with advancing time, granite presence is resolved mostly within the erosion pit leading close to the left bank the migration of the bed wave. Considering the doubling of thickness at the front stretch, it is more likely that the more mobile gravel fed at the upstream stretch (which demonstrated erosion), covered the less mobile granite at the front. The latter nevertheless was not immobile. It can finally be argued that erosional conditions have led to preferential erosion of finer gravel if any surpassed the granite at the leading erosional pit leaving the granite more exposed to the bed surface compared to stretch 1.

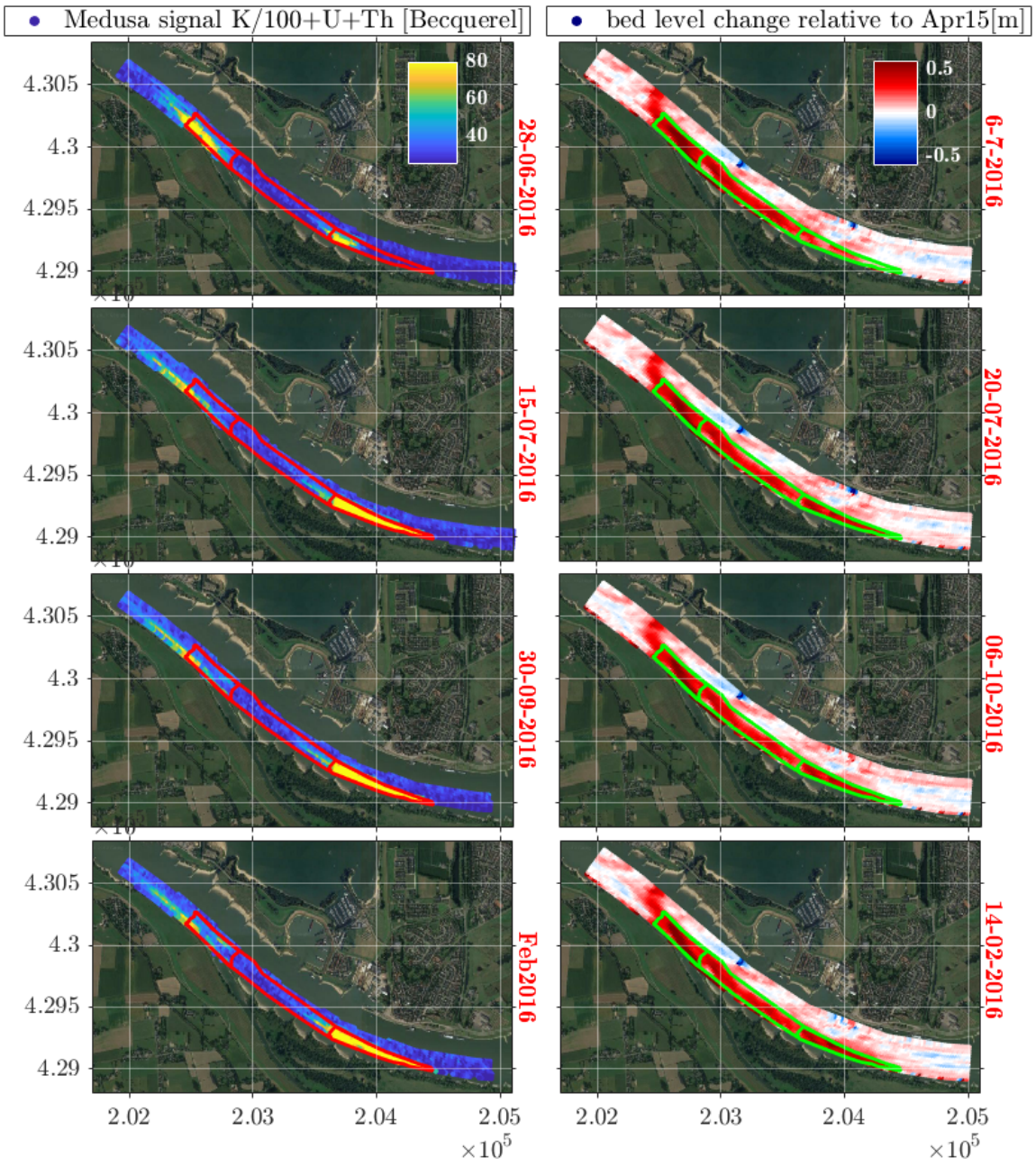

Figure 3.13: Medusa signal ($K/100+Th+U$) plotted next to the evolution of the bed wave for respective measurements conducted close in time. In y-axis the y-coordinates are given in meters whereas in x-axis the x-coordinates.

From Fig.3.14 it can be seen that since August 2016, the gravel can be identified at the front (left at figure) at some lateral locations (i.e., $-140-120-100-80$ and less at -60 meters from the axis of the river) closer to the left bank bank. However there is an indication that it has migrated more downstream as the distance from the left bank increases. This is also the case for granite at stretch 3, which however after its completion has migrated only marginally downstream. The signal of the latter is retained closer to design levels (120 Bq) but its nourishment was completed after the occurrence of the high water event which is associated with most of the morphodynamic changes during the monitoring period.

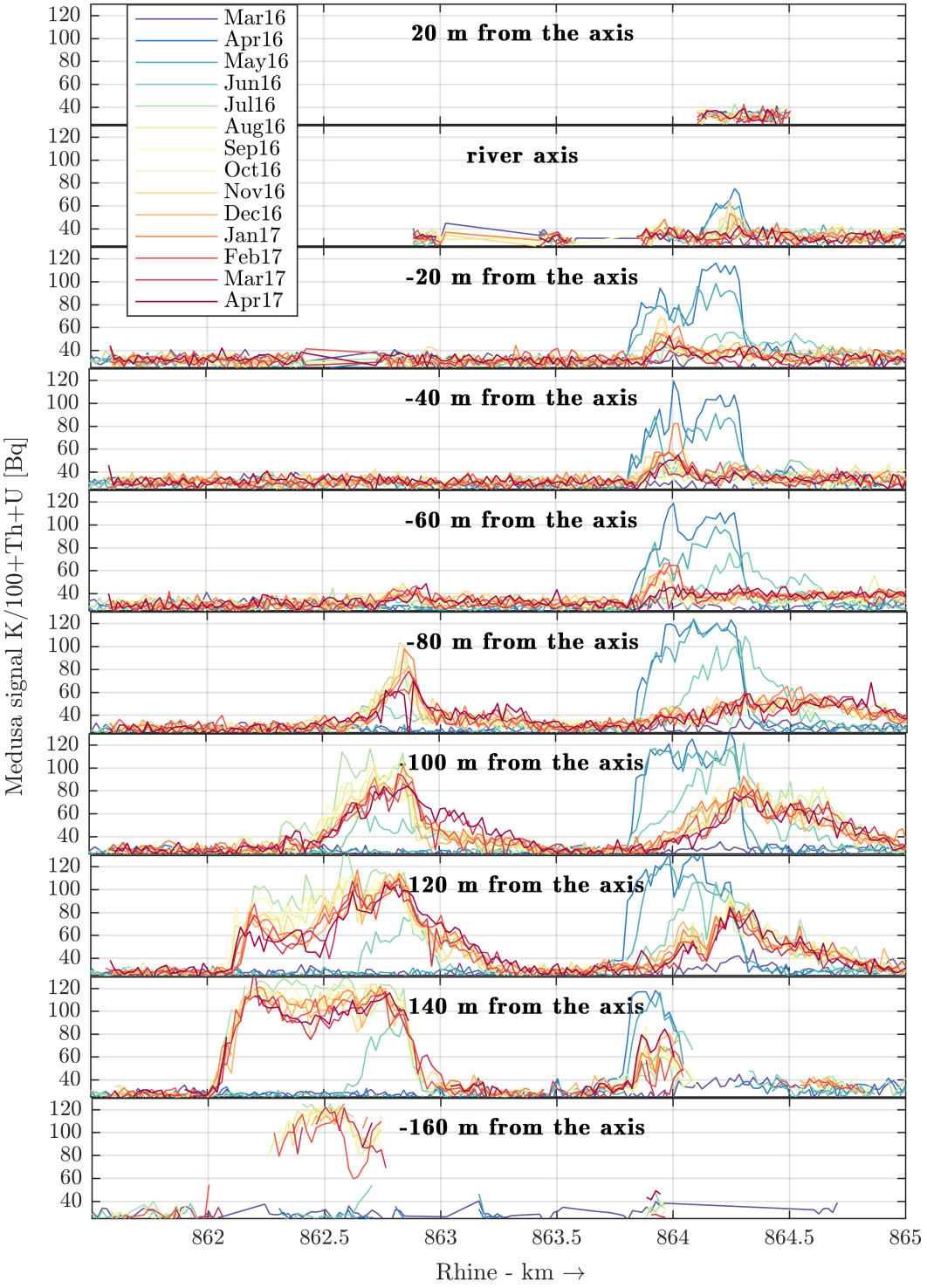

Figure 3.14: Medusa signal $(K/100 + Th + U)$ per lateral location along Rhine-km 861.5 to 865 km.

To further explore the migration of the granite we repeat the cross-correlation analysis that was described in detail earlier. Now the Medusa signals are cross-correlated instead of the bed wave signals. For this a narrower stretch is considered than before and the focus is only on the downstream migration of the granite at stretch 1. For this we chose the window of Rhine-km $863.5 - 865$ (see Fig.3.14). The results of this analysis are shown in Fig.3.15. The cumulative downstream migration of the granite (Medusa signals) is found to reach a maximum of ca. 200 metres, 100 metres left from

the river axis. 150 days after the execution of stretch 1, no further downstream migration of the granite is observed.

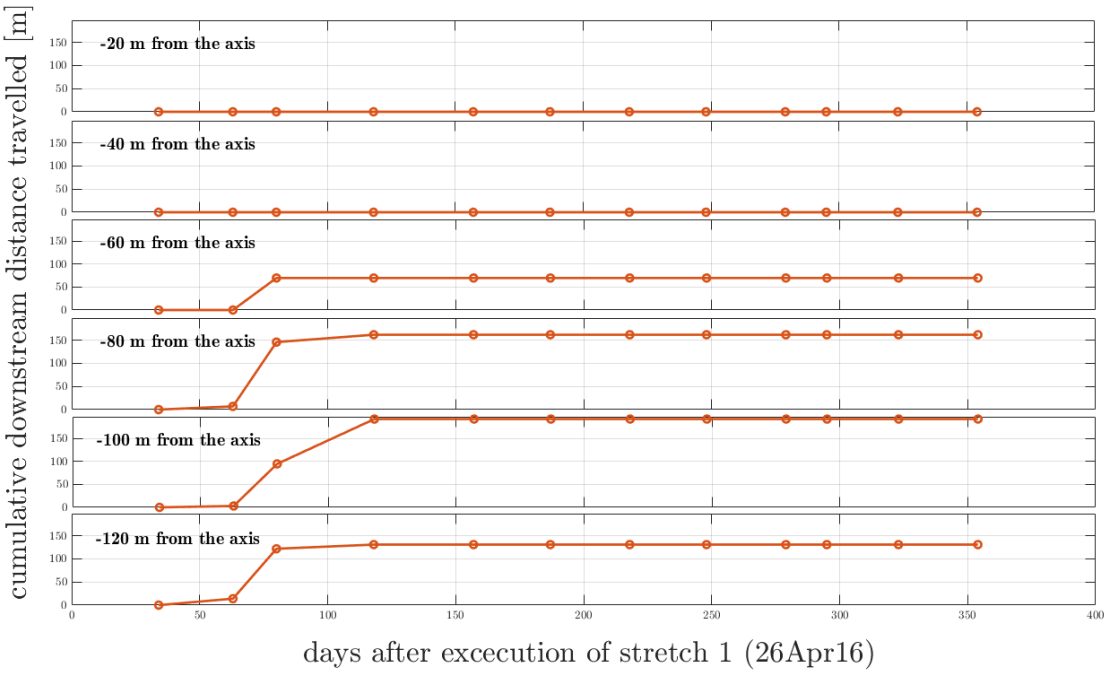

Figure 3.15: Downstream migration of Medusa signal ($K/100 + Th + U$) per lateral location along Rhine-km 863.5 to 865 km. (stretch 1)

3.3 Conclusions

Concerning the textural changes in the study reach as revealed from the analysis of samples taken from the bed surface in 1995, 2008 and 2016 the main findings can be summarized in the following;

a. The surface texture of the Bovenrijn has coarsened significantly during 1995-2008.

b. The coarsening was more prominent closer to the upstream end of the Bovenrijn, especially for the period 2008-2016.

c. The added sediment is somewhat coarser than the present bed surface sediment since the finer bed fractions are not included.

The main findings from the analysis on the temporal changes in topography can be summarized in the following;

a. The front of the bed wave migrated slowly, with a diagonal direction crossing from one outer bend to the next.

b. An erosion pit was leading close to the left bank of the river the slowly migrating bed wave.

c. The thickness of the front granite stretch more than doubled during the high water event. At least part of the deposited sediment there, originates from the upstream gravel stretch where erosion was more enhanced during the flood wave.

d. The cross-sectionally averaged migration correlates well with the water discharge.

Finally, the main conclusions from the analysis of the Medusa signals that reveal the presence of granite at the top surface layer, can be summarized as follows;

a. A part of the granite has migrated downstream and its presence is mostly observed in the leading erosion pit.

b. Granite is observed progressively less at the front stretch 1. The doubling of thickness of the stretch has resulted most probably in the burial of the front granite under added gravel and other sediment transported from upstream.

c. While the bed wave crossed towards the next outer bend, the granite was observed at the south part of the river. However, it is not sure whether any granite is buried below the sediment deposited at the front of the stretch 1 and in a diagonal direction.

By comparing rough estimates of the downstream migration celerity between Medusa and bed wave signal fronts (presented in the Appendix) the main conclusions are the following.

a. The downstream migration of the Medusa signals (per 20 meter lateral position from the axis) was found to be larger compared to the downstream migration of the respective bed wave signals. The former varied for three studied periods between 3.3 and 0.6 km/year while the latter between 0.6 and 0.2 km/year.

b. The roughly estimated celerities of the fronts were found to be larger compared to the estimates taken from the cross-correlation analyses both for topographic and Medusa changes. Since the roughly estimated celerities concern the migration of the signal fronts, whereas the celerities taken from the cross-correlation analyses concern the full signals extent, it can be argued that both topographic and Medusa signals are dispersive.

chapter

FOUR

MAIN PHYSICAL MECHANISMS

4.1 Introduction

In the present Chapter we focus on the main findings of the previous Chapters where data from the Iffezheim and Bovenrijn field experiments were analysed. Until now we aimed at assessing the characterization and quantification of the temporal evolution of nourished sediment. In the following we will concentrate on assessing the main physical processes stemming from the interaction between flow and mixed-sediment morphodynamics that control the temporal changes (in streamwise, vertical and lateral direction) and the effects exerted on the bed levels and surface texture of the mitigated reaches. To this end we will provide argumentation on the physical mechanisms by employing simple hand-calculations, reviewing available literature and finally analysing further data from the study reaches when needed.

We will first assess the main physical mechanisms that control the trajectory of nourished sediment and related topographic changes along the meanders of the study reaches. Then we will focus on the vertical mixing of nourished sediment and finally on the temporal changes evolving over the streamwise direction. This structure follows -as we will see later- from the fact that we estimate that vertical mixing and lateral dispersion of nourished sediment may affect its downstream migration and hence need to be discussed earlier in the present chapter. Finally, we will focus on assessing the morphodynamic controls on the coarsening of the Bovenrijn surface texture and discussing any possible relevance with sediment nourishments.

4.2 Lateral dispersion

4.2.1 Findings, hypotheses and further analysis

In the previous chapters we focused on two different study cases of sediment nourishments in meandering reaches, with respect to the physical processes that arise for flow and sediment transport. This follows mainly from the differences concerning the dumping location of sediment across the cross-sections of the respective feeding stretches in Iffezheim and Bovenrijn. While in Iffezheim the sediment was uniformly distributed in the cross section, in the Bovenrijn the sediment was fed left from the river axis across the deep outer bend. Nevertheless, the layer that was formed had a thickness of 30 cm resulting in a local increase of the bed level that was not possible to reverse the bar pool topography. i.e., the deeper part of the cross-section remained at the outer bend.

The data analysis of the Iffezheim study case concerned only the trajectory of the total volume of nourished sediment and the various fractional components. In the data analysis of the Bovenrijn experiment we studied not only the trajectory of the coarse wave of tracer granite but also the migration of the bed wave that resulted from the presence of the nourishment.

The **findings** for the Iffezheim study case indicate that the trajectory of nourished sediment follows the deep outer bends of the navigational channel, crossing from one outer bend to the next at the locations of bend crossings. We did not observe any differences concerning the discussed behaviour between the various gravel fractions monitored during the field study. The **hypothesis**,

is that since the tracer fractions correspond to the coarser range of transported sediments in the reach (gravel), they are subject to the physical mechanisms that bring coarser sediments in the deep parts of the meanders closer to the outer bends. Such physical mechanisms are for instance gravity pull along trasverse slopes and shoaling of flow along the upstream part of the point bars.

The main **finding** concerning the Bovenrijn case, is that the granite follows the downstream inner bend despite the fact that it corresponds to the coarser range of the transported sediment spectrum. Nevertheless, the bed wave resulted from the presence of the nourishment, followed a trajectory towards the downstream outer bend. The **hypothesis** is that since the granite has only migrated a little distance downstream from the front of stretch 1 which corresponds to the crossing location between the upstream and downstream meander, there was not enough time and space for the lateral sorting mechanisms to become effective. This is hypothesized under the assumption that the Medusa signals obtained from the downstream area, allow us to observe the real characteristics of the granite's migration without it being buried below other deposited sediment. The validity of this assumption is discussed earlier.

4.2.2 Physics of flow and sediment transport in river bends

First, let us focus on the physical processes that govern sediment transport in river meanders. The flow pattern along a meander is governed by a centrifugal force that brings water towards the outer bank leading to an increase of water level combined with a decrease of the water level at the inner bend. Result of this cross-stream water level gradient is a cross-stream pressure gradient that forces the slower moving water near the bed surface towards the inner bed. In that way a secondary flow arises that strives sediment into moving towards the inner bend.

Dietrich et al. (1979) studied the flow and sediment transport in a river meander of the sand bedded Muddy Creek river. They additionally noted a flow acceleration over the point bar at the upstream inner bend. This follows from a downstream pressure gradient due to the decrease of water level downstream (owing to the increase of centrifugal force upstream) and an increase of the bed level from the presence of the point bar. The overall effect locally is a lateral exchange of momentum, that counteracts the effect of the secondary flow and forms an area of strong outward directed bed shear stress. They demonstrate this flow pattern with a schematic of cross-stream velocities at an upstream cross-section of a meander (see Fig.4.1).

This outward bed shear stress brings coarser sediment entering the meander at the upstream point bar towards the outer bend. Together with the preferential rolling, and avalanching of coarser sediment downslope from the inner bend (due the enhanced effect of gravity on larger grains compared to finer grains), eventually a lateral sorting pattern between the finer and coarser sediment is established, with the former transported closer to the inner bend and the latter closer to the outer bend of the meander.

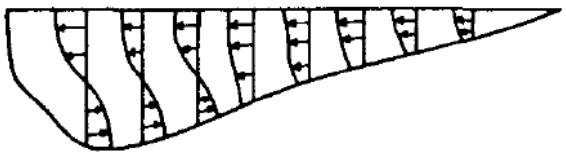

Figure 4.1: Schematic of cross-stream velocities at the entrance of a meander by (Dietrich et al., 1979). Outward flow over the point bar urges coarser entering sediment towards the downstream pool.

The conceptual schematic of Fig.4.2 shows the crossing of the trajectories between finer and coarser sediment. Eventually, an equilibrium topography may be established with the more mobile finer grains lying at the shallow bars and the less mobile coarser grains in the deep outer bends.

Following studies by Clayton (2010) on gravel bedded rivers suggested that in meanders with poorly-sorted sediment (in contrast to the meanders studied by Dietrich and Smith (1984)) and strong lateral sorting patterns, the entrainment and transport rate of individual grains is not only a function of flow and gravitational forces, but also a function of the size of neighbouring grains. This is due to the armouring and hiding processes that emerge in conditions of mixed-sediment, and yield a grain size of the transported sediment finer than the bed sediment.

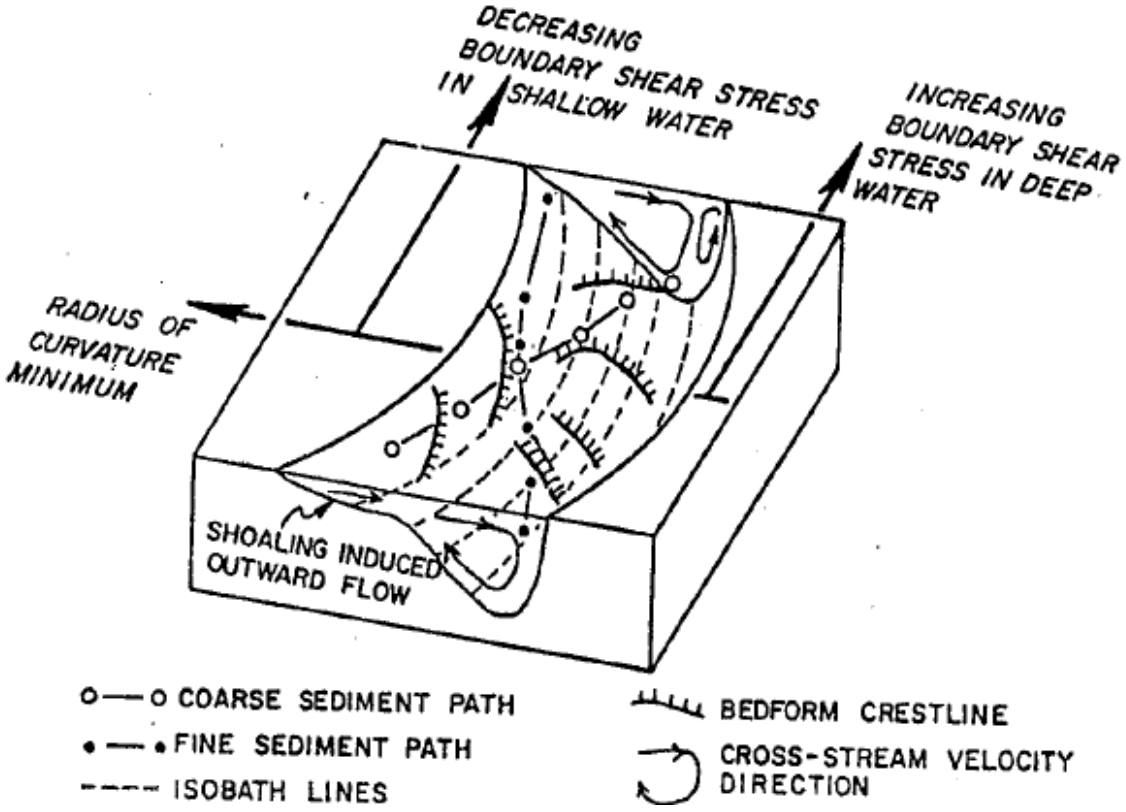

Figure 4.2: A schematic for the trajectory of coarse and fine sediment along a meander (Dietrich et al., 1979).

4.2.3 Trajectory of tracer sediment in the meanders below Iffezheim

The findings of the data analysis that the gravel tracer fractions follow the outer bends of the study reach, can be explained from the theoretical background discussed above. As explained, coarser fractions are expected to travel downstream following predominantly the outer bends of the meanders. In our case, 70 % of the tracer sediment corresponds to the coarse gravel range ($> 16mm$) transported which means that an enhanced effect of rolling downslope the point bars can be expected by the coarse tracer grains.

Further, sediment transport is expected to occur more frequently and with larger intensity closer to the deeper outer bends, since low water depths (approximately 3 m) are associated with the discharge of the highest probability of occurrence. That means that for the larger period of time flow is predominantly concentrated at the deeper parts of the cross-sections as well as the higher bed shear stresses controlling downstream sediment transport. During higher less probable flows though, it can be expected that sediment transport spreads throughout the whole cross-section.

In Fig.4.3, sediment transport measurements at various discharge rates are plotted for a station located in the middle of a meander near Philipsburg within our study reach (Rkm-390), where information is available for the cross sectional shape. Measured sediment transport rates at multiple transverse locations along the cross-section are presented for three gravel ranges corresponding to the three merged tracer fractions (studied in Chapter 2), as well as for the total load, sand load, and the load of the fine gravel fraction excluded from tracer fractions (2/4 mm). Measurements are normalized for demonstration purposes against the maximum sediment transport rates per considered fraction f and per discharge rate. This is done as follows;

$$S_N(f,n)[-] = \frac{S(f,n)}{max(S(f,n))} \tag{4.1}$$

where,
S_N denotes the normalized fractional sediment transport and $max(S)$ the maximum fractional transport per discharge rate.

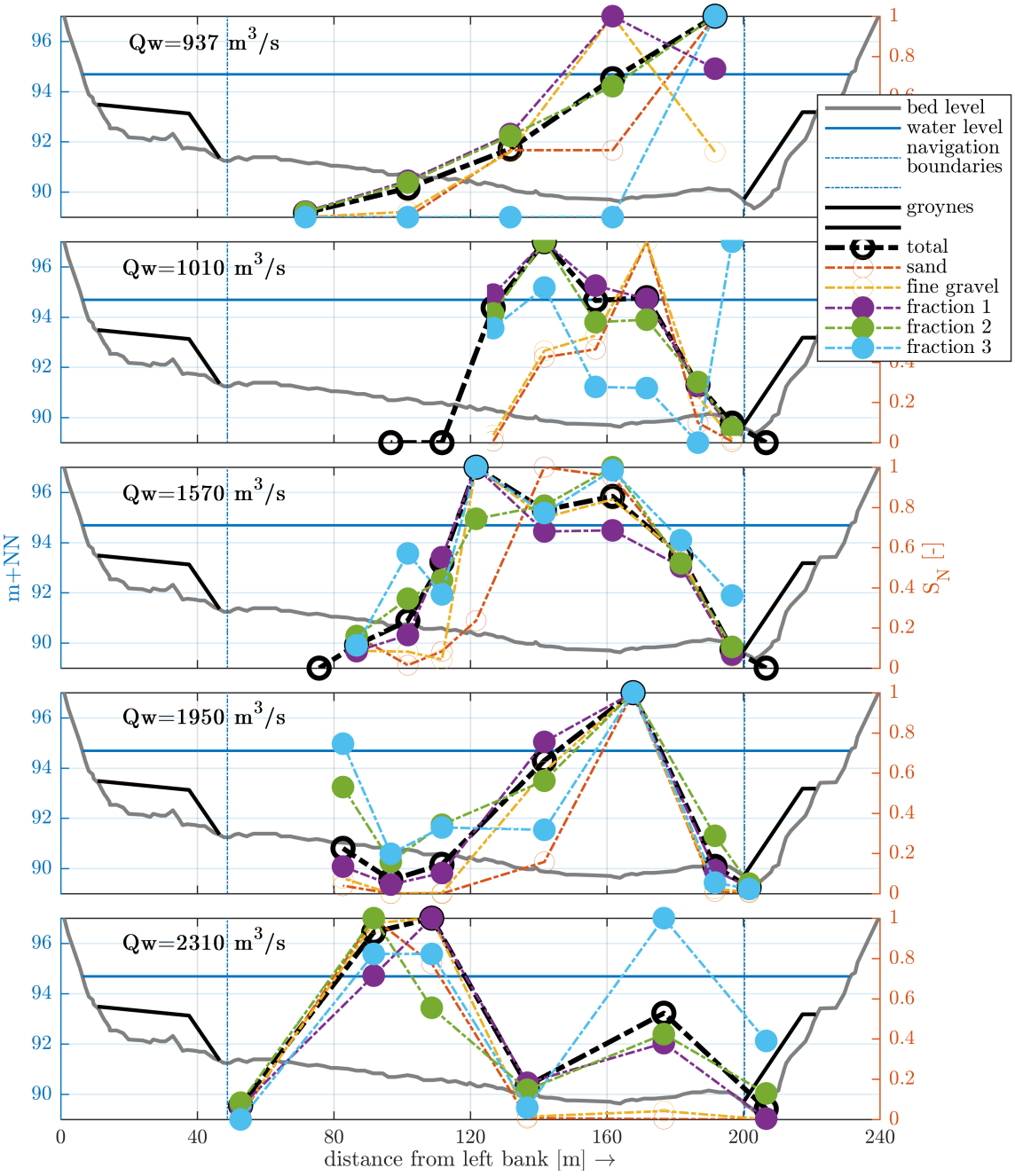

Figure 4.3: Sediment transport measurements at Philipsburg (Rkm-390) during the study period at various discharge rates. The normalized transport rates are given for the total load (0.063/63 mm) (black dashed line), for the sand load (0.063/2 mm) (red dashed line), for the fine gravel range of 2/4 mm (orange dashed line), and for the three merged gravel fractions studied in Chapter 2. These are the fine gravel fraction 4/16 mm (purple dashed line), the 16/31.5 mm gravel fraction (green dashed line), and finally the 31.5/63 mm gravel fraction (blue dashed line). source of data: BfG

First, it can be seen that normalized fractional sediment transports do not always span the whole cross section. This is due to the fact that measurements were not taken any closer to the left bank when zero sediment transports were measured closer to the axis (e.g. for the second panel during Qw=1010 m^3/s). When no data are plotted for certain fractions at certain lateral positions it may be assumed that the fractional transports measured are zero. The maximum measured fractional sediment transports per discharge rate examined are presented in Table 4.1.

Table 4.1: Maximum fractional transport rates (in Kg/s/m) per examined discharge rate.

water discharge [mˆ3/s]	**fraction 0.063/63 mm**	**fraction 0.063/2 mm**	**fraction 2/4 mm**	**fraction 4/16 mm**	**fraction 16/31.5 mm**	**fraction 31.5/63 mm**
937	0.0162	$4 * 10^{-5}$	$2 * 10^{-4}$	0.0065	0.0067	0.0046
1010	0.1292	0.0052	0.0061	0.0663	0.0544	0.0044
1570	0.3796	0.0066	0.0191	0.2671	0.1067	0.0125
1950	0.8606	0.0404	0.0687	0.5508	0.1708	0.0299
2310	0.1958	0.0114	0.0166	0.1353	0.0511	0.0081

It can be seen from Fig.4.3 first that the total bedload transport is concentrated closer to the right half of the navigation channel for most of the measurements. This is not the case only for the highest examined water discharge (bottom subplot in Fig.4.3), during which measurements surprisingly yield lower sediment transport rates (see Table 4.1) compared to the rest.

The mean discharge measured in Maxau is 1310 m^3/s. When higher and less probable water discharges are considered a tendency for increased spreading of sediment transport is observed closer to the left bank. In fact as previously noted, the spatial pattern reverses for the highest examined discharge rate. On the contrary for more probable lower flows, sediment transport increases significantly closer to the outer bend (right bank).

Although some variations can be visually detected in the cross-sectional distribution of fractional transport, the overall trend is that lateral sorting is weak. Only for the coarsest studied fraction there is an enhanced tendency for transport closer to the outer bend during discharges lower than the mean discharge at Maxau (e.g. two top subplots in Fig.4.3). In conclusion, there is a first order effect of the discharge rate and hence the water level on the sediment transport in our study reach. This is also supported by other measurements which are not presented here due to absence of information about the cross-sectional shape. During lower and more probable flows, sediment transport is concentrated closer to the deep outer bends where the bed shear stress is apparently sufficient to mobilize and transport sediment downstream. The lateral sorting observed is weak even between gravel and sand fractions and hence is not expected to dominate the entrainment and transport of tracer fractions in the study reach.

4.2.4 Trajectory of granite in the meanders of the Bovenrijn

Let us now focus on the trajectory of the coarse granite wave monitored at the Bovenrijn. The coarse granite although being fed at the crossing between the two meanders upstream from Pannerdensche Kop, did not show any migration towards the next outer bend. Grain size measurements at the study reach (see Fig.3.2), reveal that strong lateral patterns have been established upstream from the Pannerdensche Kop despite the low sinuosity of the meanders, implying crossing of coarse transported sediment to the downstream outer bend. Nevertheless, at the area of crossing between the two meanders a nearly uniform grain size distribution is observed. This is the area that initially the front of the nourishment was located.

Although it is possible that granite has migrated diagonally towards the next outer bend at an area where other deposited sediment may have led to its burial at deeper strata from where it could not be detected by Medusa measurements, focusing on the physical mechanisms controlling the lateral sorting of sediment at meanders, we could explain why it was observed to have stayed close to the south bank during the monitoring period treated in the present study. To this end, the bed topography at the study reach and the streamwise extent of the observed granite migration are presented in Fig.4.4 and will be considered in conjunction with the data presented in Fig.3.2.A.

The bed topography clearly demonstrates how deeper cross-sectional locations are found close to the south bank in the upstream meander and close to the north bank in the downstream meander. The streamwise crossing of deeper cross-sectional locations, is indicated by the red dashed arrow and is initiated at the front area of the nourished sediment where only granite was fed (blue box). Despite the fast crossing of deepest locations, Fig.3.2 suggests that sediment at the bed surface is well-sorted at least along the cross-sections between Rkm-864.5 and Rkm-865.5. This corresponds to the full streamwise extent presented in Fig.4.4 downstream from the nourishment's front. In the conceptual schematic of Dietrich et al. (1979) (see Fig.4.2) the crossing of deepest locations occurs

earlier in the meander compared to the crossing of trajectories of the gravel and sand. This implies that lateral sorting of transported sediment is effective further downstream from the entrance in a meander and does not necessarily correspond to the crossing of the deepest locations.

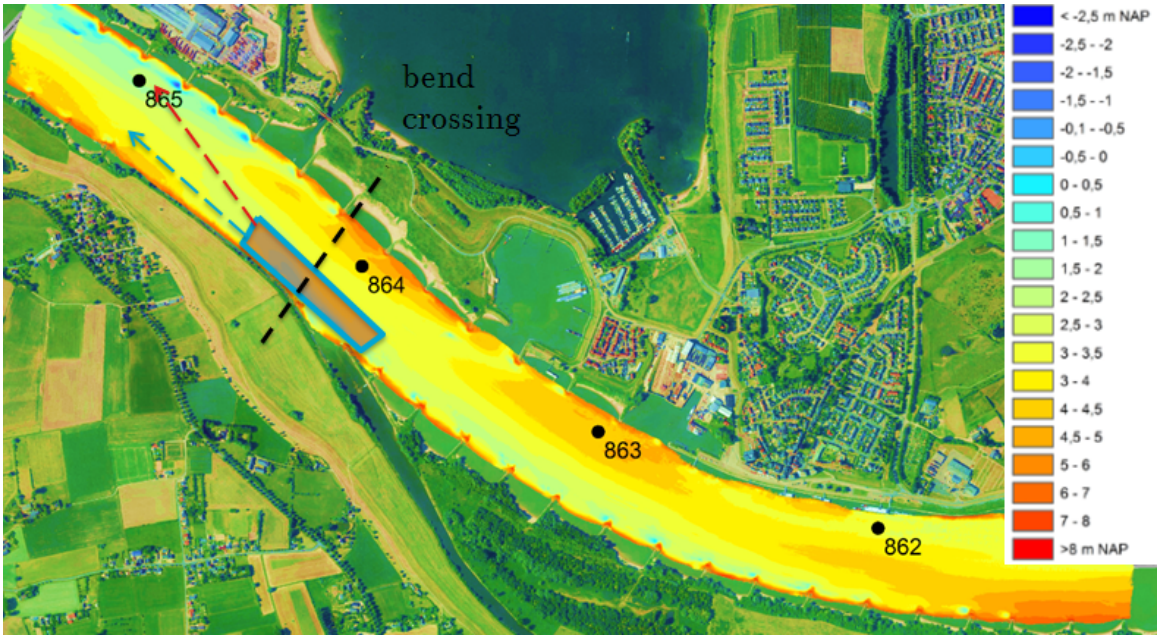

Figure 4.4: Flow is from right to left. Topographic data at the Bovenrijn taken with Multi-beam measurements during the monitoring of the pilot study (source: Sieben (2017)). The approximate location of the bend crossing between the two meanders is indicated by a black dashed line whereas the stretch 1 area is indicated from the blue rectangle. The red dashed arrow indicates the path of the deepest downstream locations while the blue dashed arrow indicates the observed granite migration.

Nevertheless, the bed topography controls the effectiveness of the main physical mechanisms that bring coarser sediment to the deep outer bend. At one hand, the point bar of the downstream meander still grows in downstream direction where granite was observed (blue dashed arrow). This implies that the transverse slopes are not maximal in this area and hence gravity pull would be not very effective in avalanching or rolling the coarse granite particles downslope (towards the downstream outer bend at the north bank). Moreover, any shoaling of flow along the point bar (of the downstream meander) due to positive pressure gradients, may be effectively counteracted by opposite pressure gradients resulting from flow deceleration along the front of the nourishment. The latter may be even more pronounced due to the observed doubling of thickness (see Fig.3.10) of the front stretch (blue box in Fig.4.4) which implies flow expansion conditions at its downstream end.

In conclusion, although it is not certain that we are able to observe the full characteristics of the granite's downstream migration (i.e., due to its possible burial at locations closer to the river axis), the existing lateral sorting patterns in conjunction with the topography at the area just downstream from the front of stretch 1 (Rkm-864.3 to Rkm-865) indicate that the physical mechanisms responsible for bringing coarser sediment towards the deep outer bends (i.e., gravity pull and shoaling of flow) may not be effective. Therefore, it is possible that coarser granite particles will cross towards the deep outer bend at the north bank at a later stage, when it will have migrated further in the downstream meander.

4.3 Vertical mixing

4.3.1 Findings, hypotheses and further analysis

In our previously presented analysis of the data from the Iffezheim field experiment, we observed that within the thin surface bed layer studied (30 cm), the finer gravel tracer fractions had systematically larger concentrations closer to the bottom 20 cm layer than in the top 10 cm layer. This tendency was reversed as the grain size of the studied tracer fractions increased.

This **finding**, denotes a vertical sorting pattern of the nourished sediment over the bed similar to the one that is present in the study reach overall leading to an armoured bed. Further, samples from a deeper layer up 30-50 cm reveal that all tracer fractions are typically mixed over larger depths in the bed. Finally, after the flood wave in 1999, the tracer sediment was found by means of freeze cores in deeper strata, with the finer fractions again lying deeper up to 1.5 m below the bed surface (Gölz et al., 2006).

The **hypothesis** is that several physical processes may be contributing to the vertical mixing of nourished sediment at various depths each one being more relevant under different flow conditions. The more prominent mixing of finer nourished sediment in the shallow surface layer examined (top 30 cm of bed), could be explained for instance by their penetration into the pores of the coarser pavement (Hassan and Church, 1990), vertical winnowing of finer material (Parker and Klingeman, 1982), or burial of bedload during the downstream migration of an avalanche face bar (Hoey and Ferguson, 1994). Concerning the preferential burial of finer material into even larger depths due to flood events (Gölz et al., 2006), the process that is hypothesized to be dominant is the formation of large transport bodies which are superimposed by fine gravel dunes during the process of fill and scour. Although, it is not trivial to conclude which of these processes are the most dominant, in the following subsections these will be discussed in larger detail concerning their relevance with the characteristics of the study reach and nourished sediment.

We need to account for these processes leading to a varying mixing between the various tracer fractions over the vertical, in later assessing which are the main mechanisms that control their streamwise sorting that was also observed in the field experiment.

4.3.2 Mechanisms controlling the vertical mixing of nourished sediment

At first, let us exclude some possible mechanisms that bury sediment into larger depths. Finer tracer fractions were found to lead the coarser, which remained closer to the main feeding area at the study reach at all times (see Fig.2.12). Further from Fig.2.3 it can be seen that aggradational conditions were more prominent during the study period with decreasing distance from the feeding area (at the upstream end of the study reach). It follows that aggradational conditions cannot straightforwardly explain the preferential burial of finer tracer into larger depths, as these would most likely affect more the coarsest material lagging behind. Another mechanism that could be associated with the findings from the data analysis is the burial of finer material below point bars as they tend to follow the shallow inner bends of the meanders. However, the findings from the analysis of the temporal changes of tracer concentration in lateral direction, indicate that even the fine gravel tracer fractions (8/16 mm) follow predominantly the deep outer bends of the study as well as the coarser fractions which correspond to the coarse gravel spectrum ($> 16mm$). Therefore, this mechanism is also not likely to be dominating the preferential burial of finer fractions.

The tracer concentrations of the various gravel fractions in our study case indicate that the added sediment below Iffezheim is quickly structured (the trend appears already 2 months after feeding) over the top vertical layer (30 cm) such that a pavement is formed/maintained by systematic preferential deposition of finer grains towards the subpavement. The study reach is characterized over its larger extent by the presence of an armour layer (Gölz et al., 2006; Frings et al., 2014b) expressed by a finer load and substrate compared to the surface texture (see Fig.2.5). Therefore, the arrangement of the tracer material over the vertical dimension (as these migrate downstream) corresponds to the natural sorting pattern in the study reach.

Static armour layers are typical for poorly sorted gravel-bed rivers especially located downstream from dams, as is our study reach. These static armour layers are often attributed to the downstream winnowing of finer grains (Dietrich et al., 1989) and the inability of flows to entrain the remaining coarser sediment at the bed surface, and extend to a certain distance downstream from the dams.

Nevertheless, the armour layer in our study reach is not static as indicated from the results of the tracer experiment. At one hand the range of the feeding sediment corresponds to the natural spectrum especially towards its coarser end (Gölz et al., 2006). In the same line of thought, all bed fractions are represented in the load since even the coarsest (nourished) tracer fractions were found to migrate slowly downstream even during low flows.

Parker and Klingeman (1982) discuss how the pavement may be maintained even when all size fractions are mobile. This is the so called mobile armour layer, which they suggested to form in order to additionally provide equal rates for all size fractions provided from upstream. A well known process that promotes equal mobility is (microscopic) hiding, which is not necessarily linked with the formation of a pavement. Following observations from the Oak Creek, Parker and Klingeman (1982) concluded that mobile armour is an additional mechanism by gravel-bedded streams trying to promote equal mobility, since (microscopic) hiding alone is not enough for this purpose. A pavement provides additional hiding (termed macroscopic), by covering the finer range of the bedload transported and deposited into the subpavement. This is assumed to be the reason why the grain size distribution of the bedload and the subpavement sediment are often observed to be very similar. In our case, what is important is the mechanism that leads to the formation of the mobile armour layer. Vertical winnowing of finer grains is a process first described by Milhus (1973) and is supported by Parker and Klingeman (1982) to be linked with the formation of the mobile armour layer. It differs from the downstream winnowing of finer sediment, which is linked with the formation of static armour, since it requires the coarser material to be relatively mobile. This process evolves by deposition of finer grains in the holes that are created from the transport of their coarser counterparts, a schematic of which is given in Fig.4.5.

Figure 4.5: A schematic of vertical winnowing of finer material given by Parker and Klingeman (1982) . Flow is from right to left.

Considering the fact that tracer material gets quickly structured in the bed such that it sustains the mobile armour layer present in our study reach, the hypothesis presented previously concerning vertical winnowing being one of the dominant physical mechanisms seems sound. Nevertheless, this is a process able to yield larger concentrations of the finer transported sediment deeper, into a shallow depth, as the one studied in the data analysis (top 30 cm).

Another physical process that potentially leads to preferential burial of finer material in this shallow depth, is the tendency of fine grains for deposition inside the pores of large framework clasts (Hassan and Church, 1990). The previously discussed pavement in our case can be seen as a clast form. According to Hassan and Church (1990), the diameter of the surface pores averages 0.4 times the framework clast diameter. If for the study reach the framework clast diameter is approximated by a representative and uniform mean diameter of the surface ($d_{50} \simeq 20mm$ and $d_{90} \simeq 50mm$ from Fig.2.3) then the surface pores diameter varies between 8 and 20 mm. Obviously the relative diameter of tracer fractions with respect to the surface pores diameter is what straightforwardly denotes the ability of grains to protrude into the deeper layer. The two finer tracer fractions range at grain sizes that have potential to protrude into the pores. This is not the case for the three coarser fractions. This conceptually also holds for the case of vertical winnowing discussed before. Table 4.2 summarizes a quantitative comparison between the characteristic grain sizes of tracer fractions and a characteristic uniform grain size for the bed surface taken as $dm_{surface} = 22mm$ according to Gölz et al. (2006). This is presented along with the monitoring period averaged FV concentrations at the two layers.

Table 4.2: Ratio expressing the relative size of tracer fractions with respect to representative diameter in the thin pavement layer. Monitoring period-averaged values of FV are also compared for the two layers.

fraction	4-8 mm	8-16 mm	16-31.5 mm	31.5-45 mm	45-63 mm
$dm_{tracer}/dm_{surface}$	0.27	0.55	1.1	1.7	2.5
$FV_{pavement}/FV_{subpavement}$	0.8	0.8	1.15	1.8	3.6

It can be seen that the vertical mixing of the tracer fractions, is closely related to their relative grain size with the grain size of the pavement layer. Finer tracer fractions are more efficient in protruding towards the sublayer.

Another mechanism that is relevant here, is the burial of sediment under the avalanching faces of advancing bedforms. Gölz et al. (2006) support that fine gravel dunes are present in the study reach even at lower more probable discharges (see Fig.2.4). Furthermore, Hoey and Ferguson (1994) while presenting a model for the routing of gravel-sized sediment along a river channel, suggest that under aggradational conditions which are mostly present at the upstream part of our study reach (see Fig. 2.3.A), the size fractions transferred from the surface to the subsurface (during deposition), are more likely to correspond to the ones transferred as bedload, in the case that the latter would be buried as an avalanche face bar migrates downstream. This relates also to the geometry of dunes which nevertheless is not known. Since bedload is somewhat finer than the coarser tracer fractions (see Fig.2.5), it is expected that this process would promote a preferential burial of finer material into the subsurface corresponding to the findings of the data analysis.

So far we assessed three physical mechanisms with respect to their relevance in preferentially transporting finer sediment to larger depths as was indicated from the findings of the data analysis. These are vertical winnowing, filling of pores and burial of bedload under advancing faces of bedforms under aggradational conditions. The assumptions behind these mechanisms may be valid for the study reach to some extent, yet it is unknown which dominate the vertical mixing processes. Other mechanisms not discussed here may also be playing a role.

Let us now consider processes that are able to mix sediment over significantly larger depths. These are especially significant to study, due to the occurrence of the 1/100 years flood in 1999 . Freeze cores taken after the flood with the use of liquid nitrogen indicate that generally all fractions were mixed deeper in the bed. Nevertheless, the finer tracer fractions were the only ones to be found at depths larger up to 1.5 meters. The results of a representative core taken after the flood wave, are presented in Fig.4.6. For more information about these measurements we refer to Gölz et al. (2006).

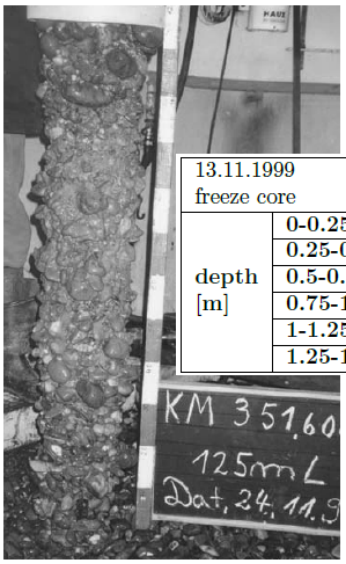

13.11.1999 freeze core		Tracer concentration in the respective fraction [%]				
		4/8 mm	8/16 mm	16/31.5 mm	31.5/45 mm	45/63 mm
depth [m]	0-0.25	0.1	0.1	0.5	7.5	0
	0.25-0.5	0.4	0.4	0.8	0	0
	0.5-0.75	0.4	0.3	1.5	0	7.5
	0.75-1	0.6	1.6	1.7	0	0
	1-1.25	0.1	0	0	0	0
	1.25-1.5	0.2	0.2	0	0	0

Figure 4.6: A photograph of a core, taken inside the diving vessel along with the results of the sieving analysis. Note that the concentrations are given as a function of depth relative to the concentrations of the respective (non-tracer) fraction Gölz et al. (2006) .

Various efforts have been made with the use of tracer stones in gravel-bed rivers in order to provide insight on the processes of burial and re-exposure (e.g. (Andrews, 1987; Hassan and Church, 1994)). Dinehart (1992) with the use of ultrasonic depth sounding, observed the fill and scour process of a gravel bed during a flood wave in North Fork Toutle river, conformed by the migration of gravel bedforms. He identified two dominant spatial scales of bed deformation, which nevertheless evolved with the passage of the flood wave. The small scale (large frequency) variations were related to fine gravel dunes and appeared first during the flood event. After reworking of the bed by the dunes, larger scale (low frequency) variability emerged. These two scales of bed deformation, can be detected in singlebeam measurements (Fig.4.7) along a short straight stretch in our study reach, at a discharge of 3000-3500 m^3/s (lower than the flood wave of 1999 that reached up to 4500 m^3/s).

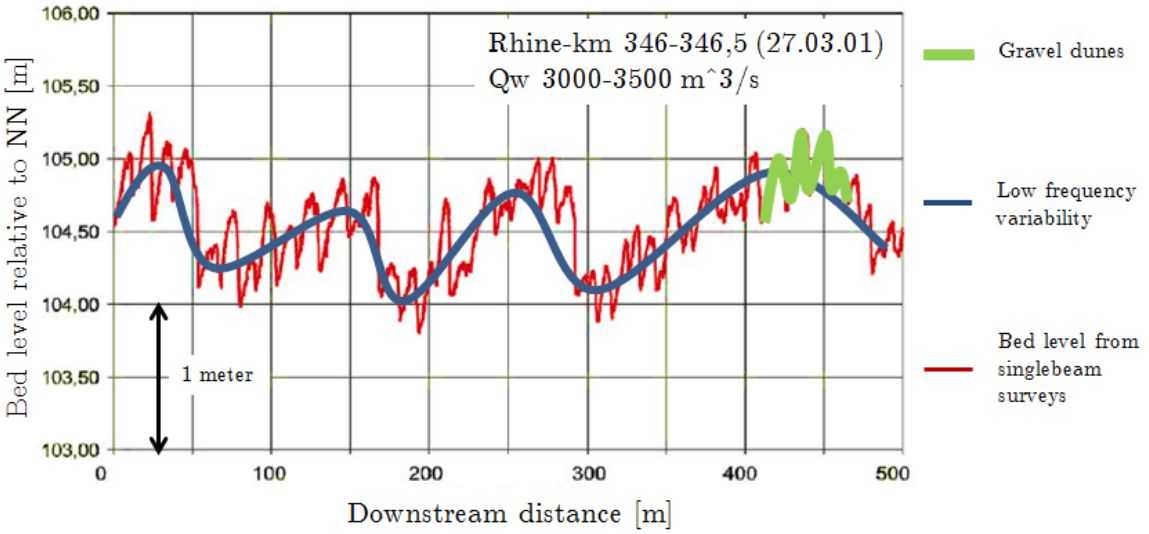

Figure 4.7: Two modes of bed deformation during a 3000 m^3/s flood in 2001 captured with singlebeam surveys by BfG within a straight section of the study reach (Rkm-346 to Rkm-346.5). The figure was modified from Gölz et al. (2006).

The low frequency variability, corresponds to large bedforms that migrate downstream by erosion of sediment at the windward slope and deposition at the troughs positioned at the leeward slope. The main agents of the downstream migration of these large bedforms, are the superimposed gravel dunes (Hassan and Church, 1994). Sediment deposited at the troughs, becomes buried by the advancing bedforms until the latter migrate further downstream. Nevertheless when the water levels drop during falling discharge and fill, the larger bedforms also reduce in size (Dinehart, 1992), and sediment that was deposited in the troughs (which are below the mean bed level to a depth dictated by the flow event and hence the growth of the large bedborms) is now buried to larger depths until a new competent flow event arises. Apparently, it is the finer material that is predominantly deposited in the troughs of the large bedforms and later preferentially buried to larger depths. This might be a result of the gravel dunes that are able to rework the finer sediment from the bed.

Hassan and Church (1994) studied the burial depth of various-sized fractions in several rivers. Their results indicate that burial of finer grains is likely to be promoted for single events in small or ephemeral streams where scour and fill is local and sporadic. Results of their study are presented in Fig.4.8 and concern studies in various rivers. Although the latter is most probably not the case for our study reach, it is worth noticing their hypothesis concerning the process controlling the preferential burial of finer grains. The increased mobility of finer grains makes it more possible for them to find the scoured areas in the bed whereas their coarser counterparts remain more or less stationary. An analogy could imply an enhanced deposition of finer sediment in the large bedform troughs, yet more mechanisms are expected to play a role in this case.

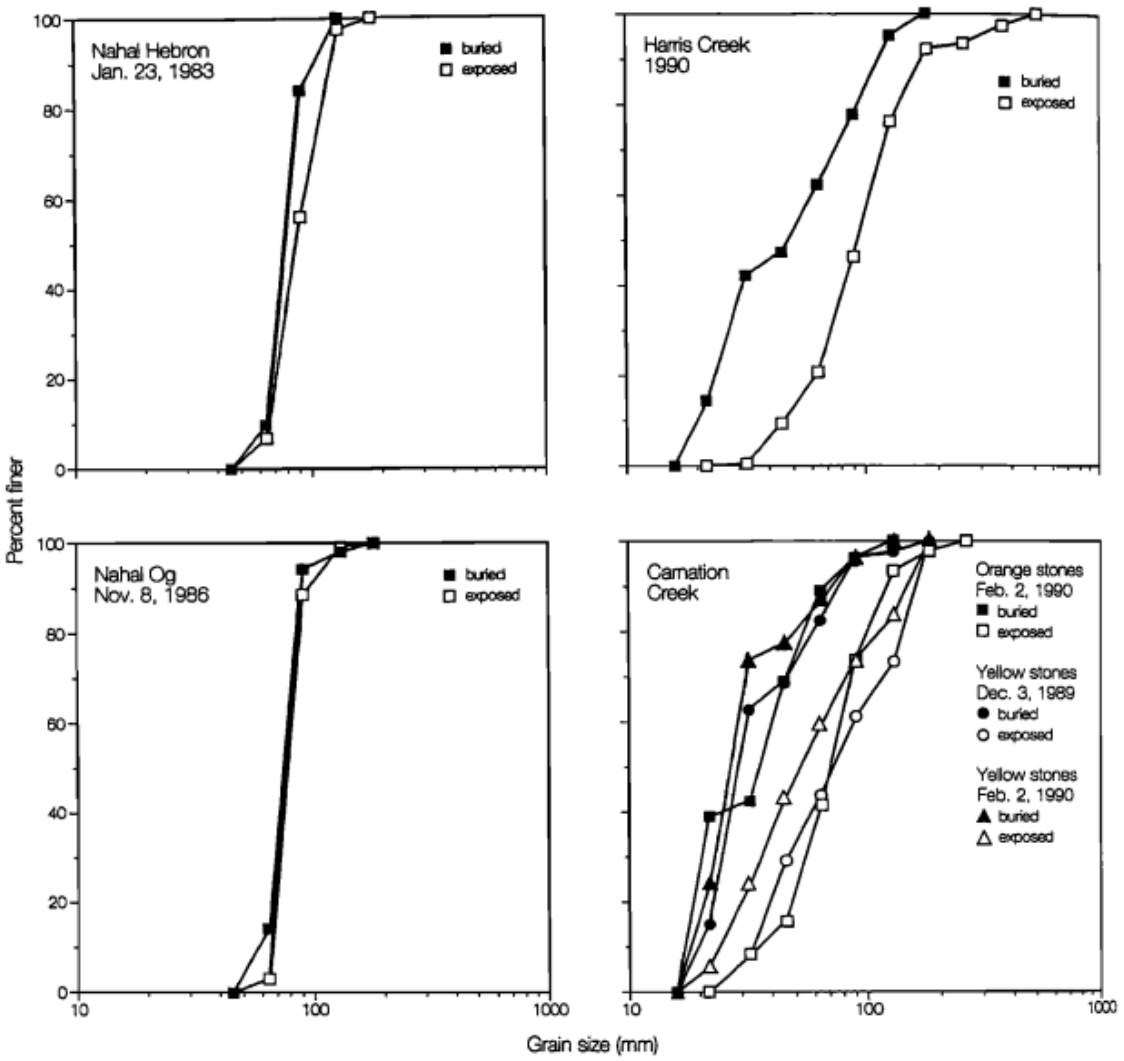

Figure 4.8: Grain size distributions of exposed and buried tracer particles after flow events in the study rivers Hassan and Church (1994) .

4.4 Downstream migration

4.4.1 Findings, hypotheses and further analysis

The main **findings** of the data analysis concerning the temporal changes of tracer concentration in streamwise direction, come from the Iffezheim field experiment. First, it was found that the signals of the various fractions migrated downstream with different speeds (see Fig.2.12). At one hand, grain size selectivity by flow is the obvious mechanism that leads to hydraulic sorting, characterized by faster downstream transport of the more mobile finer grains compared to their coarser counterparts. Nevertheless, the signal of the finest fraction (4/8 mm) was seen to migrate downstream having nearly same (or even lower) speed as the slightly coarser fraction (8/16 mm) (see Fig.2.14). Furthermore, the hydraulic sorting between the finer and coarser fractions was seen to intensify late in the monitoring period with the two finest fractions partly forming distinct signals leading at the front of the bulk nourished sediment volume. Therefore, it can be argued that there are more physical processes than grain size selectivity that affect the downstream migration of nourished sediment.

Moreover, a result of streamwise sorting between the various tracer fractions was that the bulk tracer volume dispersed downstream (e.g. Fig.2.10). Obviously, a nourishment is expected to disperse at a degree proportional to the hydraulic streamwise sorting between its fractions and hence to the sorting degree of the supplied mixture. Another finding from the analysis of measured data, partly opposing the above, was that the narrow-ranged finer tracer fractions dispersed somewhat more downstream compared to the wide-ranged coarser tracer fractions (see Table 2.3). This implies that at least on a fractional level, the grain size range of the various fractions (and hence streamwise sorting at a fractional level) is not the dominant control on regulating the degree of dispersion.

The **hypothesis** that will be discussed in more detail later, is that there are several controls both on streamwise sorting and on the dispersion of the various tracer fractions studied. At first, we consider the effect of flow on the downstream migration and dispersion of the nourished sediment. This effect is expressed by streamwise changes in bed shear stress, as well as by flow temporal variability. With decreasing longitudinal shear stress in a downstream direction, streamwise sorting between the various fractions may be promoted, whereas the opposite may be expected in cases that flood waves bring the faster moving finer sediment to deeper inactive areas of the bed. The latter also implies that the longitudinal dispersion of various fractions may vary accordingly to the varying degree that these are mixed over the vertical direction and thus partly deprived from entrainment and downstream transport.

The streamwise sorting may additionally be controlled by (microscopic) hiding that could explain the nearly identical behaviour between the finest and slightly coarser tracer fraction as well as by (macroscopic) hiding due to the fact that tracer sediment was seen to be vertically arranged while it is transported downstream, such that the finer fractions are found in larger concentrations in the shallow subpavement layer. Finally, it is not only the grain size range of the nourished sediment that defines the degree of streamwise sorting but also the share of each fraction in the designed mixture. That being said, it can be expected that the middle tracer fraction would be faster transported downstream since it has a larger share in the nourished volume and hence will be represented more in the bed as well as in the load. In the same line of thought, the progressively lower availability with time of the finer tracer fractions at the the trailing edge of the bulk volume, in conjunction with the fast downstream advancement of their fronts, may provide an additional explanation (to vertical mixing discussed before), for the increased dispersion of finer fractions.

Although it is not going to be considered in the following as it was not found to be significant for the study reach below Iffezheim, it is worth noticing that different trajectories between nourished fractions along meandering reaches could also control the streamwise sorting and hence the dispersive behaviour of nourished sediment under certain conditions. In the following of the present document, flow and mixed-sediment morphodynamics are going to be discussed in larger detail with respect to their effects on the speeds and dispersion rates of the downstream migrating tracer fractions fed below Iffezheim. The downstream migration of the topographic changes in the Bovenrijn field experiment are briefly discussed in the Appendix.

4.4.2 Mechanisms controlling the speeds and dispersion of the various tracer fractions

Slowdown of coarser tracer fractions along a concave profile .
To start with, let us consider the effect of the longitudinal shear stress on the downstream migration of the various tracer fractions. Rivers tend to have decreasing bed level gradients in a downstream direction accompanied by downstream fining patterns in their bed texture. According to the concept of graded river introduced by Mackin (1948) and supported by later studies (e.g. (Blom et al., 2016)), rivers build concave profiles as they strive towards equilibrium such that they can transport all sediment supplied from upstream. The concave profile is a result of abrasion that breaks larger particles into smaller ones (mainly clay) as they are transported downstream, and selective transport in the sense that a finer particle requires a milder slope to be mobilized. Such decrease in longitudinal slope is associated with a decrease of the longitudinal bed shear stress.

The concave profile of our study reach over a sufficiently large time scale is likely to promote hydraulic sorting between the transported fractions due to a preferential slowdown of the coarser fractions. The time scale for slowdown of transported tracer sediment can be expected to be a function of its relative grain size with the grain size of the bed sediment (Ferguson and Wathen, 1998). This is why particles corresponding to the coarser spectrum of the supplied mixture are expected to experience a preferential slowdown compared to the finer ones when they arrive to reaches of significantly decreasing shear stress.

The study reach below Iffezheim is characterized by a constant shear stress and mild downstream fining to its larger extent (see Fig.2.3). This can partly explain why the speeds of the tracer fractions are nearly constant for the larger period of the monitoring (e.g. Fig.2.13). Downstream from approximately Rkm-380, the hydraulic conditions drastically change in the study reach. In this sense, this is more or less the location where a morphodynamic nickpoint arises. The abrupt increase of the river width (accompanied by a decrease of longitudinal bed slope), leads to relatively rapid downstream fining and lower available bed shear stress for sediment transport. From Fig.2.12 (lower subplot), it can be seen that only the two finer fractions have migrated downstream from the considered nickpoint and only after the campaign of 1999. By 2001 the coarser fractions (16/31.5 mm and 31.5/45 mm) have their fronts at the location of the nickpoint. As a result a strong streamwise sorting arises at the front of the bulk tracer volume, which is mainly a consequence of the slowdown of coarser fractions at the area of the nickpoint. This assumption is made since it is unlikely that the finer tracer fractions would accelerate while entering a region of decreasing longitudinal shear stress.

The effect of flow variability on downstream migration .
One could argue that the overall migration of sorting waves would be augmented with increasing water discharge as a larger bed shear stress becomes available for sediment transport. This would be true, under the condition that the layer of the bed from where sediment is entrained varies proportionally less than the increase of discharge or does not vary at all. While this could be expected for a range of relatively low flows as in the case of the Bovenrijn pilot study (note that the downstream migration of granite was closely correlated with measured discharge at Lobith (see Fig. 3.15)), it is likely not the case for flood wave of 1999 in the study reach below Iffezheim. In fact, despite the fact that fractional waves were migrating at a reach with more or less uniform shear stress (well upstream from Rkm-380), their measured speed was not increased after the occurence of the 1/100 years flood wave (the downstream speeds of the centroids remained more or less constant in Fig.2.13).

At this stage it would be useful to consider an approximation for the migration celerity of a linear sorting wave carrying changes in the bed composition, in order to explain the physics behind this behaviour. Since the fractional waves change the composition of the bed sediment as they migrate downstream, can be seen as sorting waves. The approximation for the kinematic sorting wave we treat here is given by Mosselman et al. (2008) and reads;

$$C_{mix} = \frac{\mu q_s}{\delta(1-\varepsilon)} \tag{4.2}$$

where $\mu = \frac{D_{mT}}{D_m}$ is the ratio between the average bedload grain size (often assumed as equal to the average grain size of the subsurface) and the average grain size in the active layer

q_s is the total bedload transport per unit width
ε is the porosity in the bed and
δ is the thickness of the active layer where from sediment of the bed is engaged in sediment transport processes.

Employing this model, we would expect that with increasing discharge increase of q_s, since a larger bed shear stress is generally exerted on the bed, but also an increase of δ for instance by emergent gravel dunes or large bedforms in our study reach that have the ability to rework sediment from deeper strata. Finally, an increase of D_{mT} following from a more competent flow, would probably lead to an increase of μ since, the activated sediment from deeper strata is finer for the study reach and therefore D_m also most probably increases. Therefore, there are certain conditions under which changes in the composition of the bed texture would be accelerated under a flood wave but this is not necessarily always true.

Overall, from the data analysis follows that the effect of 1999 flood was more prominent in enhancing vertical mixing of the tracer sediment compared to accelerating the downstream migration. In fact, since finer tracer gravel fractions were buried in larger depths compared to coarser gravel fractions, it could be expected that they experienced larger residence periods in inactive areas of the substrate, before the were mobilized again by a next high flow event. This implies that floods capable of forming large transport bodies (resulting from scour and fill), may be overall more efficient in arresting streamwise sorting by mixing the finer nourished sediment over larger depths. This has also consequences for the dispersion rates of the various tracer fractions. If part of the finer fractions is to be buried deeper, where it is less probable to be entrained by flow and transported downstream, the longitudinal dispersion rate would increase. This is because the part that is still transported by the flow still advances the front of the finer fractional wave downstream.

Mixed-sediment morphodynamic processes .
Let us now focus on processes controlling the entrainment and transport of the various tracer fractions from the bed, considering for simplicity flows closer to the representative mean discharge. At gravel beds with poorly sorted sediment (microscopic) hiding effects may become very important in controlling the transport of various fractions at the bed surface. Under these conditions finer grains hide behind coarser ones and therefore require a larger shear stress to be entrained. On the contrary, the exposure of coarser grains to the flow increases. From the data analysis it was seen that the finer tracer fraction inside the fine gravel spectrum ($< 16mm$) lagged behind the coarser fine gravel throughout the larger part of the monitoring period. A rough estimate reveals that the critical Shields parameter for incipient of motion increases by a factor 3 for the finest fraction in the mixture (4/8 mm) and by a factor 1.5 for the coarser fine gravel fraction (8/16 mm) if hiding effects are explicitly accounted for, using the Ashida and Michiue formulation.

Not only grain size selective transport but also hiding effects are regulated by the availability of the various considered fractions in the bed surface. At one hand, the more available a fraction becomes at the bed, the more probable it is to be transported downstream. Additionally, (microscopic) hiding depends on the degree that finer or coarser fractions are available at the bed surface. In turn, the availability of a certain fraction at the bed surface is partly controlled by its share in the nourished volume. That being said, we would expect for instance the 16/31.5 mm fraction to be relatively more represented in the load, owing to its largest share in the nourished volume (see Fig.2.6). This means that it is transported downstream relatively faster compared to a hypothetical case that all fractions would have been fed at equal amounts. Nevertheless, the effect of the supplied mixtures on the availability of a certain fraction at the bed surface can be expected to be more dominant with decreasing time from the feeding.

A more persistent effect on the availability of the various fractions at the bed surface results in the Iffezheim study case, from the fact that nourished sediment is quickly structured over the bed such that additional (macroscopic) hiding is provided for the finer fractions. Although the active layer of the bed may be expected to exceed the shallow depth of 30 cm studied even for more probable low flows, the finer fractions will still experience additional sheltering due to the fact that they have larger concentrations at the subpavement. Since the opposite is true for the coarser tracer fractions, eventually it can be assumed that the effect of macroscopic hiding is to arrest streamwise sorting, adding to the effects of microscopic hiding and mixing of finer material to deeper strata from flood waves. At the same time considering the presence of a downstream fining pattern in a mitigated reach, this enhanced vertical mixing of finer tracer fractions provides conditions for

relatively delayed entrainment at the upstream parts compared to downstream parts (due to an increased ability of finer grains in protruding into the subsurface when the pores of the bed surface are generally larger). Nevertheless, abrasion processes may be relevant in regulating this behaviour since they tend to reduce the size of the grains during transport. Overall, such a relatively delayed entrainment upstream would act as an agent of longitudinal dispersion for the finer grains. The relevance of this assumption for the study reach is questionable as the downstream fining patterns are mild for its larger extent.

To conclude, it is reasonable to assume that the finer fractional waves migrated downstream relatively decelerated compared to the rest, experiencing microscopic hiding effects, enhanced vertical mixing both close to the bed surface (macroscopic hiding) and towards deeper inactive zones (from the flood wave of 1999), and finally due to their under-representation in the feeding volume. Only the longitudinal decrease of the bed shear stress can be expected to have decelerated the coarser fractions, yet late in the monitoring period. When only the two finer fractions are under consideration, it can be assumed that mainly grain size selectivity and (microscopic) hiding effects differentiate their downstream migration, yielding overall a nearly identical downstream migration between the two. This is stated since their vertical mixing was found to be also more or less identical (see Table 4.2), while they shared equal volumes in the nourished sediment.

When it comes to the different dispersion rates between the fractional waves studied, enhanced vertical mixing of the finer fractions may be well assumed to dominate their behaviour.

4.5 Coarsening of Bovenrijn

4.5.1 Findings, hypotheses, and set-up of further analysis

In Chapter 3 we discussed about the textural changes in the Bovenrijn. The main **finding** was that the sediment of the bed surface has coarsened from 1995 to 2016. It was seen that during the period 1995-2008 the d_{50} of the bed sediment increased by almost 5 mm while the d_{90} by ca. 10 mm across the study reach (see Fig.3.7 and 3.8). Moreover, a spatial trend was revealed with respect to the temporal increase in the diameter of the grain size. Especially for the period 2008-2016 the increase in grain size was stronger with decreasing distance from the upstream end of the study reach. The **hypothesis** is that there are two main potential reasons for the coarsening observed in our study reach. These are river bed degradation and coarsening of upstream load.

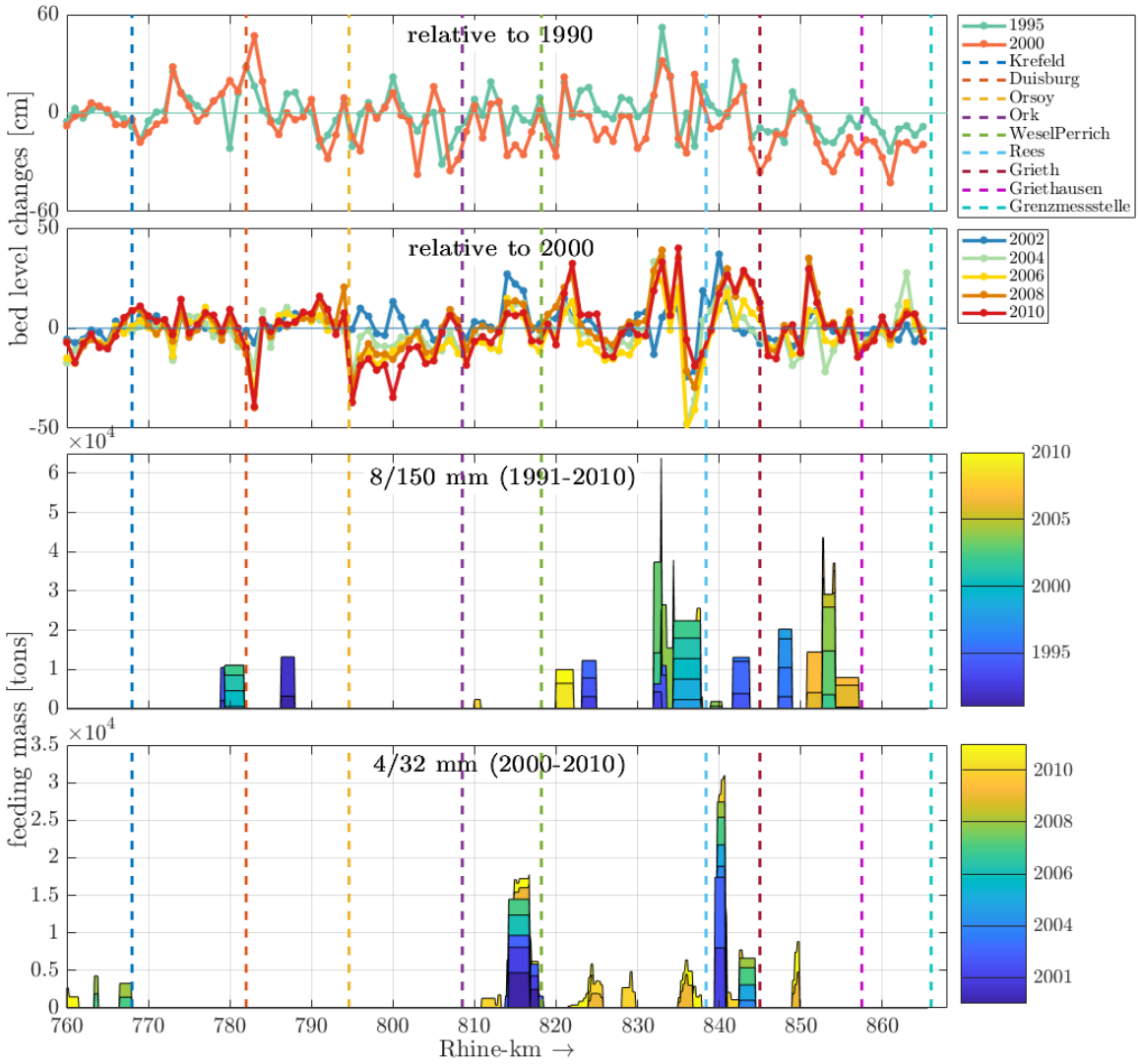

Figure 4.9: At the top two panels, the bed level changes in the Lower Niederrhein are demonstrated for the periods 1990-2000 and 2000-2010. The study reach is located at the downstream end between Griethausen and Grenzmessstelle (data source: RWS-ON, (Frings et al., 2014a)). The bed in the depicted reach has stabilized overall after 2010. At the bottom panels, the mass of feeding in the Lower Niederrhein is given up to 2010. The two figures differentiate based on the grain size characteristics of added sediment (data source: BfG, (Frings et al., 2014a)).

Coarsening of the surface texture is a known response of rivers subjected to degradation (e.g. (Frings et al., 2014a; Blom, 2016)). This was prominent during the period 1990-2000 when the bed has lowered across the whole stretch by nearly 20 cm. This can be seen from the top panel of

Fig.4.9 where the bed level changes during the period 1990-2010 are presented. The study reach is located downstream from Griethausen at the right hand side of the subplots. There may be several contributing factors for the observed degradation. It could follow for instance from a deficit of sediment supply from upstream or dredging activities at the reach. Sieben (2009) argued that both were contributing to the bed level changes in the study reach to some degree. Another possible cause could be an increase of the overall sediment transport capacity as a response to narrowing of the past to which the river may still be responding by down-cutting. An increase of transport capacity could also follow from degradation at the downstream adjacent reaches and consequent lowering of the base level. To conclude, it is also likely that a combination of all the mentioned triggers may be controlling the past, present and possibly the future adjustment of the bed levels in the study reach, with each one of them having a more significant signature in different time periods. Although the core objective of the present analysis is not to assess the causes of bed degradation at the study reach, it is a morphodynamic response which potentially closely relates to bed texture coarsening.

Not only degradational conditions may lead to coarsening of the bed. An increase of the caliber of the supplied load from upstream could also coarsen the texture, not necessarily accompanied by significant bed level changes. Several factors may be contributing to the coarsening of the upstream load. For example, the texture of the upstream adjacent Niederrhein has coarsened between 1980 and 1995 (Frings et al., 2014a) (see Fig.4.10). This may be due to the past degradation (Fig.1.5) but also due to the feeding of sediment that is significantly coarser that the bed sediment. Such a coarsening of the texture further implies that the sediment available to be transported by the flow gets coarser leading eventually to a coarsening of the load. In the same line of thought, we have already seen how coarse sorting waves monitored during the Iffezheim field experiment migrated slowly downstream. Similarly, we can now imagine sorting waves of coarse nourished sediment supplied at the downstream reaches of Lower Niederrhein, entering Bovenrijn and coarsening its texture.

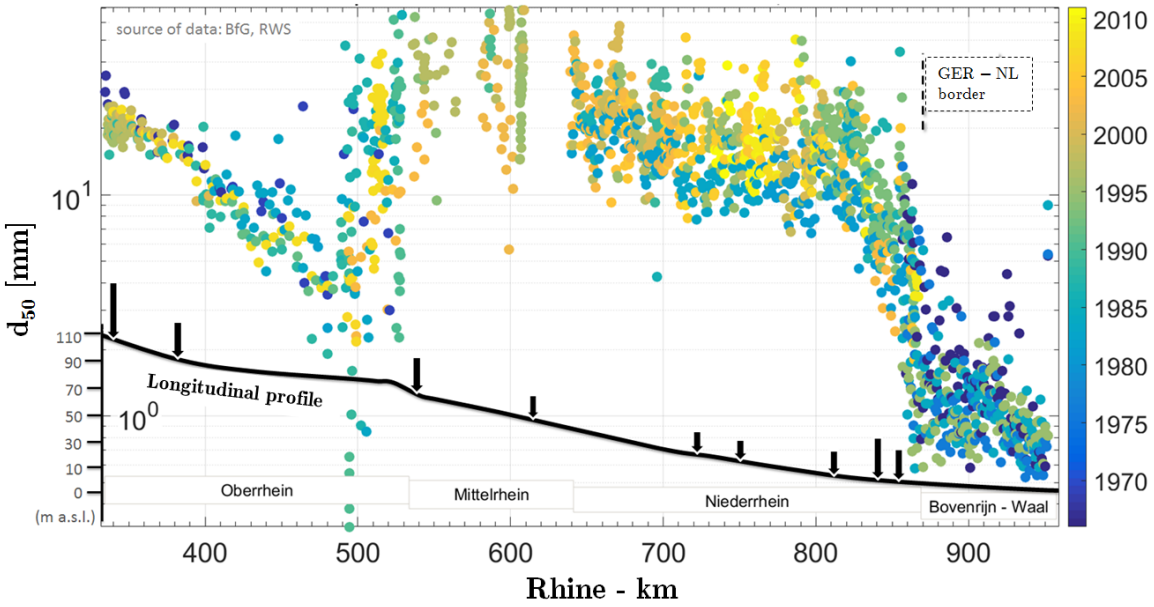

Figure 4.10: The temporal evolution of bed surface texture is given for the freely-flowing Rhine in log-scale (Emmanouil, 2017). Along the longitudinal profile (solid black line) the main sediment dumping locations are denoted with black arrows. For the Niederrhein reach, a large part of the supplied sediment consists of very coarse gravel and cobbles. A coarsening of the the bed texture relative to 1980s, (when no nourishments were performed) can be observed. source of data: Frings et al. (2014a) and Rijkswaterstaat

.

So, what additional processes come into play in the bed coarsening of the Bovenrijn, and how are the spatial patterns explained? Obviously there is no simple answer to these questions. Nevertheless, in the following we will attempt to provide reasonable explanations focusing on a) temporal variations of the controls and b) potential important processes during the adjustment of the reach.

4.5.2 Bed degradation

Let us focus on the bed coarsening of Bovenrijn between 1995 and 2008 as revealed by the soil samples. This corresponds to a period of enhanced degradation (1995-2000) and a period of stabilizing or even aggrading bed levels (2000-2008). Vibracore measurements at the study reach taken in 2000 reveal a coarser texture compared to 1995. Therefore degradation overlapped in time with the coarsening of the Bovenrijn.

Characteristic examples of bed coarsening associated with bed degradation can be found at reaches situated downstream from dams. There the lack of sediment supply leads to rapid degradation and extreme coarsening expressed by preferential erosion (or winnowing) of finer bed material by the flow (Dietrich et al., 1989). This follows from grain size selectivity; finer grains are more mobile than coarser grains and thus easier for the flow to erode. Examples have been reported for many rivers such as the Colorado river and the Clackamas river where static armour layers have formed downstream from dams paving the river beds (Grant, 2012). Additionally, Frings et al. (2014a) underline how bed degradation in the Lower Niederrhein was more prominent at the reaches where the sand content of the bed subsurface (10-50 cm) was larger, especially indicating the downstream part of the gravel-sand transition where our study reach is located.

Another process that comes into play in degradational conditions and can add to the coarsening is the exposure of coarser historical deposits that may lie in deeper strata. Such a stratigraphy (taken by lithographic surveys) is presented for the study reach in Fig.4.11.

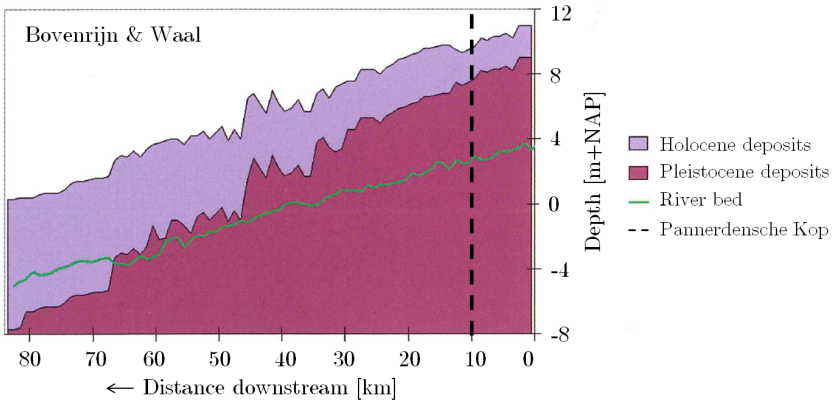

Figure 4.11: Historical deposits of the Bovenrijn and Waal as taken by lithographic surveys, plotted with the level of the Rhine in 2000s. source: Ten Brinke (2005)

It can be seen that coarser Pleistocene deposits lie beneath finer Holocene sediment. Nevertheless, since in the study reach (right from the dashed black line) the river bed has cut for several years well into the coarser Pleistocene deposits, we may assume that this process is not very likely to have controlled the temporal coarsening during 1995-2000.

So far we assessed the relevance of morphodynamic processes that come into play in coarsening under degradational conditions. Nevertheless, coarsening can act as an opposite triggering factor on the bed levels by limiting degradation. This is the case since as the mean grain size of the bed increases, a larger shear stress in required by the flow to mobilize sediment. Elaborating, if we now consider poorly sorted sediment which is typical for our study reach, rather than a mean diameter for expressing bed texture, we can assume that after the depletion of the finer grains even a larger shear stress is needed by the flow than before, to transport the coarser grains that remain in the bed. This is due to the fact that the latter become less exposed to the flow as the content of the finer grains in the bed decreases (Parker and Klingeman, 1982).

In that sense the coarsening of the bed surface texture over the study reach may explain to some extent the stabilized bed levels after a long period of degradation up to 2000. At this point it is worth to note that a comparison of earlier soil samples taken during a period with continued degradation of the study reach (i.e. 1976 and 1984) with 1995 samples revealed no temporal trend in grain size of the bed sediment in a previous study (Emmanouil, 2017).

4.5.3 Coarsening of the sediment supply

So far we assessed the coarsening of the Bovenrijn as a response to its degrading bed during 1995-2000, and we additionally discussed the limiting effect of the former on the latter. Let us now focus on a larger period and assess how the caliber of the load entering from upstream might have influenced the texture in our study reach. To this end we focus on the transport rates of the bedload with its grain size distribution measured at Giethausen located exactly at the upstream end of Bovenrijn (km 857.5) and 7 other stations located further upstream at Lower Niederrhein (Rhine-km 760-857.5). The available measurements span from 1990 to 2010 and thus correspond partly to the period that the soil samples revealed coarsening in Bovenrijn. Tab.4.3 summarizes the locations and the available period of measurements per measuring station studied.

Table 4.3: Sediment transport measuring stations

station	Krefeld	Duisburg	Orsoy	Ork
km	768	782	794.6	808.5
period	1990-2010	1991-2010	1994-2006	1991-2010
station	WeselPerich	Rees	Grieth	Griethausen
km	818.2	838.4	845	857.5
period	1990-2009	1990-2009	1992-2009	1990-2009

At this point it is worth to mention that by studying the bed load we capture only a part of the supply to Bovenrijn. According to Frings et al. (2014a), half of the morphologically active supplied sediment to Bovenrijn enters as suspended load. Moreover, washload (clay, silt) exceeds by an order of magnitude the load entering as suspended sand and bed-load combined. Unfortunately, available data do not allow for assessing temporal trends in the suspended load and wash load at the upstream end. Finally, sediment transport measurements are inherently associated with large uncertainty and so does their analysis. In the Appendix the related uncertainty is discussed and motivation for certain choices made for the following analysis are explained. The main conclusion from the uncertainty analysis is that temporal trends concerning the total bedload rates may not be considered (although included in the figures presented in the following). On the contrary, we may consider temporal changes concerning the grain size distribution of the load.

Analysis of temporal trends in grain size distribution of bedload .
Focusing on the temporal evolution of various contents in the load measured at Griethausen during 1991-2010 (dashed lines in Fig.4.12), we can observe the following:

- The transported load consists of coarse gravel less than 10% before 2000. Afterwards, until the end of available measurements the coarse gravel content scatters systematically up to 20% even for discharges lower than the mean discharge at Lobith.
- The temporal redistribution of fractional contents evolves predominantly between sand and fine gravel that consist the larger part of the load (ca. 80%).
- The sand content decreases slightly up to 2000 starting at 1994, while later increases to 60% before finally it reaches down to 10%.

From the above observations it is useful to consider from now on two periods; 1990-2000 and 2000-2009. Before drawing final conclusions about how these findings may relate to the coarsening of Bovenrijn, let us first search for possible controls resulting in these trends.

The discussed trends in respective periods are also revealed in measurements taken from other stations along Lower Niederrhein. The time series we will refer hereby can be found in the Appendix.

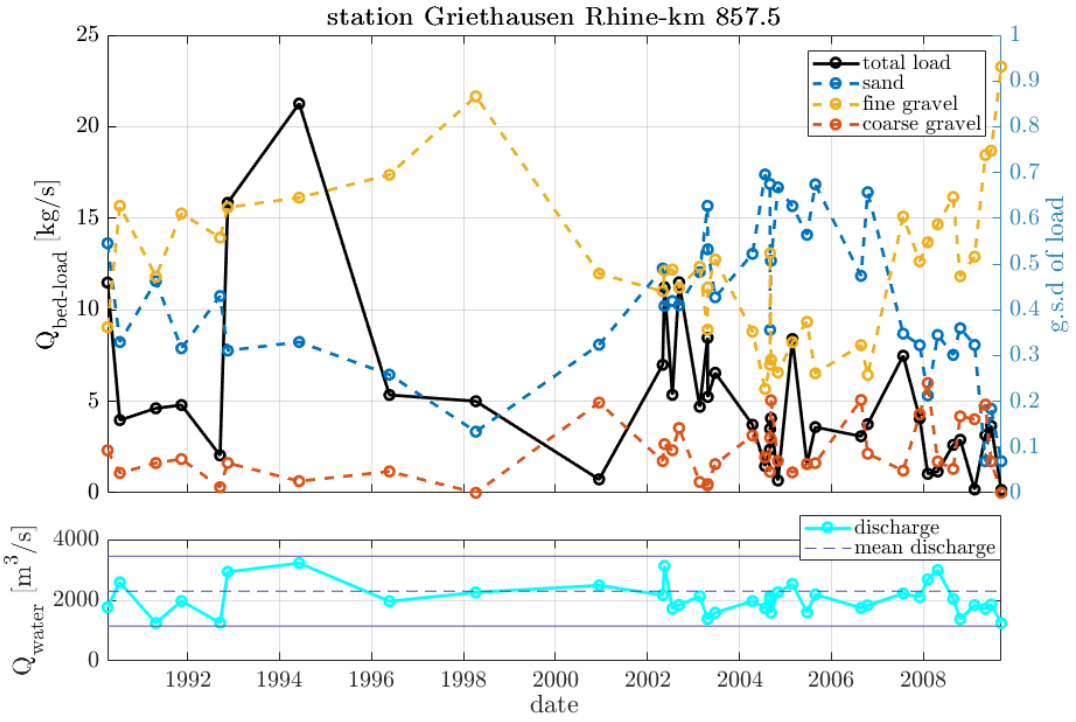

Figure 4.12: Sediment transport measurements at discharges ±50% $2300 m^3/s$ at Griethausen during 1990-2009. data source: BfG, Frings et al. (2014a)

Morphodynamic trends at Lower Niederrhein during 1990-2000 .
Focusing on the first period i.e., 1990-2000 the decrease in sand content transported as bed-load can be identified also in measurements taken in Duisburg (Fig.G.2), Rees (Fig.G.6) and Grieth (Fig.G.7). Measurements of other stations do not reveal such a systematic increase of gravel content at the expense of sand content.

So why is this trend revealed in measurements only for specific stations? To address this question we may concentrate on differences between the controls on the reaches of various stations. Bed degradation as can be seen in the top subplot of Fig.4.9, would have had an effect (by coarsening of the bed texture and consequently of the transported load) for most of the measuring sites concerning the first period; by erosion either at the stretch were measurements were taken or at the adjacent upstream short reaches. Nevertheless, it was most profound at Grieth where the bed incised at a rate of 3 cm/y during the whole studied period. Other potentially affected measuring sites are found in Giethausen (after 1995), Ork (up to 1995 at the upstream reach), WeselPerrich (after 1995 at the upstream reach) and Orsoy (up to 1995 at the upstream reach).

At the start of the study period in 1990, sediment nourishments were initiated in the Lower Niederrhein reach aiming at stabilizing the bed (Frings et al., 2014a). These consisted mostly of coarse gravel and pebbles (8/150 mm) generally coarser than the bed sediment. The third subplot of Fig.4.9 presents the feeding mass per stretch and year at Lower Niederrhein. The locations of the sediment transport measuring stations are denoted by dashed vertical lines. For all stations whose measurements revealed an increase of gravel content at the expense of sand content between 1990 and 2000 (Duisburg, Rees, Grieth and Giethausen), at a distance of $\leq 10km$ we can observe nourishments at the same period (denoted by dark blue color in Fig.4.9). Upstream from Krefeld, Ork, and WeselPerrich no such nourishments were reported. Note also, that sand transported as bedload increases significantly with downstream distance after km-820, where the gravel-sand transition starts (Frings et al., 2014a). That being said, a growing effect from 8/150 mm nourishments should be also expected with downstream distance.

Morphodynamic trends at Lower Niederrhein during 2000-2010 .
Let us now focus on the period of measurements after 2000. We already mentioned that at Gri-

ethausen measuring station, we observe a systematic increase of coarse gravel content in the transported load together with an increase of sand content. Nevertheless, only the former persists throughout the whole considered period. The sand content decreases again significantly after 2007 as the fine gravel content abruptly increases to 60% or more until the last available measurement (see Fig.4.12). We can also observe the mirroring between the temporal trends of sand and fine gravel, at Grieth and less clearly at Rees, WeselPerrich and Ork where the scatter increases. Measurements at other monitoring stations located further upstream (Orsoy, Duisburg and Krefeld), scatter strongly around stable values.

Shifting our attention to the controls at Lower Niederrhein after 2000, bed incision was demonstrated at at two stretches. First, during the whole studied period (2000-2010) along 795 to 805 Rhine-km which was more or less stable before (see Fig.4.9). At this stretch Tertiary deposits of clay and sand lie very close to the bed surface (Frings et al., 2014a). Second erosion continued up to 2006 at a short stretch upstream from Rees. Very little erosion was seen only locally elsewhere while the general trend reveals aggradation. Note that the Bovenrijn bed has also stabilized during this period.

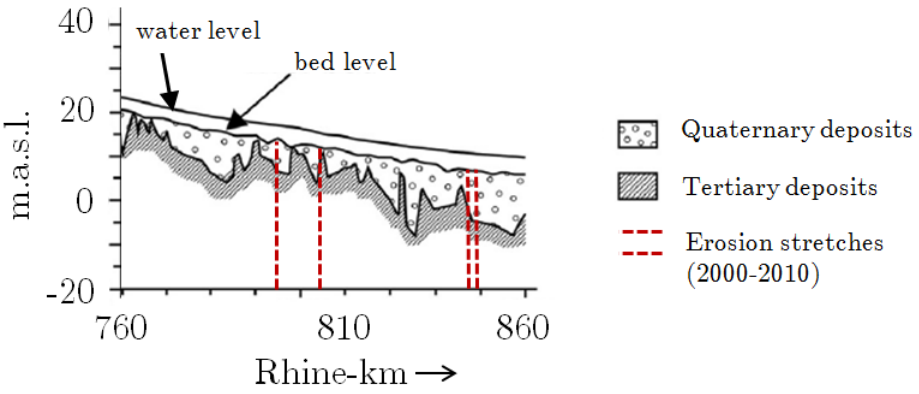

Figure 4.13: Stratigraphy of the Lower Niederrhein by (Frings et al., 2014a). Erosional stretches during 2000-2010 are denoted by red dashed lines. Quaternary deposits consist of sand and gravel while Tertiary deposits of sand with varying clay contents.

Moreover concerning the feeding operations, sediment at the range 8/150 mm was nourished predominantly just upstream from Bovenrijn in two periods; 2002 to 2005 and 2006 to 2007. At slightly earlier periods sediment was also nourished upstream from Rees at the stretch with continued erosion up to 2006. Furthermore, finer gravel (4/32 mm) was added in the river system also concentrated at two locations; upstream from WeselPerrich and downstream from Rees. Again owing to the downstream fining of the bed texture at Lower Niederrhein we can consider that these nourishments (typically consisting of equal mass between the fractions of 4/8 mm, 8/16 mm, and 16/32 mm), were relatively coarser at downstream from Rees.

Based on the complex controls on Lower Niederrhein during this period, it would be crude to make strong statements about the temporal increase of sand content after 2000 that we observe in some monitoring stations. Nevertheless, we can assume three processes potentially responsible for this. First, newly introduced 4/32 mm nourishments (typically not including sand) might have mobilized the coarse sediment previously fed to the system. The latter would mean that sand previously protected from entrainment by the immobile coarse gravel and pebbles would now be more exposed to the flow. Such a mobilization is possible since addition of finer sediment to the bed may lead to increasing exposure of coarser grains to flow. Additionally, flume experiments conducted by Venditti et al. (2005) proved the ability of fine gravel addition to mobilize static armor, by increasing the smoothness of the bed, and hence the shear stress exerted by the flow.

Another assumption is that the sand content was increasing to some extent, due to the continued degradation at 795-805 Rhine-km, wehre sand and clay Tertiary deposits lie very close to the river bed. It is likely that eroded sand from this stretch migrated downstream as a very fast sorting wave leaving its signature in the bedload nourishments taken further downstream almost instantly.

Finally, we can assume that the temporal increase of sand content simply denotes that the sorting waves in the range of fine gravel -excited by sediment feeding in the beginning of 1990- have

effectively migrated further downstream with their trails exiting the respective sediment transport measuring sites by 2000. Further the fact that this increase is only seen temporarily, in the same line of thought, denotes that new sorting waves appeared due to the continued nourishments after 2000. If this is the case we can estimate a time scale of 5 years for the duration that their effects were felt at downstream locations from the feeding stretches. In fact, a tracer study at Lower Niederrhein (fed at km 817-818) in 2001 (Abel, 2001), revealed that sorting waves in the range of fine gravel migrated downstream with a celerity of ca. 7-10 km/year corresponding well with our estimate above extracted by the sediment transport measurements. This is presented in Fig.4.14, where we can additionally observe the streamwise hydraulic sorting between the fine and coarse gravel tracer fractions.

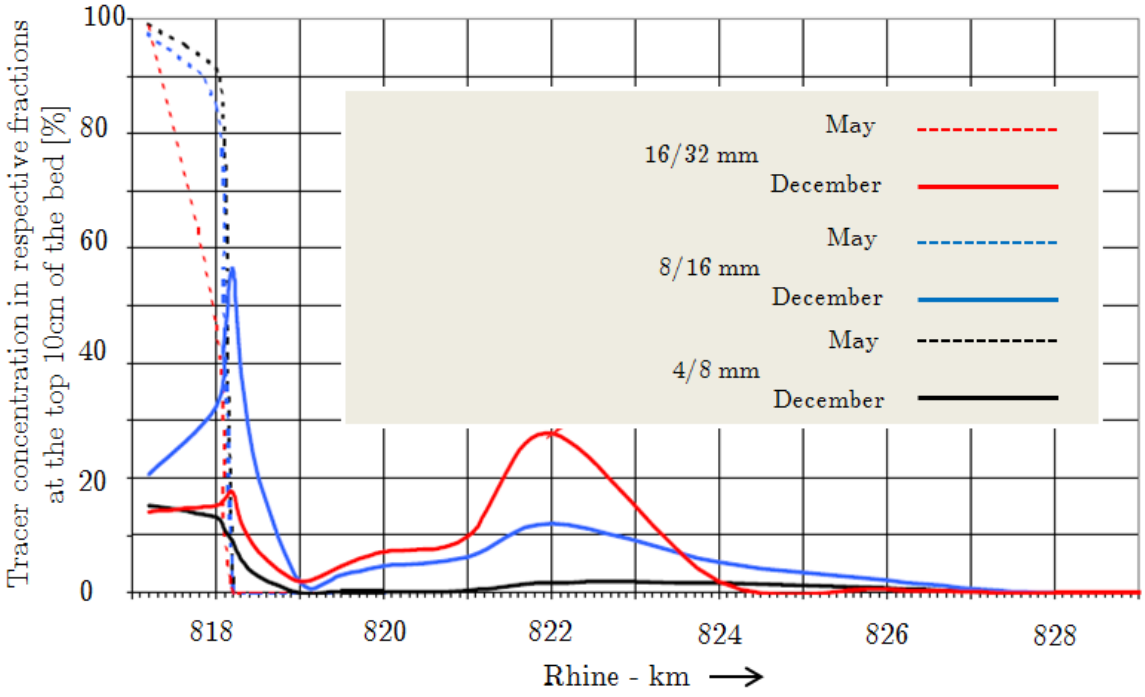

Figure 4.14: Monitoring of the 4/32 mm tracer fractions in Niederrhein in 2001. source: Abel (2001)

Sorting waves captured at Griethausen measuring station .
Having said that let us now focus on the measurements of Griethausen measuring station and the contextual morphodynamics at the short upstream adjacent reach. The sorting seen in Fig.4.14 can be expected to be more pronounced at the reaches located further downstream at Lower Niederrhein. This is because the presence of the gravel-sand transition yields a streamwise fining of the bed texture, combined with decreasing slope in a downstream direction starting from Rhine-km 820 (Frings, 2011). As we explained earlier, tracer fractions may experience a long-term slowdown as they migrate downstream on a concave bed. This slowdown is likely to affect more the coarser fractions enhancing the hydraulic sorting.

If our theory about the ability of sediment transport measurements to capture such sorting waves is true, this additionally implies that the persistent increase of coarse gravel content after 2000 at Griethausen, may be better assigned to slowly migrating sorting waves linked with coarse gravel and excited by earlier nourishments (8/150 mm in 1995) 10 km upstream, rather the ones possibly excited by similar nourishments during 2002-2007 at a closer distance upstream. We assume this, since a new sorting wave related with fine gravel (from the later nourishments) which is expected to lead appears at the measured data after 2007. This assumption corresponds to a celerity of 2 km/year for coarser gravel sorting waves, which is plausible considering the propagation of similar waves at the Iffezheim field experiment. The longer residence time of these waves (more than 10 years) compared to the sorting waves linked with fine gravel fractions (less than 5 years) follows directly from their lower speed. An additional implication is that the effect of new sorting waves linked with coarse gravel fractions is not yet resolved in the available measurements at the upstream

end of Bovenrijn. Said in other words, this increase of coarse gravel content in the bedload supplied to Bovenrijn is likely to have persisted or even aggravated after 2010.

4.6 Conclusions

Concerning the main physical mechanisms that control the lateral dispersion of nourished sediment in the Iffezeheim the conclusions drawn can be summarized as follows.

- Since the larger part of the nourished sediment corresponds to the coarse gravel spectrum, mechanisms such as gravity pull and shoaling of flow that bring sediment to the deep outer bends of the meanders are likely to be dominant.
- Sediment transport measurements indicate that for more probable low flows, sediment transport take part predominantly at the deep outer bends of the study reach, with little sorting even between gravel and sand fractions.

Under the assumption that the actual characteristics of granite migration are observed from Medusa measurements in the Bovenrijn, the main conclusions concerning granite's trajectory are as follows.

- The fact that the transverse slopes are far from maximal at the area where granite has reached so far denotes that gravity pull is not very effective on its coarser grains.
- Moreover, any shoaling of flow over the point bar is most probably counteracted by negative pressure gradients resulting from deceleration over the nourishment.
- Due to the topography and the relevance of mechanisms discussed above, at that area of crossing between the two meanders, lateral sorting patterns were absent, as indicated from the vibracore measurements taken in the past. Further downstream, it may be expected that the coarser granite grains will be sorted under the effect of the relevant physical mechanisms.

Concerning the vertical mixing of tracer sediment in Iffezheim field experiment the main conclusions concerning the dominant physical mechanisms are the following.

- The mechanisms that were excluded from being relevant in the study reach were burial due to degradation as well as under point bars at meander inner bends. The former would affect mostly the vertical mixing of coarser material as they reside further upstream where aggradational conditions are dominant, whereas the latter would be the case only if the various tracer fractions would follow a different trajectory which was not indicated from the analysis of lateral dispersion of nourished sediment.
- For the preferential mixing of finer tracer concentrations deeper into a shallow bed layer three mechanisms were found to have the potential to be dominant. The first was vertical winnowing of finer material when larger grains move.
- The second mechanism discussed was depositional tendency and filling of pores of the surface framework clasts by the finer material.
- Finally, under aggradational conditions a depositional flux may bring finer bedload sediment buried as bedforms advance downstream.
- The overall vertical structure of tracer sediment denotes that nourished sediment tends to maintain the vertical sorting pattern in the study reach, by forming a mobile armour which provides additional sheltering to the finer sediment (macroscopic hiding).
- During higher flows, as the flood wave of 1999, there are two main scales of deformation in the study reach. Finer gravel dunes (larger frequency) are superimposed over large bedforms (low frequency), and have as a result the preferential burial of finer material in the deep troughs. This is related with the increased mobility of finer fractions compared to their coarser counterparts.

Concerning the dominant physical mechanisms on the temporal changes of tracer concentration in downstream direction the main conclusions about Iffezheim field experiment are summarized in the following.

- The longitudinal decrease of bed shear stress promoted streamwise sorting between the various fractions by preferential slowdown of coarser sediment. This was effective later in the monitoring campaign.
- Although an increase of discharge was linked with faster downstream migration in the Bovenrijn, the flood wave in 1999 was not found to have increased the speeds of various tracer fractions nourished below Iffezheim. It is likely that instead vertical mixing processes were enhanced. The latter is assumed to arrest streamwise sorting by burial of faster finer fractions in deeper inactive bed areas. In turn dispersion of finer fractions is enhanced due to vertical mixing processes.
- Hiding effects at the bed surface are likely to arrest streamwise sorting between the various tracer fractions. This was the most dominant mechanism on the lagging of the finest fractions behind the slightly coarser fraction.
- Initially, the larger availability of the middle tracer fraction in the supplied volume is expected to have increased its downstream migration speed compared to a case that all fractions would have been supplied at equal volumes. This also implies that the downstream migration of finer fractions was less promoted compared to their coarser counterparts.
- Macroscopic hiding as well as microscopic hiding is expected to have arrested strong streamwise sorting by decelerating the finer tracer fractions. Nevertheless, the most prominent effect of the larger mixing of finer fractions concerns the observed dispersion rates.

Finally the conclusions drawn with respect to the main physical mechanisms controlling the textural changes in Bovenrijn can be summarized as follows.

- During the first studied period (1995-2008), both degradation and increased caliber of upstream load are associated with the coarsening of the bed texture. Especially degradation is expected to have coarsened the texture of the Bovenrijn, predominantly by downstream winnowing of finer sediment from the bed.
- The coarsening of the texture during this period has probably also contributed to the halting of degradation which was initiated more or less since 1934.
- Coarsening of upstream load during this first period is expressed by a persistent increase in the representation of coarser gravel ($\geq 16mm$) in the supplied bedload from upstream. This was detected since 2000 in the available sediment transport measurements at Griethausen. We assume that it is more likely that this might have been a result from sorting waves excited by the nourishments of 8/150 mm material approximately 10 km upstream during 1995-1998. The nearly uniform pattern of coarsening in Bovenrijn, as revealed from the comparison of 1995 and 2008 soil samples implies that the contribution of the bed degradation during 1995-2000, was at least as important as the increase of caliber of the upstream supplied load.
- Concerning the second period of coarsening (2008-2016), we hypothesized a continued input or even further increase of the representation of coarse gravel in the supply (the available sediment transport measurements span up to 2009), as a result of the 8/150 mm nourishments concentrated exactly at the upstream end of the reach during 2005-2007. Therefore, accounting for the stability of bed levels, we conclude that the continued coarsening especially closer to the upstream end of the reach is closely linked with nourishments performed upstream.

chapter

FIVE

CONCLUSIONS AND RECOMMENDATIONS

5.1 Conclusions

Sediment nourishments with mixed-sediment have become an attractive alternative to hard measures in counteracting river bed degradation. Due to the large degree of uncertainty concerning mixed-sediment morphodynamics, river authorities conduct field studies to collect data that will help in the calibration of morphological models, used to design effective nourishments.

In the present study, we conducted an analysis on available data from two field experiments that monitored the fate of mixed-size nourished sediments at the mitigated reaches. In the first case, we study data from a 5 year monitoring campaign at the reach below the most downstream weir in the Rhine river (Iffezheim). Second, we studied the early evolution of the nourishment of the pilot study initiated in 2016 in Bovenrijn, another reach of the Rhine situated further downstream. Despite the early stage of morphodynamic changes linked with the nourishment, because of intensive monitoring of the pilot data are collected in dense time intervals from bed surveys, radioactivity measurements for the detection of tracer sediment as well as soil samples.

In both study cases we focus on the migration of nourished sediment and the main physical processes resulting from the feedback between flow and mixed sediment morphodynamics. For the Bovenrijn case we additionally focus on the textural changes that to some extent are a result of the nourishments performed upstream. Answering the research questions presented in Chapter 1, the main conclusions of the present study are summarized in the following.

5.1.1 Downstream migration of mixed-size nourished sediment

What characterizes the downstream migration of mixed-size nourished sediment fed in lowland rivers?

When mixed-size sediment is fed into river reaches, it migrates downstream having a dispersive behaviour, as a result of the streamwise sorting between its various fractions. From the data analysis of the Iffezheim field experiment the main conclusions from this study concern first the fact despite the dominance of dispersive behaviour, all parts of the bulk tracer volume (front, centroid and trailing edge) were found to migrate downstream, i.e., a significant component of translation was observed. Furthermore, in most cases the degree of downstream migration varied between the various tracer fractions, yet was more or less constant throughout the study period for each one of them despite the occurrence of a 1/100 years flood event. Finally, we found that not only the downstream migration speeds varied between the various fractions but also the dispersion rates. The finer sediment were seen to disperse more compared to their coarser counterparts. Partly opposing the findings concerning Iffezheim field experiment, the early migration of tracer sediment in the Bovenrijn was found to have a strong correlation with water discharge.

Which are the main physical mechanisms that control the observed behaviour?

We conclude that several mechanisms have controlled the streamwise sorting between the various tracer fractions in Iffezheim field experiment. At first, the longitudinal decrease in bed shear stress

have promoted sorting by a preferential slowdown of coarser fractions late in the monitoring period. We also found that the effect of the 1/100 years flood wave was to enhance vertical mixing processes, affecting predominantly the finer faster moving fractions which were buried in deeper inactive areas. Therefore, the flood wave arrested strong streamwise sorting. Moreover, while we differentiated between the different mechanisms of microscopic and macroscopic hiding, we have concluded that both tend to arrest strong hydraulic sorting by preferential sheltering of finer sediment. Nevertheless, we consider only hiding at the bed surface (microscopic) as responsible for the lagging of the finest fraction behind its slightly coarser counterpart. This is due to the fact that both had equal shares in the initial volume and have not demonstrated significant differences with respect to the macroscopic hiding.

Concerning the increased downstream dispersion of narrow-ranged finer fractions compared to the wide-ranged coarser tracer sediment, we conclude that the most effective physical process is the increased vertical mixing of finer fractions rather the grain size selectivity by flow.

5.1.2 Trajectory of mixed-size nourished sediment in meandering reaches

What is the trajectory of mixed-size nourished sediment fed in meandering reaches?

The conclusion of the present study concerning the trajectory of nourished sediment in meandering rivers is that it depends very much on the reach-specific hydraulic conditions but also possibly on the characteristics of the nourished sediment. We found that the sediment fed below Iffezheim followed the deep outer bends of the study reach crossing fast at the locations of crossings from one bend to the other. This was expressed by the fact that the maximum cross-sectional concentrations were found closer to the deep outer bends in the middle of the meanders (where curvature is minimum) whereas closer to the river axis at the locations of crossings. No significant variations were observed when studying the respective components of nourished sediment.

Concerning the Bovenrijn pilot study, where sediment was nourished at the deep outer bend near Lobith, we observed that the tracer sediment placed at the location of meander crossing, followed the southern bank of the river without crossing towards the next outer bend. Nevertheless, we note that it is not certain from the measurements whether we are able to observe the real characteristics of nourished sediment due to limitations related with the monitoring method, as well as that the morhpodynamic changes are at an early stage.

Which are the main physical mechanisms that control the observed behaviour?

We conclude that the nourished sediment follows the deep outer bends below Iffezheim, due to the fact that its largest part corresponds to the coarse gravel spectrum of transported sediment in the reach. That follows from the fact that physical processes like gravity pull along transverse slopes, and shoaling of flow along the upstream parts of the point bars are likely to have a larger effect on its grains. Another finding that additionally explains the little sorting observed between the various fractions, is that during low and more probable flows sediment transport occurs predominantly at the deep parts of the cross-sections, mostly as a result of the apparently low water depths closer to the inner bends.

Under the assumption that we observe the real characteristics of the granite migration in the Bovenrijn despite the limitations of the monitoring method applied, we conclude that the coarser granite sediment has stayed close to the left bank without crossing towards the next outer bend, mainly because it has only marginally migrated downstream at an area of nearly uniform lateral sorting. This is related with the fact that this area is close to the bend crossing between the meanders of the study reach and does not provide transverse slopes able to roll coarser sediment downslope. Further any shoaling of flow along the point bar of the downstream meander, is counteracted by negative pressure gradients resulting from deceleration of flow over the front of the nourishment.

5.1.3 Vertical mixing of mixed-size nourished sediment

What characterizes the vertical mixing of mixed-size nourished sediment at lowland rivers?

Concerning the vertical mixing of the nourished sediment, we were able to observe from the analysis of the Iffezheim field experiment that there were differences between the various tracer

fractions. The finer fractions were found to have larger concentration deeper in a shallow layer of 30 cm, compared to the bed surface. On the other hand, with increasing grain size of the tracer fraction considered, a larger concentration was found to the surface layer compared to the bottom layer studied. This vertical sorting of the nourished sediment was apparent already from the first monitoring campaign 2 months after the feeding.

From the analysis of the Bovenrijn field experiment we observed that the arrangement of the nourished sediment in areas of sediment with uniform mobility, led to a burial of the less mobile granite placed in the front from more mobile gravel nourished just upstream and possibly other deposited sediment.

Which are the main physical mechanisms that control the observed behaviour?

Whereas in the case of the Bovenrijn experiment it is straightforward that the burial of coarser granite nourished at the front is mainly a result of the difference in mobility with the sediment nourished and transported from upstream, in the case of the Iffezheim field experiment we mainly discussed the validity and relevance of certain hypotheses. The conclusion is that the vertical mixing of the nourished sediment, evolves such that a mobile armour is quickly formed or maintained. Physical processes that can bring finer sediment to the deeper parts of the shallow layer studied were found to be the vertical winnowing of finer sediment, the filling of framework clast pores by finer grains and finally, the burial of bedload beneath advancing bedforms under aggradational conditions. All of the above are to a certain extent relevant with the characteristics of the study case yet, it is unknown which one is likely to be more dominant. We further concluded that aggradational conditions closer to the upstream end are not likely to have preferentially buried finer sediment in deeper strata since the latter was leading throughout the monitoring period. Moreover, the fact that all tracer fractions were found to propagate closer to the outer bends also renders unlikely that the finer sediment has deposited under the point bars of the inner bends.

5.1.4 Textural adjustment in the Bovenrijn

Which are the effects of sediment nourishments on textural changes in the studied reaches?

We were able to observe textural changes only in the case of Bovenrijn and in fact these were not associated with the pilot nourishment but partly to the the nourishments performed further upstream. Studying the period of 1995 to 2016, we concluded that a textural adjustment has increased the grain size of bed surface sediment in the Bovenrijn.

Due to the multiple and time-varying controls on the Bovenrijn as well as on the upstream adjacent reach of Lower Niederrhein we are only able to hypothesize concerning the effects of sediment nourishment on the coarsening of bed surface texture. Our hypothesis is that mixed-size and coarser than the bed nourished sediment at the upstream adjacent reach of Bovenrijn has contributed throughout the study period to changes in the grain size distribution of the upstream supply. A close correspondence in time was found between the nourishments performed upstream with an increase of the coarse gravel content in the supplied bedload to Bovenrijn detected since 2000. More recent nourishments exactly at the upstream end of the Bovenrijn (performed during 2005-2007), are expected to have prolonged the increased coarse gravel representation even after 2009 (up to when available data on upstream sediment supply span), while we hypothesize that are associated with the rapid increase of finer gravel content observed since 2007. Both explain the spatial pattern of stronger coarsening with decreasing distance from the upstream end of Bovenrijn between 2008-2016.

The effects of nourishments at the upstream adjacent reach have most probably conformed the textural adjustment of the Bovenrijn in conjunction with the effects of bed degradation in the study reach as well as further upstream.

5.2 Recommendations

From the present study the following recommendations are made.

- In the present study we analysed trends from soil samples, sediment transport measurements, and from radioactivity measurements amongst others. The Medusa measurements were hard to analyse since they did not provide the confidence that the full spatial extent of the tracer sediment was resolved. On the contrary soil samples from the bed with sieving analyses to determine the concentrations of tracer granite fractions despite any limitations, provided larger confidence in the analysis of the results. Therefore it is recommended for the continuation of the monitoring in the Bovenrijn, that soil samples with sieving analysis accounting for tracer fractions is applied. Finally consistent sediment transport measurements of the bed load can be very useful in detecting the migration of sorting waves (e.g. resulting from nourishments) if they provide information on the grain size distribution of the transported load.
- The reaches of the Rhine near the border of Germany and Netherlands, i.e., Lower Niederrhein and Bovenrijn are characterized by a multitude of controls, yet the presence of mixed-size sediment nourishments is likely to have been dominant over the past two decades. To this end, further efforts in assessing the behaviour of mixed-size sediment and the possible effects on the mitigated reaches should definitely consider this area as a potential study reach.
- In order to extract tracer concentrations as a function of some location in a river, the weighting process is of critical importance and should be closely related to the objective of the study. If various locations are compared for their content in a certain tracer fraction f one should keep in mind if it is needed to account (or not) for the lateral, vertical, and streamwise sorting patterns. This has to do in specific with the normalization approach in which, in order to arrive to the fractional concentration, the **tracer** mass of fraction f as a function of some location, is weighted against the **total** mass of fraction f. The differences that may be produced in a quantitative comparison over some direction (between the same fraction) by this approach, or by weighting against the total mass of all fractions in the soil sample are very significant.

BIBLIOGRAPHY

Abel, D. (2001). Geschibezugabe niederrhein untersuchungsmethoden wirkungsweisen. Presented at the Colloqium of BAW in Karlsruhe.

Andrews, E. D. (1987). Vertical exhange of coarse bedload in desert streams. *Geological Society*, Special Publication(35):7–16.

Berkhout, B. (2015). Waves arising from Hirano conservation model for mixed-size sediment morphodynamics. Master's thesis, Delft University of Technology.

Blom, A. (2016). Bed degradation in the Rhine river. *Waterview*.

Blom, A., Viparelli, E., and Chavarrías, V. (2016). The graded alluvial river: Profile concavity and downstream fining. *Geophysical Research Letters*, 43:1–9. 2016GL068898.

Buck, W. (1993). Eingriffe und ereignisse im 19. und 20. jahrhundert: Oberrhein bis zum neckar. in: Kalweit, h. (ed.), der rhein unter der einwirkung desmenschen ? ausbau, schiffahrt, wasserwirtschaft. Technical report, CHR/KHR, Lelystad, The Netherlands.

Bunte, K. (2004). Gravel mitigation and augmentation below hydroelectric dams: A geomorphological perspective. Technical report, USDA Forest Service Rocky Mountain Research Station.

Clayton, A. J. (2010). Local sorting, bend curvature and particle mobility in meandering gravel bed rivers. *Water Resour. Res.*, 46:W02601.

Cui, Y., Parker, G., Lisle, T., Gott, J., Hansler-Ball, M., Pizzuto, J., Allmendinger, N., and Reed, J. (2003). Sediment pulses in mountain rivers: 1. experiments. *Water Resources Research*, 39(9):1239.

de Vries, M. (1965). Considerations about non-steady bed load transport in open channels. Technical Report 36, Delft Hydraulics Laboratory.

Dietrich, W. E., Kirchner, J., Ikeda, H., and Iseya, F. (1989). Sediment supply and the development of the coarse surface layer in gravel-bedded rivers. *Nature*, 340:215–216.

Dietrich, W. E. and Smith, J. D. (1984). Bed load transport in a river meander. *Water Resources Research*, 20(10):1355–1380.

Dietrich, W. E., Smith, J. D., and Dunne, T. (1979). Flow and sediment transport in a sand bedded meander. *Journal of geology*, 87:305–315.

Dinehart, R. (1992). Gravel-bed deposition and erosion by bedform migration observed ultrasonically during storm flow, north fork toutle river, washington. *Journal of Hydrology*, 136:51–71.

Droge, B., Engel, H., and Gölz, E. (1992). Channel erosion and erosion monitoring along the rhine river. In *Proceedings of the Oslo Symposium, August 1992*, pages 493–503.

Eelkema, M. (2008). Measuring sediment properties in the field using medusa rhoc. Master's thesis, Delft University of Technology.

Emmanouil, A. (2017). Morphodynamic trends in the freely flowing Rhine: A literature review. Addit. Master's thesis, Delft University of Technology.

Ferguson, R. and Wathen, S. (1998). Tracer-pebble movement along a concave river profile: Virtual velocity in relation to grain size and shear stress. *Water Resources Research*, pages 2031–2038.

Frings, R. M. (2008). Downstream fining in large sand-bed rivers. *Earth-Science Reviews*, 87(1–2):39–60.

Frings, R. M. (2011). Sedimentary characteristics of the gravel-sand transition in the River Rhine. *Journal of Sedimentary Research*, 81(1):52–63.

Frings, R. M., Düring, R., Beckhausen, C., Schüttrumpf, H., and Vollmer, S. (2014a). Fluvial sediment budget of a modern, restrained river: The lower reach of the Rhine in Germany. *Catena*, 122(0):91–102.

Frings, R. M., Gehres, N., Promny, M., Middelkoop, H., Schüttrumpf, H., and Vollmer, S. (2014b). Today's sediment budget of the rhine river channel, focusing on the upper rhine graben and rhenish massif. *Geomorphology*, 204:573–587.

Gabriel, T., Kühne, E., Klos, S., Anlauf, A., Gölz, E., Faulhaber, P., Puhlmann, G., and Groger, T. (2009). Sohlstabilisierungskonzept für die Elbe: von mühlberg bis zur saalemündung. Technical report, WSV, BfG, BAW.

Gölz, E. (1994). Bed degradation-nature, causes, countermeasures. *Water Science & Technology*, 29(3):325–333.

Gölz, E. (2008). Improved sediment-management strategies for the sustainable development of German waterways. In 325, I. P., editor, *The Symposium on Sediment Dynamics in Changing Environments*.

Gölz, E., Theis, H., and Trompeter, U. (2006). Tracerversuch Iffezheim. Technical Report BfG-JAP-Nr. 2348, Bundesanstalt für Gewässerkunde. Germany.

Grant, E. G. (2012). *Dynamics of Gravel-bed Rivers*, chapter The Geomorphic Response of Gravel-Bed Rivers to Dams: Perspectives and Prospects, pages 165–181. J. Wiley and Sons.

Guerrero, M., Re, M., Kazimierski, L. D., Menéndez, A. N., and Ugarelli, R. (2013). Effect of climate change on navigation channel dredging of the Parana river. *International Journal of River Basin Management*, 11(4):439–448.

Habersack, H., Hein, T., Stanica, A., Liska, I., Mair, R., J?ger, E., Hauer, C., and C., B. (2015). Challenges of river basin management: Current status of, and prospects for, the river Danube from a river engineering perspective. *Sci Total Environ*, 543(A):828–845.

Habersack, H., J?ger, E., and Hauer, C. (2013). The status of the Danube river sediment regime and morphology as a basis for future basin management. *Intl. J. River Basin Management*, 11(2):153–166.

Hassan, A. M. and Church, M. (1990). Scour, fill, and burial depth of coarse material in gravel bed streams. *Earth Surface Processes and Landforms*, 15:341–356.

Hassan, A. M. and Church, M. (1994). Vertical mixing of coarse particles in gravel bed rivers: A kinematic model. *Water resources research*, 30:1173–1185.

Hirano, M. (1971). River bed degradation with armouring. *Trans. Jpn. Soc. Civ. Eng*, 3(2):194–195.

Hirano, M. (1972). Studies on variation and equilibrium state of a river bed composed of nonuniform material. *Trans. Jpn. Soc. Civ. Eng*, 4:128–129.

Hoey, T. and Ferguson, R. (1994). Numerical simulation of downstream fining by selective transport in gravel bed rivers: Model development and illustration. *Water Resources Research*, 30(7):2251–2260.

Humphries, R., Venditti, J. G., Sklar, L. S., and Wooster, J. K. (2012). Experimental evidence for the effect of hydrographs on sediment pulse dynamics in gravel-bedded rivers. *Water Resour. Res.*, 48(1):W01533.

Kantoush, S. A. and Sumi, T. (2010). River morphology and sediment management strategies for sustainable reservoir in Japan and European Alps. *Ann Disas Prev Res Inst Kyoto Univ*, 53(B):821–839.

Kleinhans, M., Wilbers, A., and Ten Brinke, W. (2007). Opposite hysteresis of sand and gravel transport upstream and downstream of a bifurcation during a flood in the river rhine, the netherlands. *Netherlands Journal of Geosciences/Geologie en Mijnbouw*, 86(3):273–285.

Kondolf, G. M. (1997). Hungry water: Effects of dams and gravel mining on river channels. *Environmental Management*, 21(4):533–551.

Kondolf, G. M. and Minear, J. T. (2004). Coarse sediment augmentation on the Trinity River below Lewiston Dam: Geomorphic perspectives and review of past projects. Technical report, Trinity River Restoration Program.

Kuhl, D. (1993). The addition of bed load downstream the weir Iffeheim from 1978-1992. Technical report, Bundesanstalt fur Wasserbau.

Lisle, T. E., Parker, G., and Dodd, A. M. ((2001)). The dominance of dispersion in the evolution of bed-material waves in gravel-bed rivers. *Earth Surface Processes and Landforms*, 26:1409?1420.

Lisle, T. E., Pizzuto, J. E., Ikeda, H., Iseya, F., and Kodama, Y. ((1997)). Evolution of a sediment wave in an experimental channel. *Water Resour. Res.*, 33(8):1971?1981.

Mackin, J. H. (1948). Concept of the graded river. *Geol. Soc. Am. Bull.*, 59(5):463–512.

Milhus, R. T. (1973). *Sediment transport in a gravel-bottomed stream.* PhD thesis, Oregon State Univ., U.S.A.

Mosselman, E., Kerssens, P., van der Knaap, F., Schwanenberg, D., and Sloff, K. (2004). Sustainable river fairway maintenance and improvement. Technical Report Q3757, Water Laboratory Delft Hydraulics.

Mosselman, E., Sloff, K., and van Vuren, S. (2008). Different sediment mixtures at constant flow conditions can produce the same celerity of bed disturbances. In *River Flow 2008, Proceedings of the International Conference on Fluvial Hydraulics, Cesme, Izmir, Turkey*, pages 3–5.

Paarlberg, A., Quartel, S., and Kater, E. (2016). Bed level measurements of niederrhein, analysis of bed level trends. Technical report, RWS-ON.

Pace, M. K., Tullos, D., Walter, C., Lancaster, S., and Segura, C. (2016). Sediment pulse behaviour following dam removal in gravel-bed rivers. *River research and applications.*

Parker, G. and Klingeman, P. C. (1982). On why gravel bed streams are paved. *Water Resour. Res.*, 18(5):1409–1423.

Pessenlehner, S., Liedermann, M., Tritthart, M., Gmeiner, P., and Habersack, H. (2016). River bed degradation and morphological development before and after river restoration measures at the Danube river east of Vienna. In *Proceedings of the 12th International Conference on Hydroscience and Engineering*, pages 343–366.

Ribberink, J. S. (1987). *Mathematical modelling of one-dimensional morphological changes in rivers with non-uniform sediment.* PhD thesis, Delft University of Technology, The Netherlands.

Schmidt, A. and Faulhaber, P. (2001). Five years of artificial bed load feeding in the river elbe. *River Basin Management*, 50:10.

Sieben, A. (2017). Overzicht ten behoeve van morfodynamiek boven-rijn: project suppletie boven-rijn. Technical report, RWS-WVL.

Sieben, J. (1997). *Modelling of hydraulics and morphology in mountain rivers.* PhD thesis, Delft University of Technology.

Sieben, J. (2009). Sediment management in the Dutch Rhine branches. *International Journal of River Basin Management*, 7(1):43–53.

Sklar, L. S., Fadde, J., Venditti, J. G., Nelson, P., Wydzga, M. A., Cui, Y., and Dietrich, W. E. (2009). Translation and dispersion of sediment pulses in flume experiments simulating gravel augmentation below dams. *Water Resources Research*, 45:W08439.

Sloff, K. and Sieben, A. (2008). Model assessment of sediment nourishment in rivers with graded sediment. In *Proceedings of the 5th IAHR Symposium on River, Coastal and Estuarine Morphodynamics, Enschede*.

Stecca, G., Siviglia, A., and Blom, A. (2014). Mathematical analysis of the Saint-Venant-Hirano model for mixed-sediment morphodynamics. *Water Resour. Res.*, 50:7563–7589.

Ten Brinke, W. (2005). *The Dutch Rhine, a Restrained River*. Veen Magazines B.V.

Ten Brinke, W. B. M. and Gölz, E. (2001). Bed level changes and sediment budget of the Rhine near the German - Dutch border. Technical Report 2001.044, RIZA.

Tögel, R. (2011). Integrated river engineering project on the Danube east of Vienna. Presented at Vienna at the Trans-European T.

Van Vuren, W. (2005). Rijntakken6, spreadsheet with processed water levels. Technical report, Rijkswaterstaat RIZA.

Venditti, J., Humphries, R., Allison, M., Nittrouer, J., and Church, M. (2010). Morphology and dynamics of a gravel-sand transition. In *9th Federal Interagency Sedimentation Conference, Las Vegas, NV*, page 11.

Venditti, J. G., Dietrich, W. E., Nelson, P. A., Wydzga, M. A., Fadde, J., and Sklar, L. S. (2005). Can coarse surface layers in gravel-bedded rivers be mobilized by finer gravel bedload? In *Eos Trans. AGU Fall Meet. Suppl.*

De Vriend, H. (2015). The long-term response of rivers to engineering works and climate change. *Civil Engineering*, 168(CE3):139–145.

Wohl, E., Angermeier, P. L., Bledsoe, B., Kondolf, G. M., MacDonnell, L., Merritt, D. M., Palmer, M. A., Poff, N. L., and Tarboton, D. (2005). River restoration. *Water Resour. Res.*, 41(10):W10301.

appendix

A

FRACTIONAL DOWNSTREAM MIGRATION OF TRACER SEDIMENT BELOW IFFEZHEIM

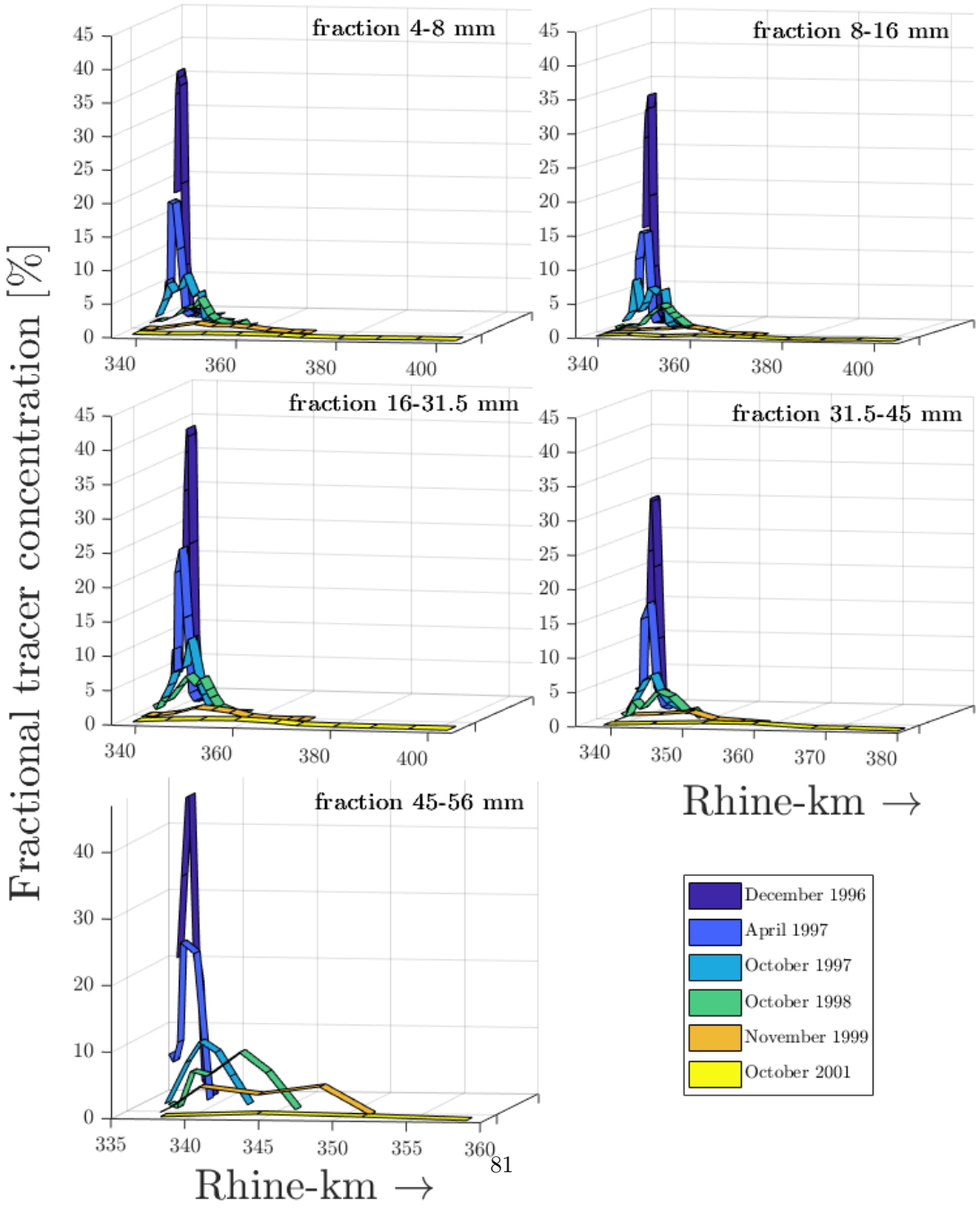

Figure A.1: Longitudinal temporal changes in the fraction tracer concentration F.

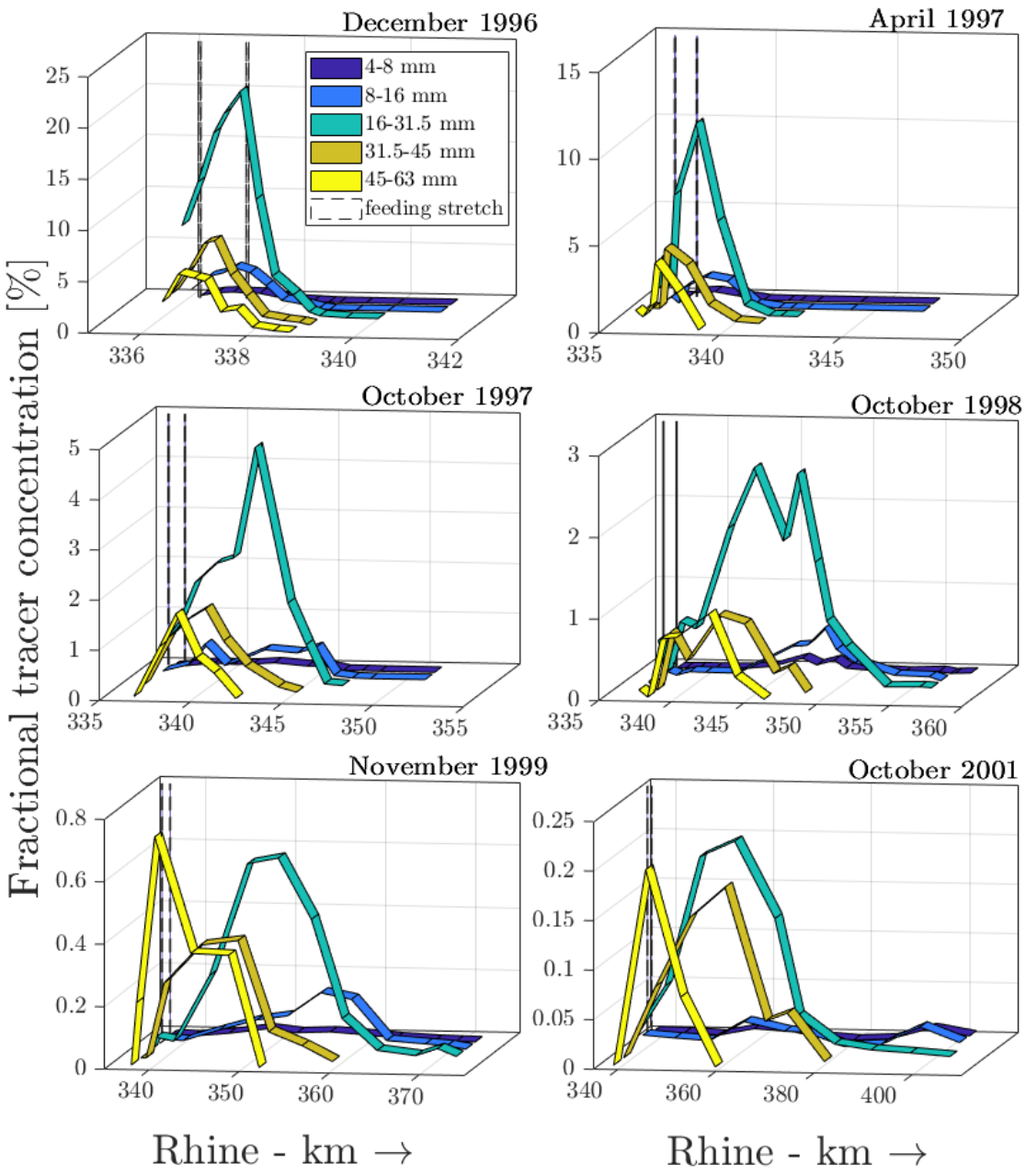

Figure A.2: Longitudinal temporal changes in the fraction tracer concentration F.

appendix

B

LATERAL MIGRATION OF TRACER SEDIMENT - IFFEZHEIM

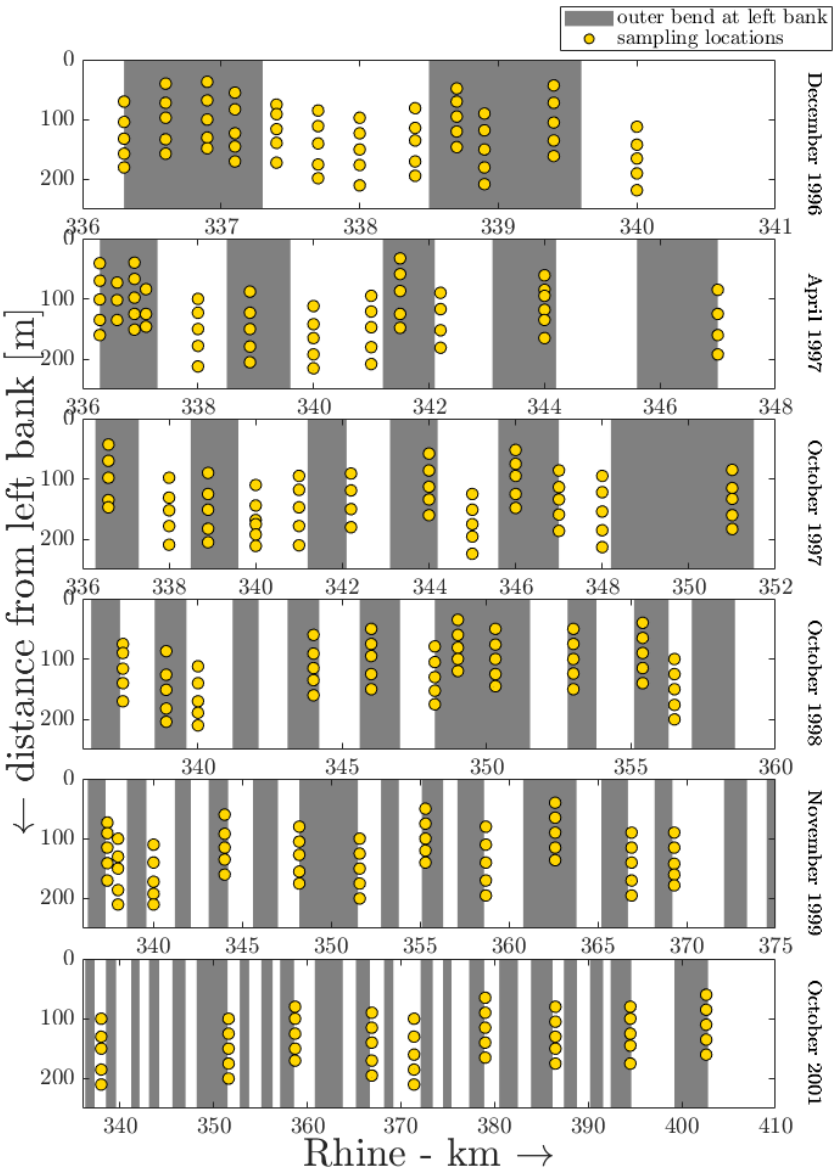

Figure B.1: Locations of sampling cross sections plotted with the locations of bend crossings.

Data preprocessing .

In order to conduct the analyses, there was a number of steps that needed to be followed. First the available data were referenced against the planform geometry of the study reach in order to express each and every sampling location with respect to its position at the meanders. Second, the dataset was inspected in order to exclude cross-sections or individual sampling locations that were irrelevant with the present analysis (e.g. samples taken from the groyne fields). These steps are presented in further detail in the following.

The dataset provides information for the streamwise position of the monitored cross section along the Rhine, and the distance of each and every sampling location from the left bank. For the vast majority of cross-sections and for all six monitoring campaigns, there were five samples taken, from well spread locations within the lateral boundaries of the navigation channel.

At this stage we are interested in extracting two pieces of information. These are the location of each sample with respect to the inner and the outer bend, and with respect to the streamwise extent of the meander (i.e., close to the bend crossing or not). The study reach is characterized by the presence of groynes alternating at its river banks, imposing a meandering morphology even along the straight sub-reaches. A representative example of the study reach is demonstrated in Fig.B.2. The groynes resemble closely the morphology of alternating bars first growing and then decreasing in width with downstream distance.

This characteristic allows to straightforwardly relate the streamwise extent and bank position of the transverse groynes, with the extent of individual meanders and the respective bank position of their inner and outer bends. In other words, the groynes can serve to extract the streamwise locations of bend crossings along the study area. An example regarding the latter, is that along a stretch were the groynes are located on the left bank, so does the inner bend of the meander while the outer bend is located at the opposite right bank and vice versa.

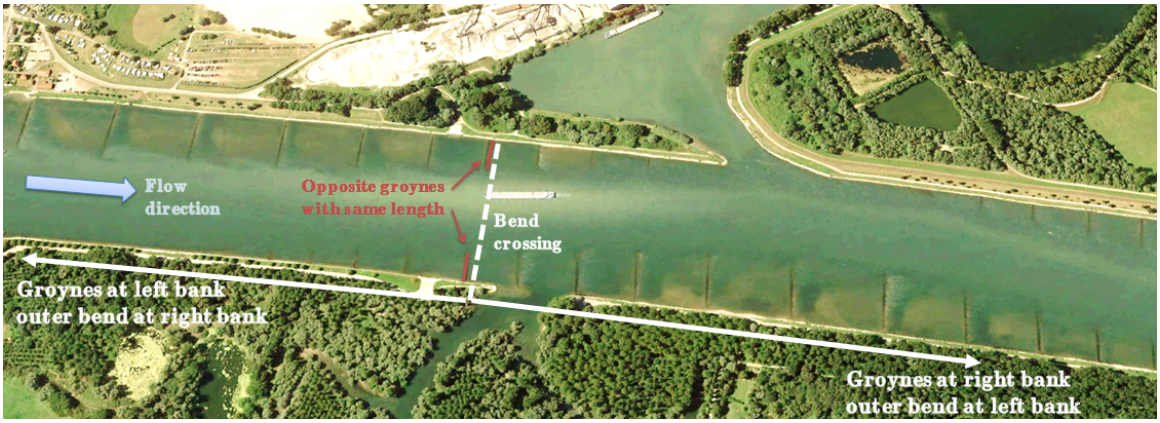

Figure B.2: Representative example of bend crossing extraction by navigation chart maps.

The streamwise positions of bend crossings were extracted by the navigation charts freely available online at `http://gpsnauticalcharts.com/`. The bend crossings were first defined at the locations where the opposite transverse groynes have same lengths. We estimate that the maximum error regarding the location of bend crossings from this approach is 100 meters and we consider that it is acceptable for the purposes of the present analysis.

It has to be mentioned that an on-map visual inspection was performed for all sampling locations during the data preprocessing phase of the present analysis. Either cross-sections that were not uniformly sampled across the lateral direction (e.g. with samples only at one half of the navigation channel) or any individual transverse samples within the groyne fields were excluded from the dataset. The analysed cross-sections (more than 90% of the initially available) with their lateral sampling locations can be found in the Appendix (Fig.B.1).

Results concerning the FL_N for each of the three merged fractions are presented below.

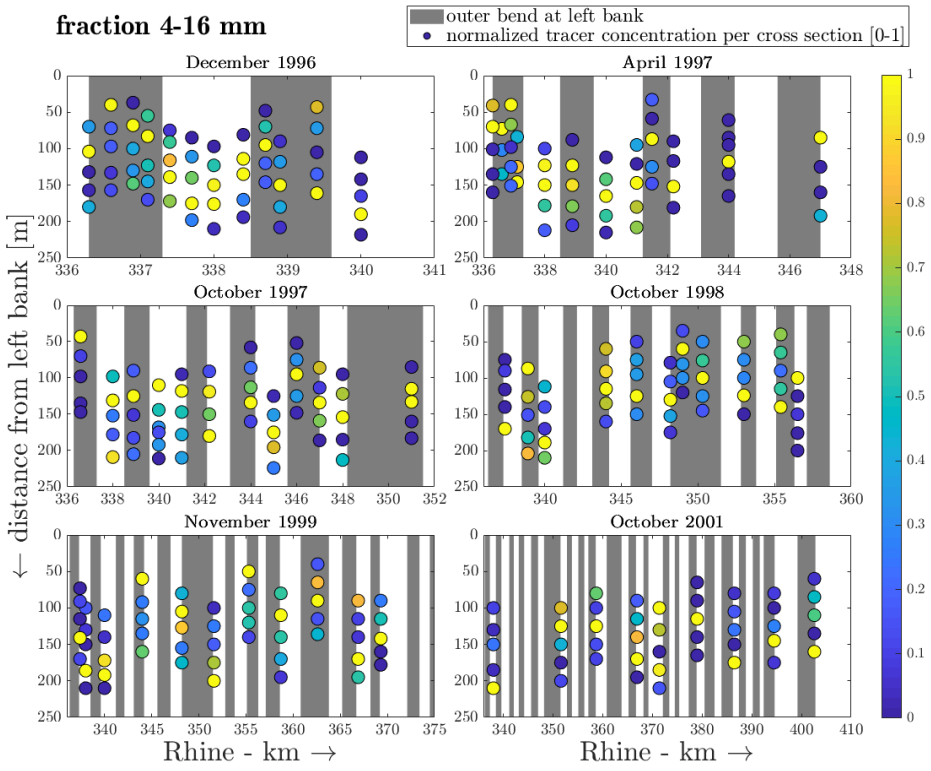

Figure B.3: Location of max tracer concentration per monitoring campaign along each cross-section for fraction 4-16 mm.

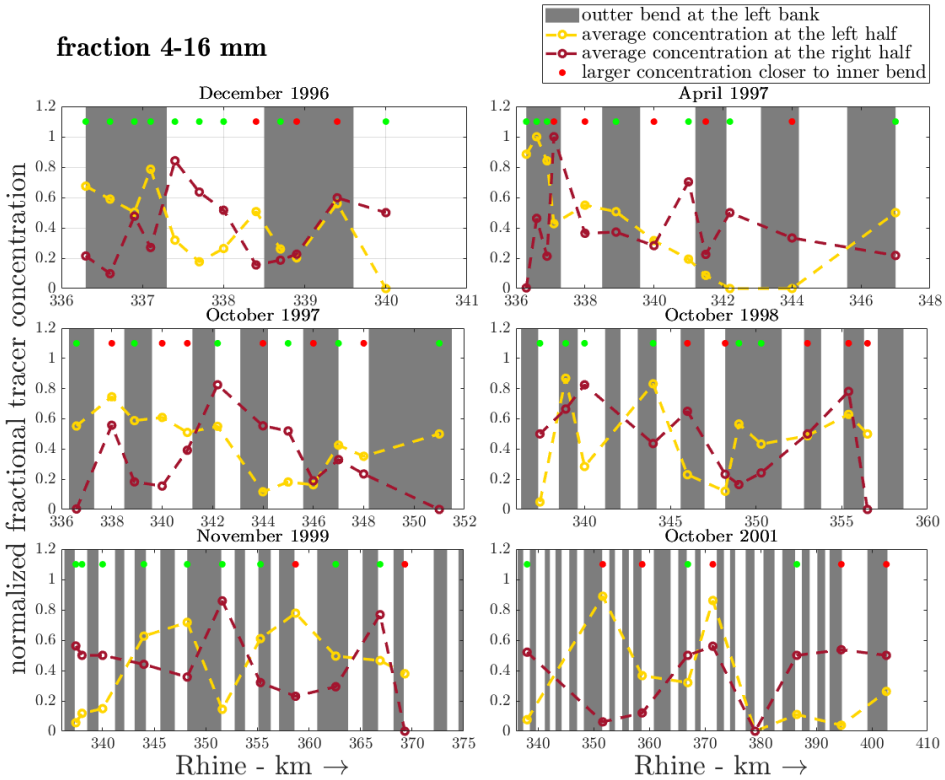

Figure B.4: Comparison of the averaged FL_N between the two halves of the navigation channel for fraction 4-16 mm.

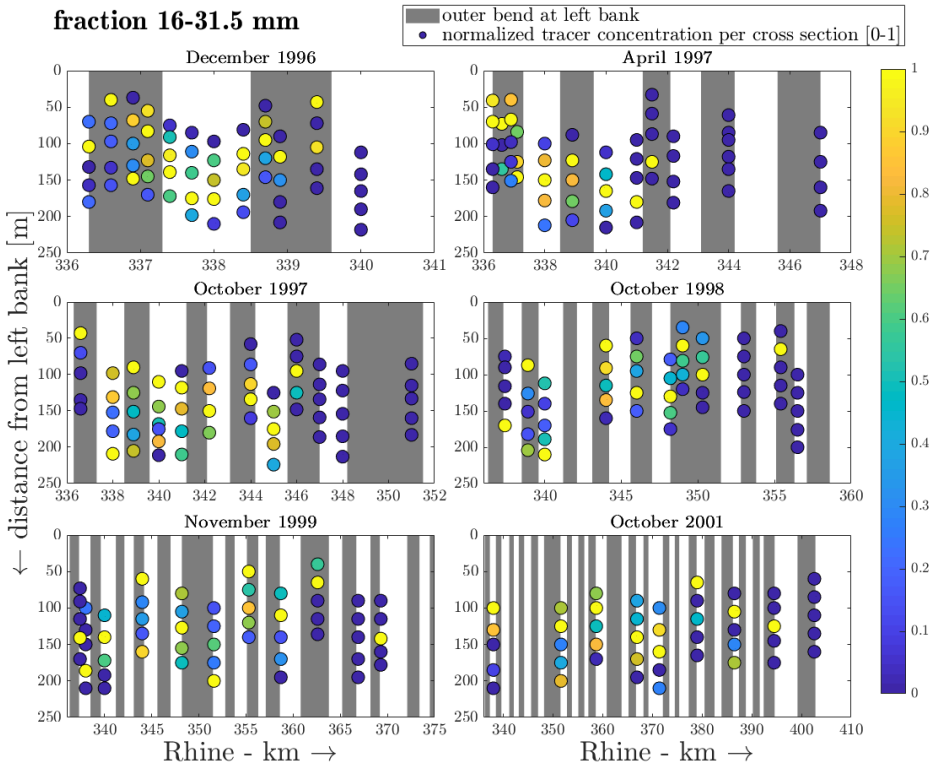

Figure B.5: Location of max tracer concentration per monitoring campaign along each cross-section for fraction 16-31.5 mm.

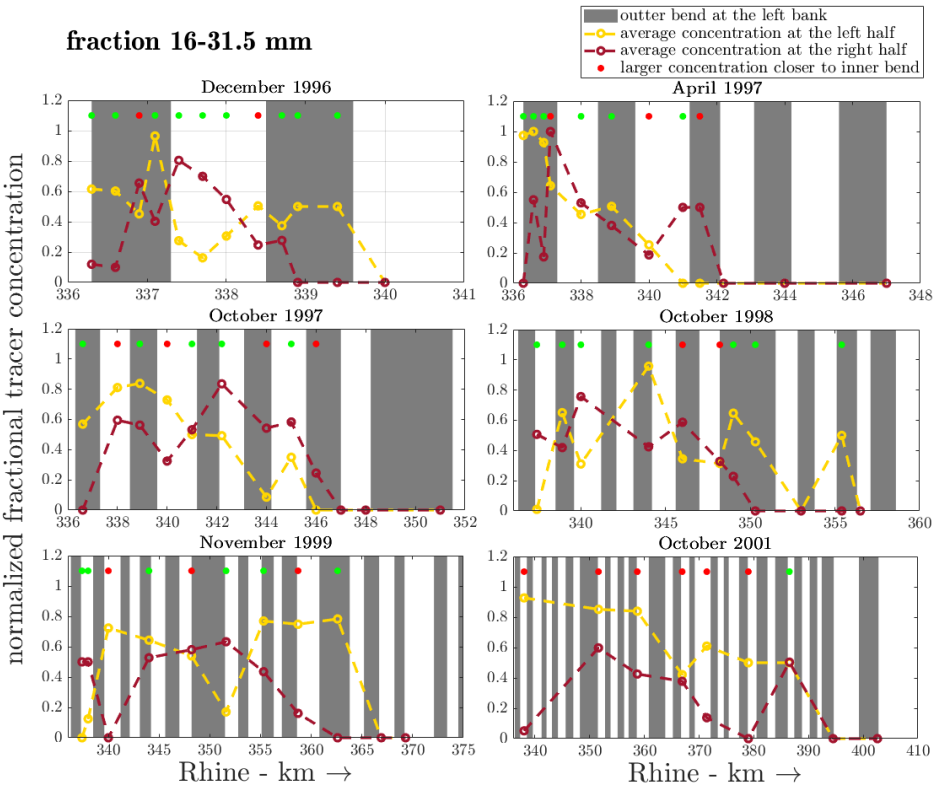

Figure B.6: Comparison of the averaged FL_N between the two halves of the navigation channel for fraction 16-31.5 mm.

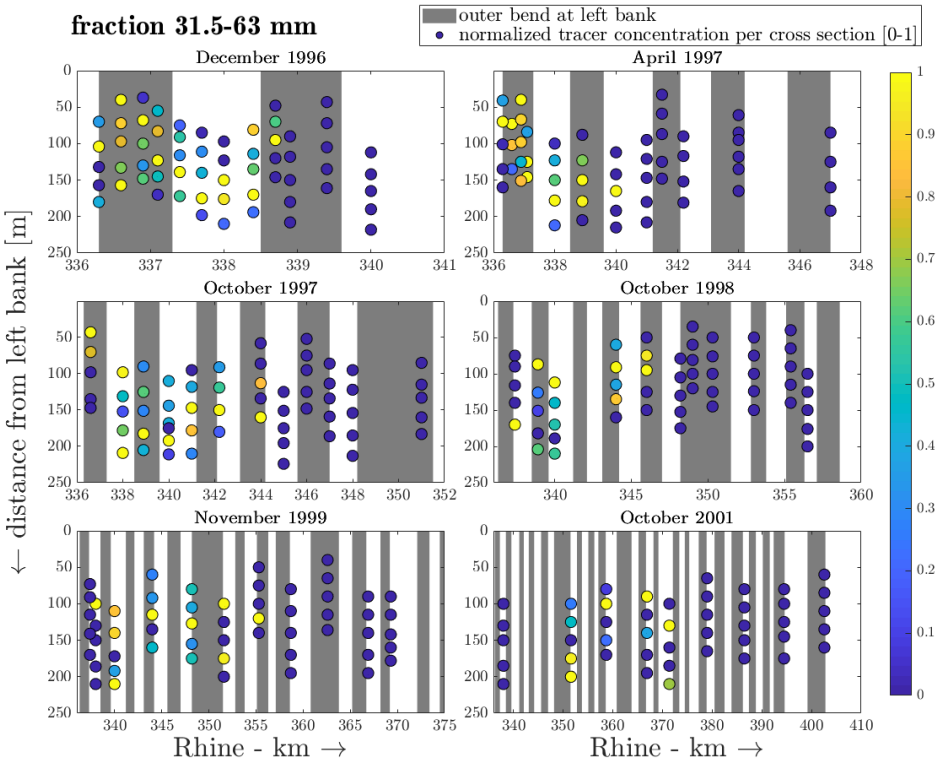

Figure B.7: Location of max tracer concentration per monitoring campaign along each cross-section for fraction 31.5-63 mm.

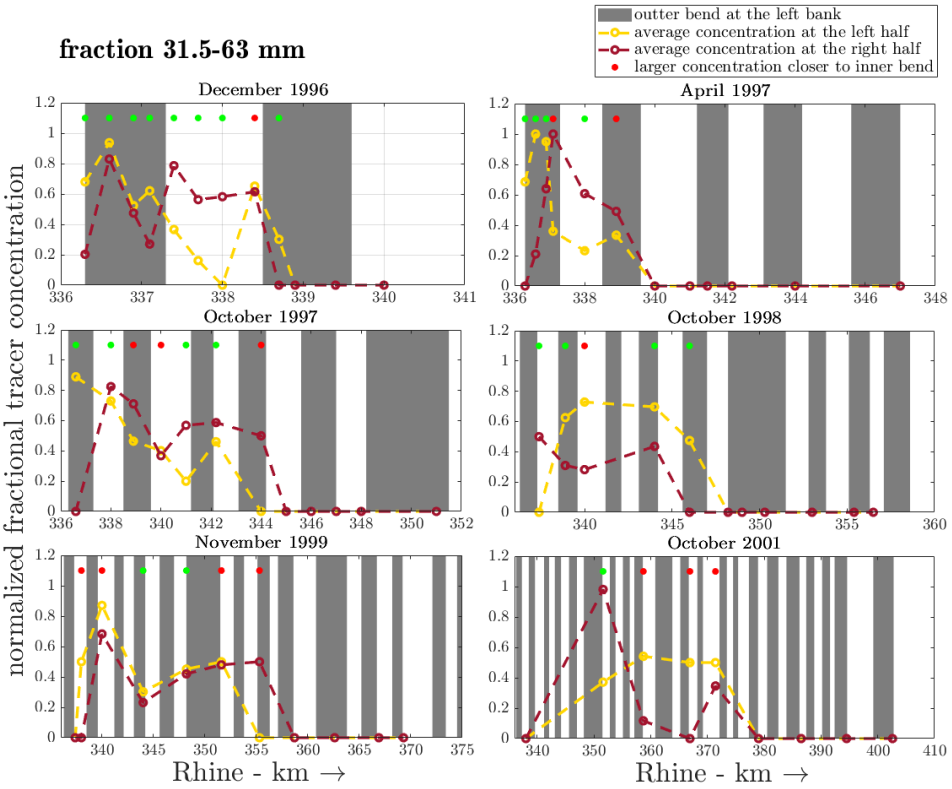

Figure B.8: Comparison of the averaged FL_N between the two halves of the navigation channel for fraction 31.5-63 mm.

appendix

C

BED LEVEL CHANGES BETWEEN SUCCESSIVE MONITORING CAMPAIGNS- BOVENRIJN

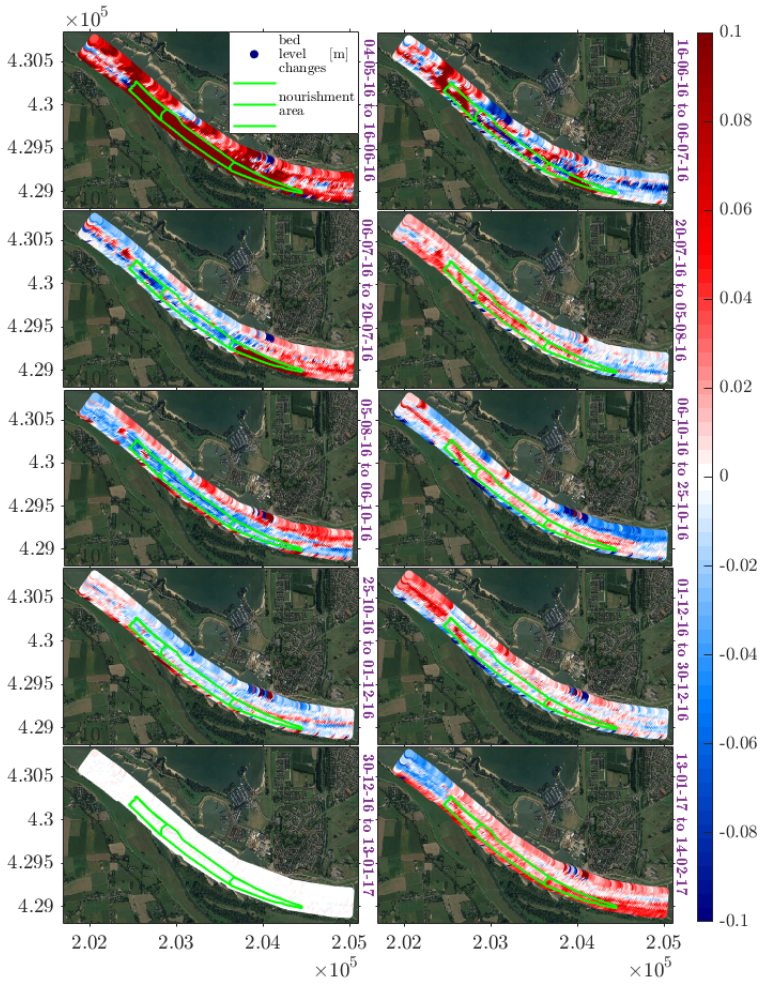

Figure C.1: Bed level changes between successive measuring campaigns.

From these figures two conclusions that can be drawn. First, the more intense erosion within the monitoring period concerned the stretch 2 in the time interval 16/06/16 to 06/07/16 corresponding to the second part of the high water period. Second, the bed level changes form distinct patches. These may evolve in a downstream or lateral direction while the nourishment itself seems to play a role in this arrangement.

appendix

D

TEMPORAL CHANGES IN MEDUSA SIGNAL BETWEEN MONITORING CAMPAIGNS - BOVENRIJN

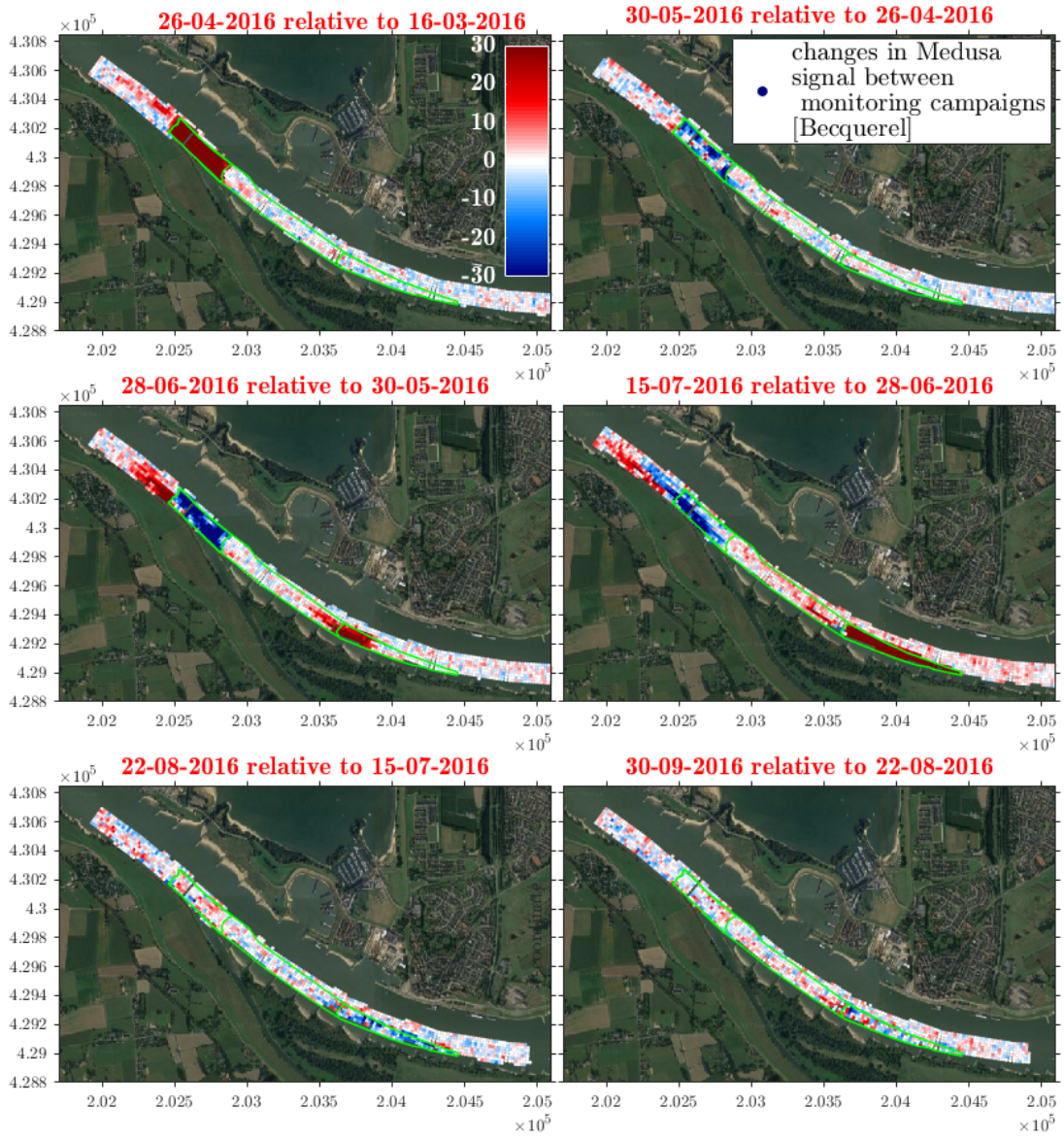

Figure D.1: Changes in Medusa signal ($K/100 + Th + U$) between monitoring campaigns. (a)

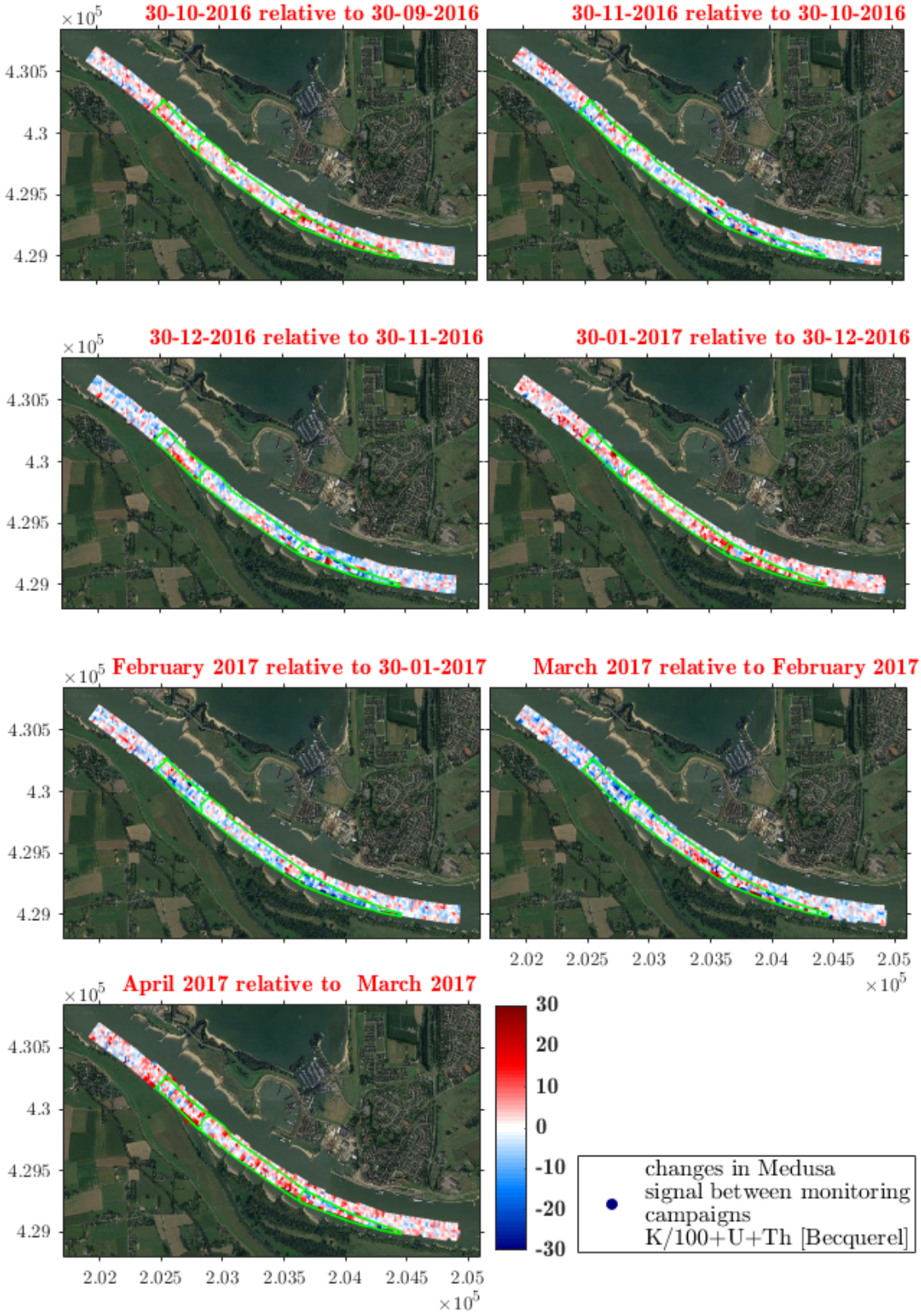

Figure D.2: Changes in Medusa signal ($K/100 + Th + U$) between monitoring campaigns. (b)

appendix

E

COMPARISON BETWEEN CHANGES IN MULTIBEAM AND MEDUSA SIGNALS IN DOWNSTREAM DIRECTION

We have previously mentioned that the Medusa signals are linked with faster downstream migration compared to the bed wave signals. We were able to detect this already from the cross-correlations of the respective signals but also visually from Fig.3.13. To provide a quantification for the discussed comparison, we now visually map the locations of the respective signal front tips at various time instances. This is done only for the lateral locations from the river axis that information is available for both signals (left from the river axis).

Fig.E.1, shows the the rough estimates taken, compared between the Multibeam and Medusa signals downstream migration for three periods (different colors). Note that all periods start at the time of feeding. The Multibeam and Medusa front migration celerities are given in solid and dashed lines respectively in meters/day. Finally, for the two latter periods studied estimates for the Medusa signals are given only close to the left bank.

It can be seen that the bed wave migrates downstream slower than the tracer granite. The migration celerities drop as larger periods are considered since lower water discharges occurred progressively with time. The average celerities from all the lateral positions studied (given in the legend of Fig.E.1) reveal that the migration celerities (in km/year) are from 3.3 to 0.6 for the Medusa signals and from 0.6 to 0.2 for the bed wave signals. The orders of magnitude for the respective periods are similar to the ones derived from the cross-correlation analysis. Now the celerities derived are larger yet concern only the front of the waves, whereas it can be expected that the cross-correlation analysis resolves the migration of the bulk nourished volume.

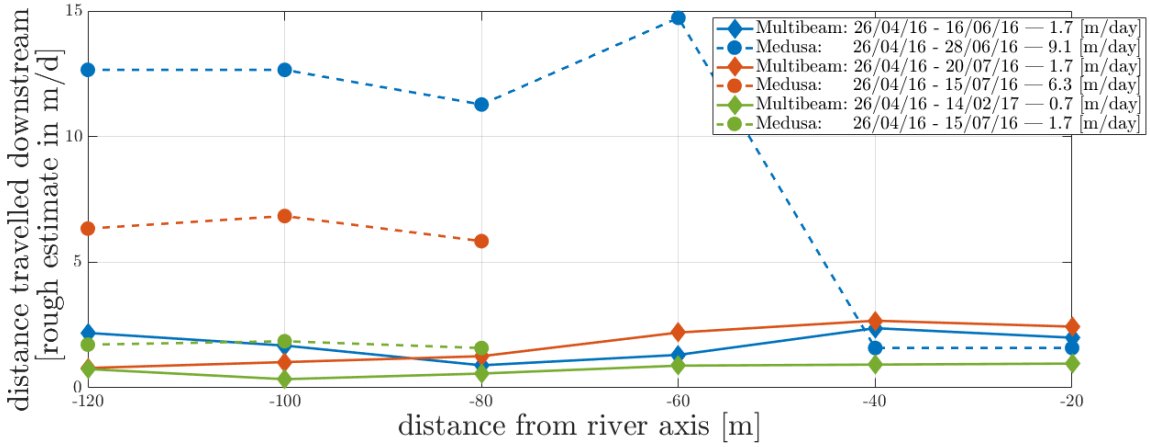

Figure E.1: Rough estimate of downstream migration of the wave front extracted for two periods.

appendix

F

THE BEHAVIOUR OF NON-LINEAR BED WAVES AND THE BED WAVE MIGRATION IN THE BOVENRIJN PILOT STUDY

A distinction between bed and sorting waves .

It is useful to make a clear distinction between the waves that we studied in the previous chapters. At one hand, regarding the data analysis of the Iffezheim, we looked into the temporal evolution of the nourished sediment, as revealed from the sieving analysis of the soil samples taken during the monitoring campaign. Even though it is possible that the presence of nourished sediment at a certain extent of the study reach may be accompanied by some bed level increase, it is crucial to clarify that we are not explicitly assessing the nourishment's temporal evolution as a bed wave. In fact, it is possible that the associated temporal evolution of bed level changes may differ significantly. A characteristic example for this, comes the analysis of the Bovenrijn experiment where we have seen that tracer nourished sediment was resolved (with radioactivity measurements) at a stretch located at the front of the bed wave (resulted from the nourishment), where actually the bed level changes were characterized by erosional conditions. Therefore, it is critical to differentiate between the various wave signals previously analysed.

To this end, the signals analysed in the Iffezheim tracer experiment can be seen as sorting waves, whereas the topographic signal at the Bovenrijn as bed wave. While the former are associated with the concentrations of tracer sediment in the bed composition of the Obberhein (n. Upper Rhine Graben), the latter is related with the bed feature resulting from the presence of the nourished sediment at Lobith.

In fact we may borrow this terminology from various theoretical studies in the past. A pioneering study by de Vries (1965) used the term bed wave to describe mathematically the propagation of a disturbance in bed elevation with a characteristic celerity, employing a model with uniform sediment and quasi-steady flow. In later studies that mixed sediment was considered, the term sorting wave was introduced supplementary to the (De Vries) bed wave, to mathematically describe changes in the sediment composition of the river bed (owing for instance to grain size disturbances) also propagating as waves with characteristic celerities along the domain (e.g. (Ribberink, 1987; Sieben, 1997)). These studies used the Hirano model to account for the conservation of mass of non-uniform sediment (Hirano, 1971, 1972) and were based on various assumptions concerning the flow and mixed-sediment morphodynamics.

In their study, Stecca et al. (2014) accounted for multiple fractions by employing multiple active layer equations, and grain size selectivity. They found distinct sorting waves propagating in the domain with different speeds. Another finding of their analysis was that the sorting waves advected significant changes not only in the composition of the bed but also in bed elevation, following from streamwise gradients in bedload transport that these waves carry as they are advected downstream.

It is worth to mention that these bed and sorting waves are treated in linearised problems and thus represent infinitesimal small disturbances that behave as kinematic or translatory waves. Although these analyses provide useful insight and rules of thumb that may be used in practice, the bed and sorting waves in nature are expected to behave in a non linear manner. This is because the disturbances arising for instance from nourishments are characterized by finite amplitudes and induce complex, time-varying feedbacks with flow. Under such conditions, friction becomes dominant and eventually the behaviour of the waves deviates from being translational.

Insight on the non-linear behaviour of bed waves can be seeked in experimental studies that simulated the evolution of sediment pulses originating from landslides and debris flows (e.g. (Lisle et al., 1997; Cui et al., 2003; Lisle et al., 2001)), releases downstream from dams (e.g. (Sklar et al., 2009; Venditti et al., 2010)) or even dam removal (e.g. (Pace et al., 2016)). These friction dominated experiments demonstrate how the natural bed waves evolve through a combination of translation and diffusion (or dispersion), with the relative importance of each defined to a large extent by the characteristics of the sediment pulses (e.g. grain size and volume) as well as from the flow conditions.

Review of studies on the evolution of non-linear bed waves .
Bed waves that form in nature, but also those that result from nourishments in rivers have a non-linear character in the sense that deviate significantly from being purely translational waves. Dispersion becomes dominant for the evolution of these waves owing to the friction they experience. (Lisle et al., 1997) studied the behaviour of non-linear waves as they occur in mountainous rivers where flow conditions are close to critical. They found that the wave they introduced into a laboratory flume, essentially evolved purely by diffusion without migrating downstream. A mathematical model they derived indicated that in flow conditions close to critical, translation processes become negligible. On the contrary, de Vries (1965) demonstrated with a mathematical analysis that when quasi-steady flow ($Fr \ll 1$) is a valid assumption, then a bed disturbance will behave as a kinematic wave negligible diffusion. While the assumption of quasi-steady flow seems to be plausible in lowland rivers, where the morphological time scale exceeds by far the time scale over which changes in flow take place, it is limited over the region of the disturbance where friction becomes increasingly important as the amplitude deviates significantly from being infinitesimal small.

Cui et al. (2003) conducted flume experiments with conditions similar to those considered by (Lisle et al., 1997) and additionally noted that translation becomes increasingly important for a finer sediment wave. More recent work by Sklar et al. (2009) showed that not only the grain size characteristics but also the volume of wave is important in determining the relative degrees of translation and dispersion as well as the rate of morphodynamic changes. Their runs also supported that finer additions promote translation as well as faster migration, but additionally showed that a time varying feedback evolves between the flow and the bed wave; initially the wave perturbs more the flow inducing backwater effects that strive it towards fast downstream advection. The feedback becomes weaker with decreasing amlitude of the wave.

Table F.1: Translation discussed for sediment waves in various mountain reaches. Superscripts explanation: a= bed material is pavement, b= Wide and uncertain range of values for entire sediment wave including reaches upstream of recent zone of aggradation, c= Order-of-magnitude value for entire wave, Large value in part caused by dispersed sediment sources. d= Fining of bed accompanies aggradation. e= Range of material sizes in wave is wider than preexisting bed. f= Wave material is bed load collected downstream of tributary; bed material is from subsurface samples from same reach. (Lisle et al., 1997)

	$\frac{amlitude}{bank-full-depth}$	$\frac{amlitude}{wavelength}$	$\frac{d_{50}wave}{d_{50}bed}$	Translation
Fall River	1	$6 * 10^{-4}$	0.1^a	yes, no
Redwood Creek	$\geqslant b$	10^{-5c}	$\leqslant 1^d$	uncertain
Navarro River	2	$4 * 10^{-3}$	$> 1^e$	no
East Fork River	<0.5	$5 * 10^{-4}$	0.3^f	yes

The bed wave in Bovenrijn .
Concerning the migration of the bed wave that resulted from the nourishment pilot at Lobith little can be concluded, mostly due to the fact that it is at an early stage of evolution. The doubling of its thickness at the most downstream stretch generally denotes a difference in mobility between the granite tracer fraction and the gravel placed upstream. This moderate mobility of the granite is also expressed by a marginal downstream migration by the front of the bed wave. In a downstream direction, the sediment supplied from the area of the nourishment is less than the capacity of flow to transport sediment. As a result a bedload gradient arises and scours the bed. This emergent erosion pit, is likely to persist and lead in front of the coarse wave as the latter will migrate downstream. It should be noted though that granite is transported downstream to a certain extent, without this being accompanied by increase in bed elevation.

Generally speaking, the evolution of the bed wave is expected to have a very significant translational component owing to its low ratio of amplitude to water depth and to the subcritical flow

conditions in Bovenrijn. However, the relatively coarse grain size associated with the bed wave is likely to promote dispersion.

appendix

G

TEMPORAL TRENDS IN SEDIMENT TRANSPORT RATES AT LOWER NIEDERRHEIN

Discharge variability and uncertainty .

Water discharges measured when the sediment transport measurements were taken demonstrate variability, which is expected to influence the analysed data. Regarding the measured transport rates, typically a power law function relates Q_w and Q_s. Also the grain size distribution of the measured load may be sensitive to changes in discharge. An increase of Q_w reduces the importance of grain size selectivity in a sense that coarser grains become relatively more mobile. To reduce the effect of discharge variability we only show analysed data taken at water discharges in the range of $\pm$ 50 $\%Q_{w,mean}$. This choice was made on the basis that further reduction of the discharge window (e.g. to $\pm$ 30 $\%Q_{w,mean}$) generally returned the same temporal variations in the measured quantities, however led to a decrease of the available timespan of measurements.

Fig.4.12 demonstrates the temporal evolution of bed-load rates and its contents; sand, fine gravel below 16 mm and finally coarse gravel at Griethausen located at the upstream end of our study reach. The sieving analysis reveals that there was hardly any content of grains coarser than 63 mm in the samples. Therefore in the following we can assume that the coarse gravel plotted reveals grains having a diameter in the range of 16 to 63 mm.

Since we were not able to completely eliminate the influence of the discharge variability, before analysing the data we are going to focus on the scatter of the various measured quantities and their correlation with the water discharge to discuss the underlying uncertainty in assessing any possible trends that may be revealed.

A first look on the graph indicates a stronger correlation between sediment and water discharge compared to the correlation of the respective contents of bedload and Q_w. More in specific, when measurements are taken at denser time intervals the variability shown in the contents of sand and fine gravel is approximately 15% (or 0.15) even when the respective discharges cross from the lower to the higher analysed boundaries. At these shorter time scales (2-4 years), the sand content variations are in some cases mirrored with the variations of water discharge implying a negative correlation according to the physics we discussed previously. Nevertheless, a larger variability is also revealed over larger time scales (8-10 years) that has a poor correlation both with the water discharge and the measured bedload transport rates. Tab G.1 demonstrates the linear correlation coefficients calculated between a) water discharge and the (total and fractional) sediment transport rates and between b) total bedload transport rate and the respective fractional rates for the studied period.

Table G.1: Linear correlations between **R1**: R(Q_w - $Q_{bedload}$), **R2**: R(Q_w - sand content), **R3**: R(Q_w - fine gravel content), **R4**: R(Q_w - coarse gravel content), **R5**: R($Q_{bedload}$ - sand content), **R6**: R($Q_{bedload}$ - fine gravel content), **R7**: R(Q_w - coarse gravel content)

station	**R1**	**R2**	**R3**	**R4**
Krefeld	0.74	0.11	0.21	-0.29
Duisburg	0.62	-0.04	0.15	-0.20
Orsoy	0.43	0.22	-0.08	-0.13
Ork	0.42	-0.09	0.30	-0.19
WeselPerrich	0.59	-0.23	0.24	-0.02
Rees	0.34	-0.24	0.33	-0.16
Grieth	0.54	-0.15	0.19	-0.11
Griethausen	0.42	-0.13	0.12	0.04
station	**R5**	**R6**	**R7**	
Krefeld	0.27	0.12	-0.33	
Duisburg	0.23	-0.16	-0.11	
Orsoy	0.40	-0.20	-0.19	
Ork	0.12	0.07	-0.20	
WeselPerrich	0.12	0.12	-0.37	
Rees	-0.05	0.07	-0.04	
Grieth	0.13	-0.05	-0.40	
Griethausen	0.02	0.07	-0.23	

It can be seen that the linear correlation between bedload transport rate and water discharge (R1) is moderate and therefore we are not able to assign any visually detected trends to generalized temporal changes. The linear correlation of the fractional contents of bedload however, demonstrate a poor relation with both measured water discharges (R2, R3, R4) and transport rates (R5, R6, R7). It is worth to note that the linear correlation between the sand content and the measured water discharge is negative, revealing a possible inverse relation of measured discharges and the sand content in the load. Moreover, the coarse gravel content also correlates systematically negatively with water discharge revealing a very week relation opposite than the one that was expected.

To conclude, it is possible to study the large scale variability of the fractional contents of the measured bedload. However, we need to underline that it is not only the variability of the water discharge that has an effect on the data. The complex processes concerning mixed sediment morphodynamics as well as the inherit limitations of the measuring methods of sediment transport have their own signature on increasing the uncertainty concerning the following analysis.

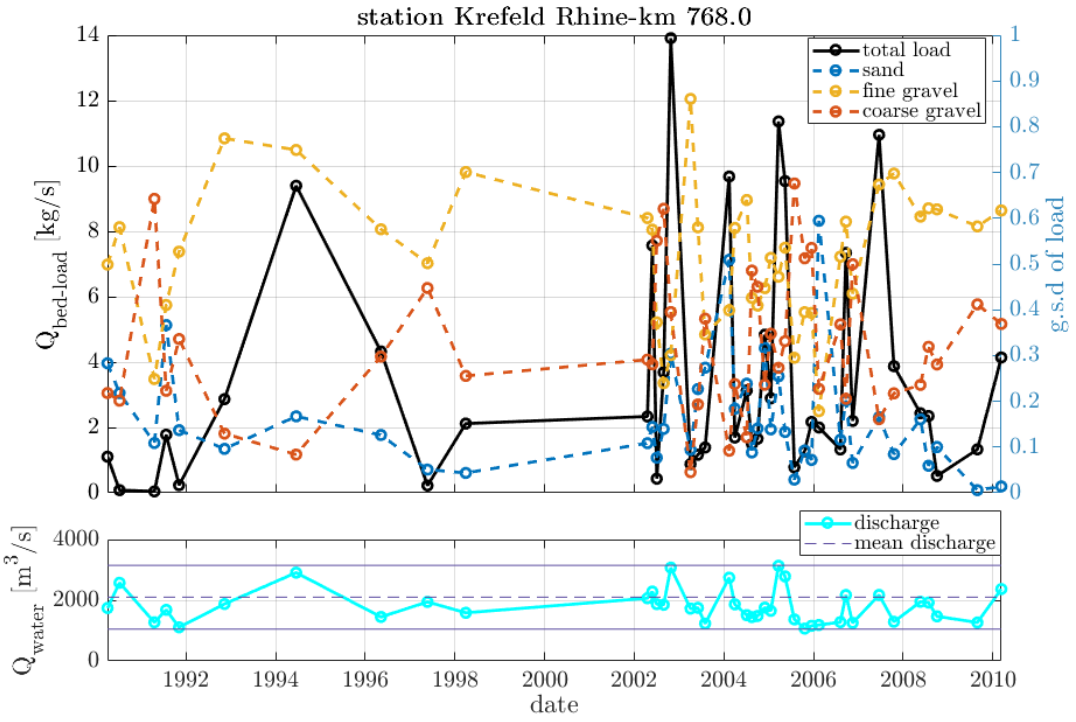

Figure G.1: Sediment transport measurements at discharges $\pm 50\% 2100 m^3/s$ at Krefeld during 1991-2011. data source: BfG, Frings et al. (2014a)

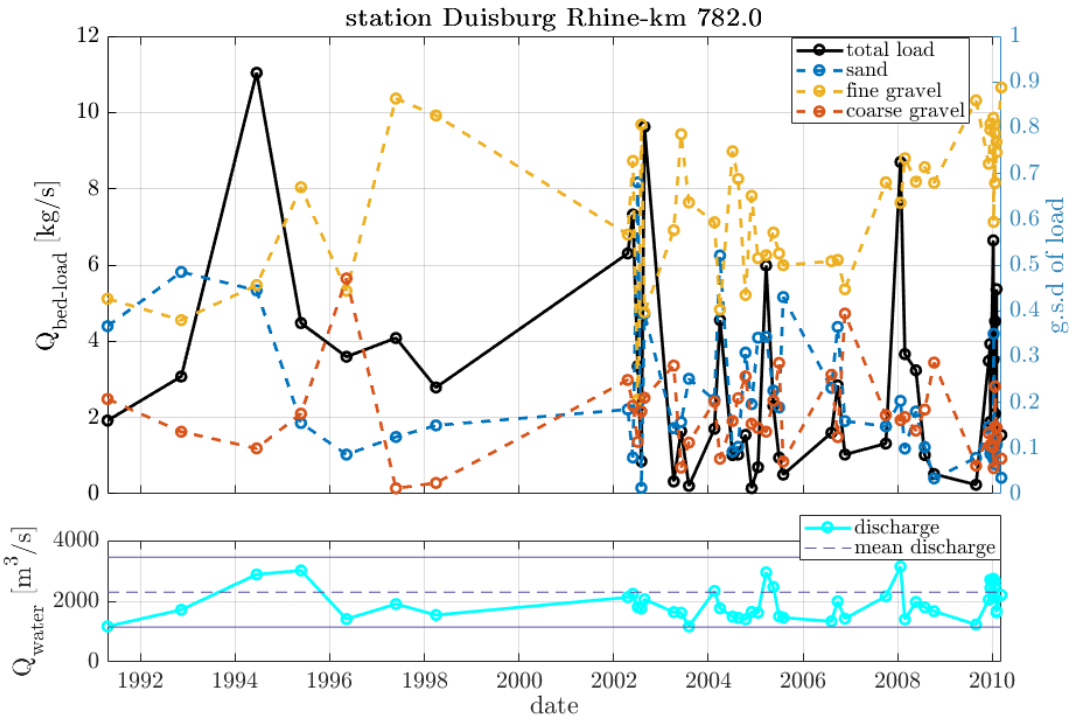

Figure G.2: Sediment transport measurements at discharges $\pm 50\% 2300 m^3/s$ at Duisburg during 1991-2011. data source: BfG, Frings et al. (2014a)

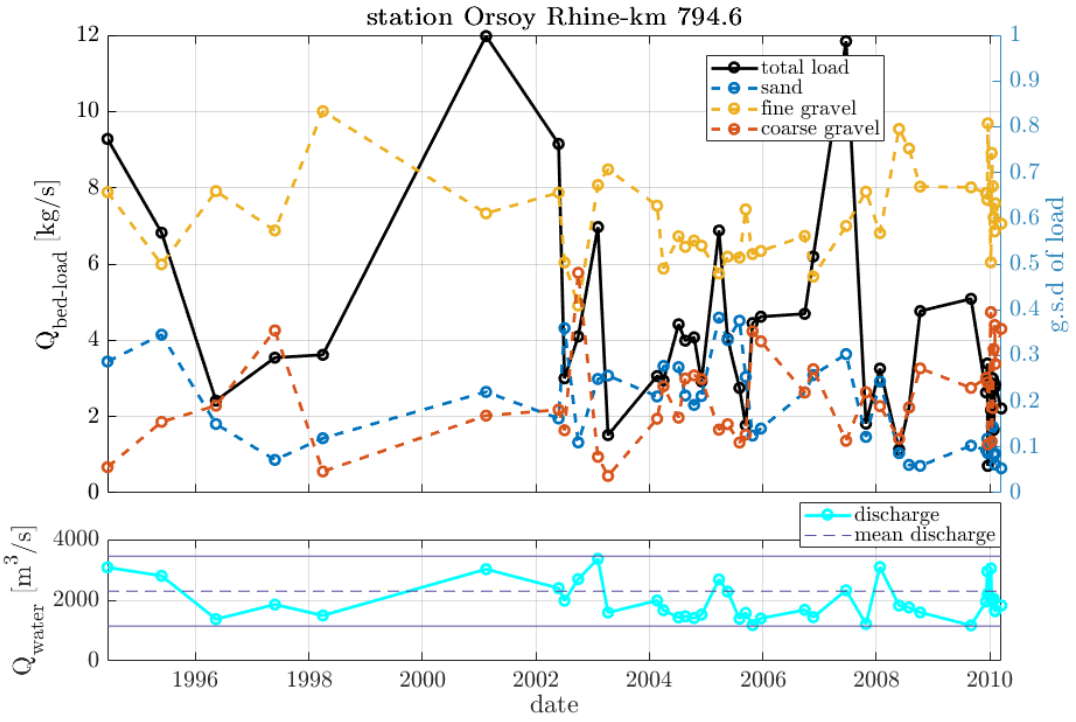

Figure G.3: Sediment transport measurements at discharges $\pm 50\% 2300 m^3/s$ at Orsoy during 1995-2011. data source: BfG, Frings et al. (2014a)

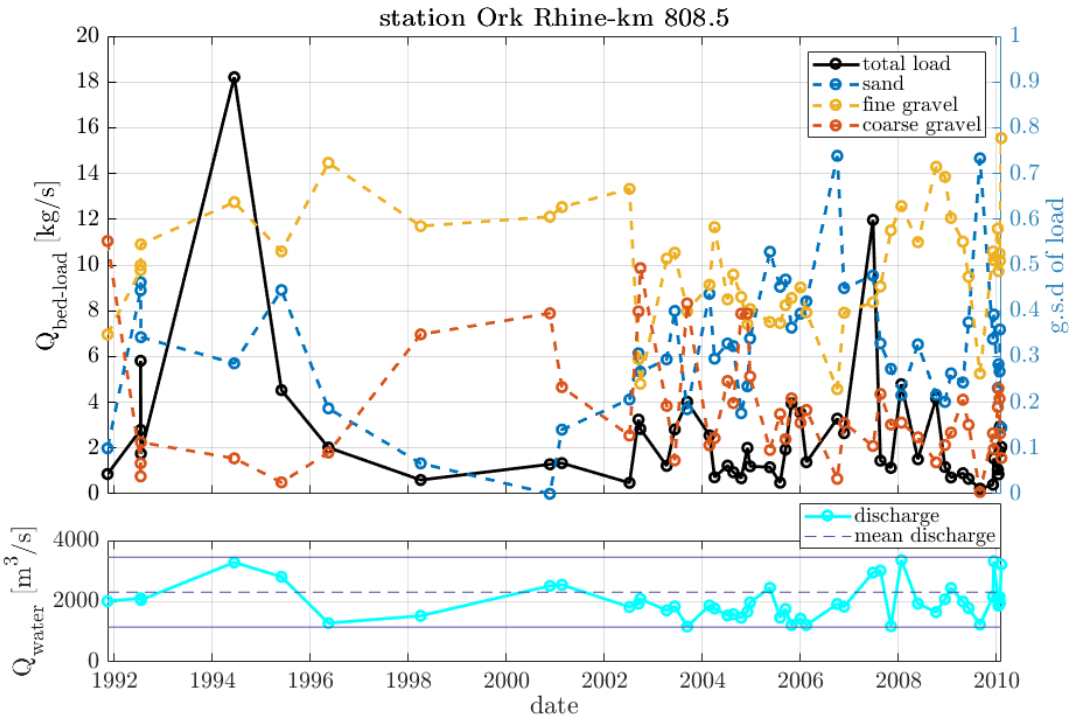

Figure G.4: Sediment transport measurements at discharges $\pm 50\% 2300 m^3/s$ at Ork during 1991-2011. data source: BfG, Frings et al. (2014a)

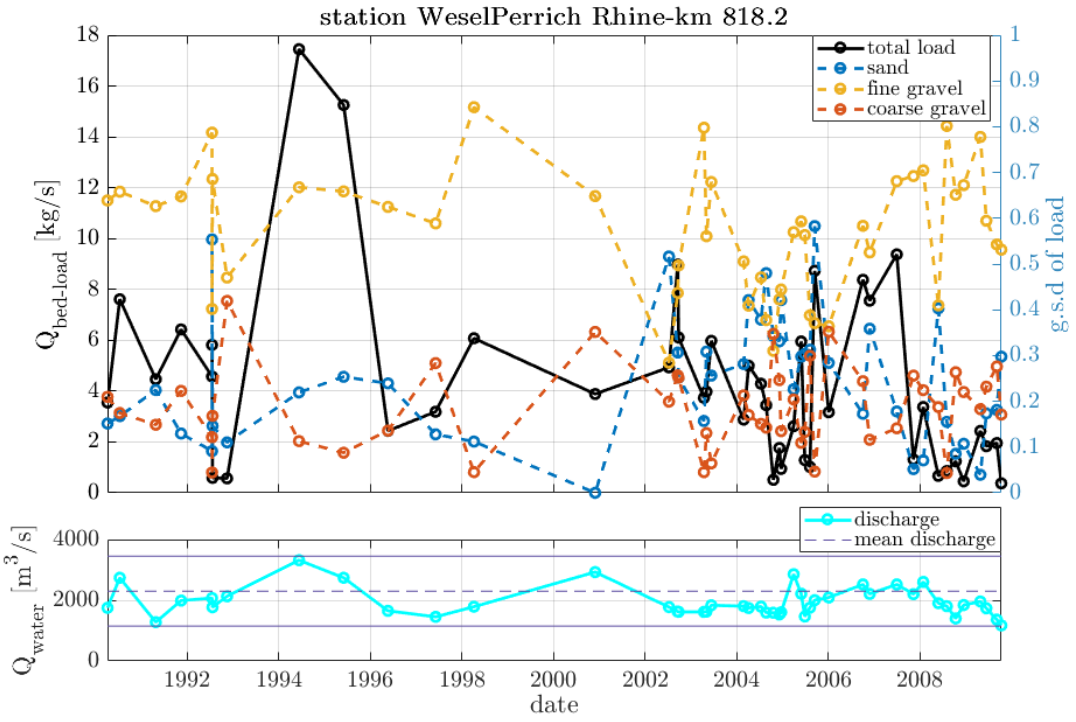

Figure G.5: Sediment transport measurements at discharges $\pm 50\% 2300 m^3/s$ at WeselPerrich during 1991-2009. data source: BfG, Frings et al. (2014a)

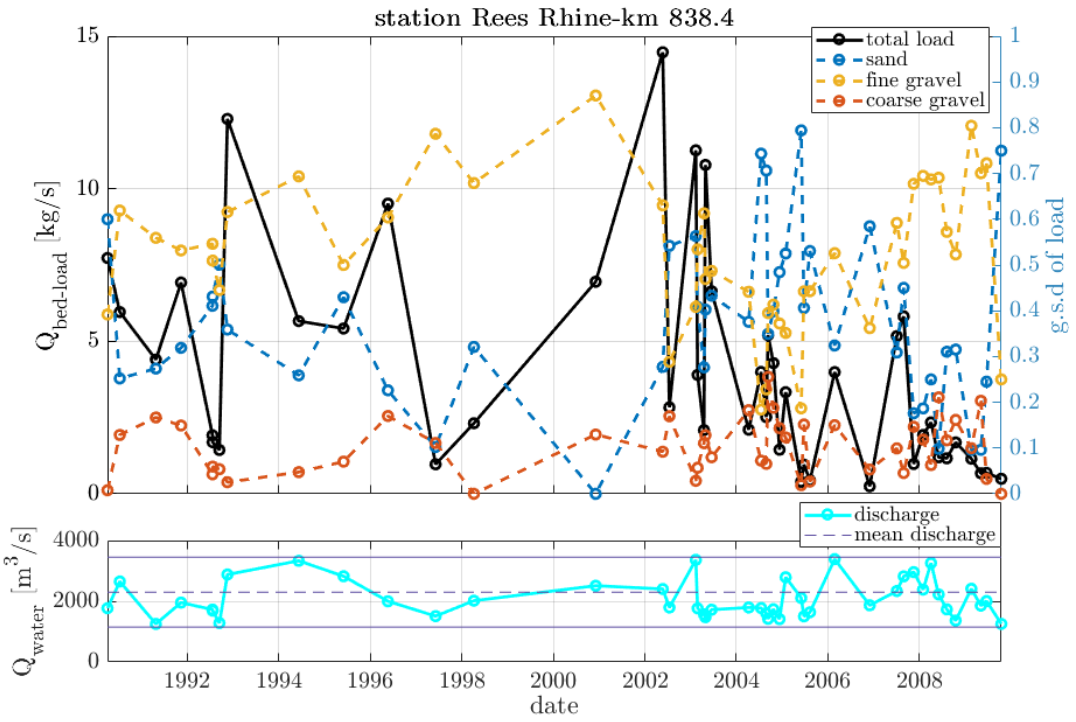

Figure G.6: Sediment transport measurements at discharges $\pm 50\% 2300 m^3/s$ at Rees during 1991-2009. data source: BfG, Frings et al. (2014a)

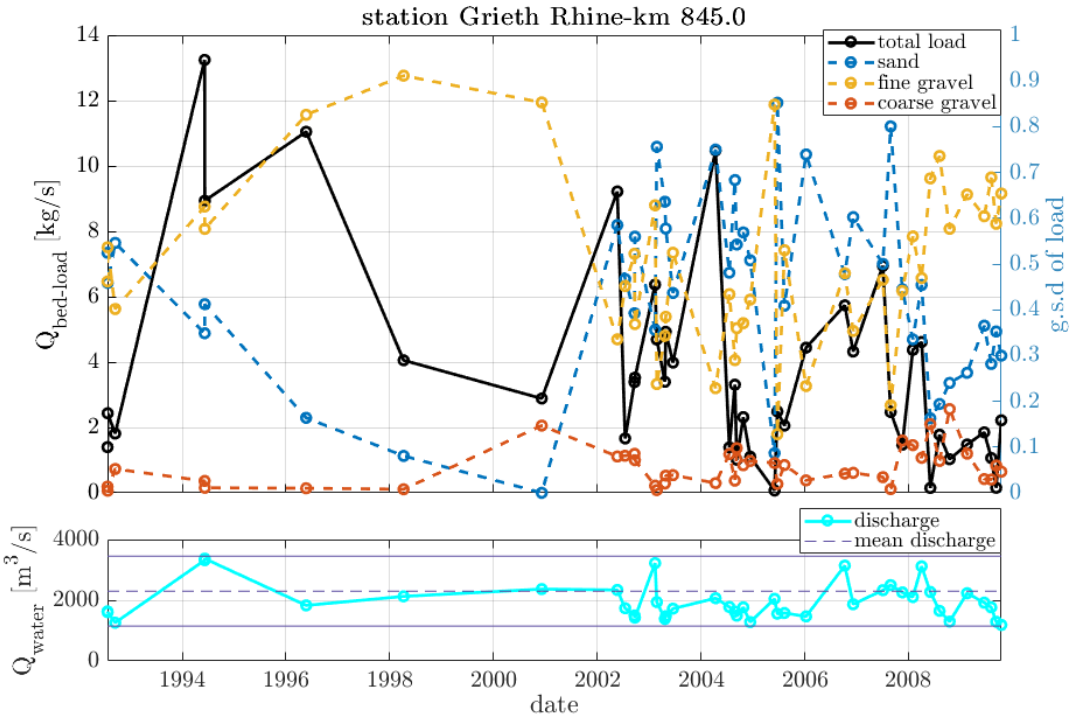

Figure G.7: Sediment transport measurements at discharges $\pm 50\% 2300 m^3/s$ at Grieth during 1992-2009. data source: BfG, Frings et al. (2014a)

LIST OF FIGURES